AD-A126 702 THE SALT-GRADIENT SOLAR POND(U) VON KARMAN INST FOR FLUID DYNAMICS RHODE-SAINT-GENESE (BELGIUM) S T BROWN FEB 83 EOARD-TR-83-4 AFOSR-82-0201 1/2

UNCLASSIFIED F/G 10/3 NL

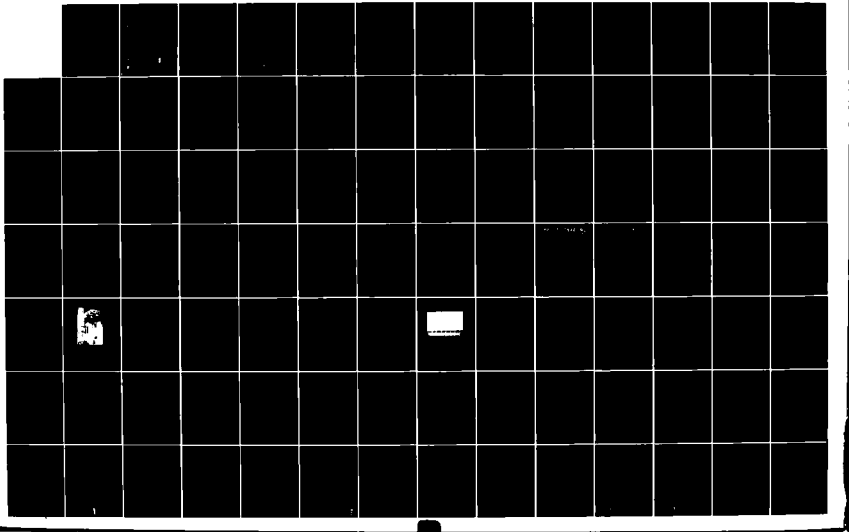

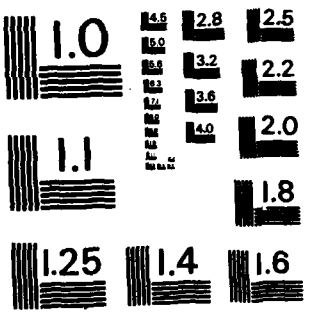

EOARD-TR-83-4

AD A126702

GRANT AFOSR 82-0201

THE SALT-GRADIENT SOLAR POND

SUSAN THOMAS BROWN
VON KARMAN INSTITUTE FOR FLUID DYNAMICS
CHAUSSÉE DE WATERLOO, 72
B - 1640 RHODE SAINT GENÈSE, BELGIUM

FEBRUARY 1983

FINAL SCIENTIFIC REPORT, 15 MAY 1982 - 14 FEBRUARY 1983

APPROVED FOR PUBLIC RELEASE: DISTRIBUTION UNLIMITED

DTIC FILE COPY

PREPARED FOR

AIR FORCE OFFICE OF SCIENTIFIC RESEARCH
BOLLING AF BASE, DC 20332

AND

EUROPEAN OFFICE OF AEROSPACE RESEARCH AND DEVELOPMENT
LONDON, UK

SECURITY CLASSIFICATION OF THIS PAGE (When Data Entered)

REPORT DOCUMENTATION PAGE		READ INSTRUCTIONS BEFORE COMPLETING FORM
1. REPORT NUMBER EOARD-TR-83-34	2. GOVT ACCESSION NO.	3. RECIPIENT'S CATALOG NUMBER
4. TITLE (and Subtitle) THE SALT-GRADIENT SOLAR POND		5. TYPE OF REPORT & PERIOD COVERED Final Scient. Rep. 15 May 82 - 14 Feb 1983 6. PERFORMING ORG. REPORT NUMBER
7. AUTHOR(s) Susan THOMAS BROWN		8. CONTRACT OR GRANT NUMBER(s) AFOSR 82-0201
9. PERFORMING ORGANIZATION NAME AND ADDRESS von Karman Institute for Fluid Dynamics, Chaussée de Waterloo, 72, B-1640 Rhode-Saint-Genèse, Belgium		10. PROGRAM ELEMENT, PROJECT, TASK AREA & WORK UNIT NUMBERS P.E. 61102F Proj/Task 2301/D1
11. CONTROLLING OFFICE NAME AND ADDRESS European Office of Aerospace R&D/CA Box 14 FPO New York 09510		12. REPORT DATE February 1983 13. NUMBER OF PAGES 109
14. MONITORING AGENCY NAME & ADDRESS(if different from Controlling Office) European Office of Aerospace Research and Development/CA Box 14 FPO New York 09510		15. SECURITY CLASS. (of this report) UNCLASSIFIED 15a. DECLASSIFICATION/DOWNGRADING SCHEDULE

16. DISTRIBUTION STATEMENT (of this Report)

Approved for public release; distribution unlimited

17. DISTRIBUTION STATEMENT (of the abstract entered in Block 20, if different from Report)

Approved for public release; distribution unlimited

18. SUPPLEMENTARY NOTES

19. KEY WORDS (Continue on reverse side if necessary and identify by block number)

SOLAR POND; SOLAR ENERGY; THERMAL ENERGY STORAGE; THERMAL STRATIFICATION

20. ABSTRACT (Continue on reverse side if necessary and identify by block number)

The salt-gradient solar pond was modelled both experimentally and numerically. The experimental model used a small-scale tank with artificial sunlight. Both temperature and concentration measurements were taken. The numerical model used a one dimensional heat conduction model to describe the heating phenomena in the pond.

The two models predicted the same type of behavior as that expected in full-scale ponds. There were small differences in the two models. These differences arose from simplifications in the numerical model.

DD FORM 1 JAN 73 1473 EDITION OF 1 NOV 65 IS OBSOLETE

SECURITY CLASSIFICATION OF THIS PAGE (When Data Entered)

EOARD-TR-83-34

This report has been reviewed by the EOARD Information Office and is releasable to the National Technical Information Service (NTIS). At NTIS it will be releasable to the general public, including foreign nations.

This technical report has been reviewed and is approved for publication.

CARY A. FISHER
Colonel, USAF
Chief Scientist

JERRY R. BETTIS
Lt Colonel, USAF
Deputy Commander

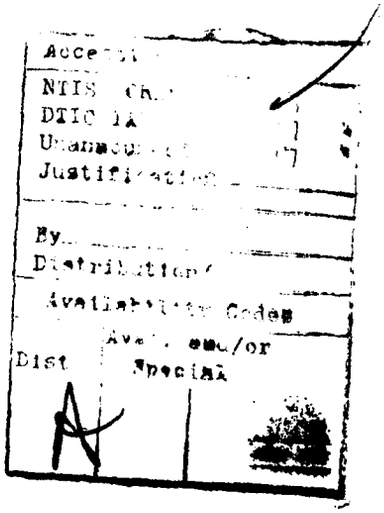

TABLE OF CONTENTS

ABSTRACT

The salt-gradient solar pond was modelled both experimentally and numerically. The experimental model used a small-scale tank with artificial sunlight. Both temperature and concentration measurements were taken. The numerical model used a one dimensional heat conduction model to describe the heating phenomena in the pond.

The two models predicted the same type of behavior as that expected in full-scale ponds. There were small differences in the two models. These differences arose from simplifications in the numerical model.

LIST OF SYMBOLS

h	distance below surface (positive downwards) [=] m
h_1	depth of the UCZ [=] m
k	thermal conductivity of the pond solution [=] W/m°C
n	refractive index of pond solution (non-dimensional)
q	salt concentration [=] kg/m^3
t	time [=] sec
C_p	heat capacity of pond solution [=] J/kg°C
D	depth of the combined UCZ and NCZ [=] m
D_s	depth of the LCZ [=] m
F	fraction of radiation which is absorbed in a small distance, δ, of solution (non-dimensional)
I_h	irradiance at a given pond depth [=] W/m^2
I_s	irradiance just beneath the pond surface [=] W/m^2
m	mass of pond [=] kg
Q_D	rate of energy transfer to load [=] J/m^2
Q_{LG}	rate of energy transfer to ground [=] J/m^2
Q_{LS}	rate of energy loss through the surface [=] J/m^2
S	pond surface area [=] m^2
T	temperature in the NCZ [=] °C
T_0	reference temperature [=] °C
T_a	ambient temperature [=] °C
T_b	temperature in the LCZ [=] °C
T_s	temperature in the UCZ [=] °C
U_{LG}	heat transfer coefficient at the pond bottom [=] $W/m^2°C$
U_{LS}	heat transfer coefficient at the surface [=] $W/m^2°C$
Z	dimensionless distance in the NCZ

α	thermal diffusivity of the pond solution [=] m^2/sec
δ	small distance in which the fraction F is absorbed [=] m
θ	dimensionless temperature in the NCZ = T/T_0
θ_a	ambient temperature in dimensionless form
θ_b	dimensionless temperature in the LCZ
θ_{GW}	ground temperature in dimensionless form
θ_r	refracted angle [=] radians
θ_s	dimensionless temperature in the UCZ
θ_z	solar zenith angle [=] radians
μ	effective attenuation coefficient [=] m^{-1}
ρ	density of pond solution [=] kg/m^3
τ	dimensionless time

1. INTRODUCTION

1.1 Definition

The salt-gradient solar pond is a body of water that is used as both collector and storage of solar energy. Salt is added to the pond such that the concentration of salt increases with depth, thus inhibiting free convection. The pond can be from 2 to 10 meters deep, with fresh water at the surface and a nearly saturated solution at the bottom. The bottom of such a pond is usually black, for high absorption. When the water in the bottom region of the salt-gradient pond is heated, it tends to remain hotter than the rest of the pond, as convection is suppressed. Thus, heat extraction is made from the bottom of the pond.

1.2 Previous investigation

The first serious research effort in the area of artificially created solar ponds was begun in 1958 by H. Tabor (Ref. 1). This work continued until 1966 when the interest in solar energy decreased due to the low cost of fuel-oil. After the energy crisis of 1973, interest in solar ponds awakened. The Scientific Research Foundation in Israel began solar pond research in 1974. Two demonstration power plants have been set up in Israel, both of which operate at temperatures near 90°C. Similar research was begun in 1974 at Ohio State University in the U.S. Most of the experimental work reported from both Israel and the U.S. has been performed on full-scale ponds, with surface areas ranging from 150 m^2 to 7000 m^2.

Some laboratory experiments have been reported, however, which investigate the concentration and temperature gradients, using tanks of 0.5 m diameter (Ref. 2). These tanks were heated from the bottom and thus did not simulate solar radiation.

Wilkins and Pinder have reported work done on a small-scale solar pond model (Ref. 3). The pond they used had surface dimensions of 65 cm × 65 cm and was 25 cm deep. Their model used partitions to separate the non-convecting layer from the convecting layers, and was exposed to actual radiation in Vancouver.

In 1981, investigators at VKI attempted to model the "saturated" solar pond, with radiation supplied by five halogen lamps (Ref. 4).

The present study differs from the others in that a non-convecting solar pond, without partitions, was modelled on a small scale with controlled artificial sunlight. The experimental results are then compared to the results from a numerical model.

1.3 The motivation for laboratory modelling

If solar ponds are to be used for energy production, a model is needed to test various designs and improvements. A typical solar pond has a surface area on the order of 1000 m^2. Thus it would be highly impractical to build a full-size solar pond to test any new idea or possible improvement. There are many existing computer simulations of solar ponds (Refs. 5,6,7,8).

Numerical models are limited, however, to the inclusion of phenomena that can be described mathematically. Although it may be argued that this is always possible, it is certainly not always practical. Thus the need for reliable small-scale laboratory models becomes evident.

2. THEORY

2.1 Basic principle

Solar radiation is received by the pond through the pond surface. Some of the incoming radiation is reflected by the surface and some is absorbed near the surface (see Fig. 1). Much of the radiation reaches the bottom of a shallow (< 10 m) pond and is absorbed by the absorbing bottom. Figure [illegible] hows the amount of transmitted radiation as a function pond d [illegible]h. It can be seen from this figure that 40% of the incoming [illegible]diation can reach the bottom of a 1.5 m pond. Thus, the bott [illegible]uld absorb the heat and consequently re-radiate it, heati[illegible]e pond from the bottom. In a pure water pond, the hot water would be lighter than the colder surface water and free convection would begin, mixing the water and allowing the heat to escape into the atmosphere through the surface. In a salt-gradient pond, however, there exist dissolved salts in the pond in proportions that increase with pond depth. That is, the solution at the pond surface contains very little salt and that at the pond bottom is nearly saturated. This increase in solution density conteracts the decrease in density due to the temperature change, thus keeping the hot solution at the bottom of the tank. The stability requirement can be expressed as :

$$\frac{\partial \rho}{\partial h} = \left(\frac{\partial \rho}{\partial T}\right)_q \frac{\partial \rho}{\partial h} + \left(\frac{\partial \rho}{\partial q}\right)_T \frac{\partial q}{\partial h} > 0 \qquad (1)$$

where :

ρ = density of pond solution [=] kg/m^3

h = distance below the surface (positive downwards) [=] m

T = temperature [=] °C

q = salt concentration [=] $\frac{kg}{m^3}$

As long as the criteria expressed in equation (1) is maintained, the pond will be non-convecting and the heating phenomena will be heat conduction.

2.2 The convective layers

If the entire pond were truly non-convective, the temperature gradient would be as shown in figure 3a. The gradients circled, however, quickly become great enough to overcome the suppressive action of the density gradient and convection begins in the zones shown in figure 3b. Thus in practice, a salt-gradient pond is composed of three layers :

(1) The upper convective zone (UCZ).

(2) The non-convective zone (NCZ).

(3) The lower convective zone (LCZ).

The parallel temperature and density gradients occur in the non-convecting zone, as shown in figure 4.

2.3 The non-dimensional equations (Ref. 5)

A heat balance over a small layer in the non-convecting zone yields the following equation :

$$\frac{\partial T}{\partial t} = \alpha \left[\frac{\partial^2 T}{\partial h^2}\right] + \frac{I_h \mu}{C_p} \sec \theta_r \qquad (2)$$

where :

t = time [=] s

α = thermal diffusivity = $\frac{k}{\rho C_p}$ [=] $\frac{m^2}{s}$

μ = effective attenuation coefficient = m^{-1}

C_p = heat capacity of solution [=] $\frac{J}{kg°C}$

I_h = radiation at a given pond depth

$$= I_s\ (1-F)\exp(-\mu[h-\delta]\sec\theta_r)\ [=]\ \frac{W}{m^2}$$

θ_r = refracted angle = $\sin^{-1}\left[\frac{\sin\theta_z}{n}\right]$ [ ] rad

θ_z = solar zenith angle [=] rad

n = refractive index of solution [=] non-dimensional

f = fraction of radiation absorbed in a small distance, δ, of solution, non dimensional

δ = small distance in which fraction F is absorbed [=] m

I_s = irradiance just beneath the pond surface [=] $\frac{W}{m^2}$

In equation (2) it is assumed that heat transfer occurs in one direction only. The depth of a solar pond is ordinarily much, much smaller than either the length or the width, making this assumption good for such an application. Also, it is assumed that all the radiation reaching the bottom is absorbed by the bottom. An equivalent situation occurs when some radiation is reflected from the bottom, in diffuse form, but is consequently absorbed in the storage zone (the lower convecting zone).

The solution of eq.(2) requires one initial condition and two boundary conditions. The initial condition can be chosen. One boundary condition evolves from a heat balance over the upper convecting zone

$$\frac{\partial T_s}{\partial t} = \frac{I_s}{\rho h_1 C_p}\left[1-(1-F)\exp\{-\mu(h-\delta)\sec\theta_r\}\right]$$

$$+ \frac{k}{\rho h_1 C_p}\left(\frac{\partial T}{\partial h}\right)_{h=h_1} - \frac{Q_{LS}}{\rho h_1 C_p} \qquad (3)$$

where :

T_s = temperature in the upper convecting zone [=] °C

h_1 = depth of the upper convecting zone [=] m

Q_{LS} = rate of energy loss at the surface [=] W/s m^2

The first term on the right represents the heat absorption in the UCZ due to radiation. The second term represents the heat conduction across the boundary between the NCZ and the UCZ. The last term represents heat lost through the pond surface. The boundary condition at the bottom can be found by performing a similar heat balance over the LCZ.

$$\frac{\partial T_b}{\partial t} = \frac{(1-F)}{\rho D_s C_p} I_s \exp\left[-\mu(D-\delta)\sec\theta_r\right] - \frac{k}{\rho D_s C_p}\left(\frac{\partial T}{\partial h}\right)_{h=D} \qquad (4)$$

$$- \frac{Q_{LG}}{\rho D_s C_p} - \frac{Q_D}{\rho D_s C_p} \qquad (4)$$

where :

T_b = temperature in the LCZ [=] °C

D_s = depth of the LCZ [=] m

D = h_1 + depth of the NCZ [=] m

k = thermal conductivity of sol'n [=] W/m°C

Q_{LG} = rate of energy lost to the ground [=] J/m^2

Q_D = rate of energy transfer to load [=] J/m^2

The first term on the right represents the heat absorption in the LCZ. The second term represents the heat conduction across the boundary between the LCZ and the NCZ. The third term represents the losses to the ground and the last term represents the heat withdrawn from the pond to meet the load.

To non-dimensionalize equations 2, 3 and 4, it is necessary to choose a characteristic time, temperature and distance. The characteristic temperature is chosen as simply T_0, a reference temperature, which can be the initial pond temperature, or the ground temperature, or in any other convenient way. The characteristic distance is chosen as D, the combined depth of NCZ and UCZ. The characteristic time is chosen as $\frac{D^2}{\alpha}$, which can be thought of as a "thermal travelling time" over the distance D. Thus equations 2, 3 and 4 become, in dimensionless form,

$$\frac{\partial\theta}{\partial\tau} = \frac{\partial^2\theta}{\partial Z^2} + \frac{D^2 I_h \mu \sec\theta_r}{kT_0} \tag{5}$$

$$\frac{\partial\theta_s}{\partial\tau} = \frac{D^2 I_S}{kT_0 h_1}\left[1-(1-F)\exp\{-\mu(h_1-\delta)\sec\theta_r\}\right]$$

$$+ \frac{D}{h_1}\left[\frac{\partial\theta}{\partial Z}\right]_{Z=Z_1} - \frac{U_{LS}D^2}{kh_1}\left(\theta_s-\theta_a\right) \tag{6}$$

$$\frac{\partial\theta_b}{\partial\tau} = \frac{D^2(1-F)I_S}{kT_0 D_s}\exp\left[-\mu(D-\delta)\sec\theta_r\right] - \frac{D}{D_s}\left[\frac{\partial\theta}{\partial Z}\right]_{Z=1}$$

$$- \frac{U_{LG}D^2}{kD_s}\left(\theta_b-\theta_{GW}\right) - \frac{Q_D D^2}{kT_0 D} \tag{7}$$

where :

$$\theta = \frac{T}{T_0}$$

$$\tau = \frac{\alpha t}{D^2}$$

$$Z = \frac{h}{D}$$

$\theta_s = \frac{T_s}{T_0}$

$\theta_b = \frac{T_b}{T_0}$

U_{LG} = heat transfer coefficient at pond bottom [=] $W/m^2 °C$

U_{LS} = heat transfer coefficient at surface [=] $W/m^2 °C$

$\theta_a = \frac{T_{ambient}}{T_0}$

θ_{GW} $\frac{T_{ground}}{T_0}$

Several dimensionless "numbers", or parameters, appear in the formulation of the above equations :

(1) The Fourier number = $F_0 = \frac{\alpha \hat{t}}{D^2}$ where t = characteristic time [=] LC ($\hat{t} \neq \frac{D^2}{\alpha}$ here, in order to choose a $\hat{t}$ to maintain the physical meaning of the numbers). F_0 gives the magnitude of the contribution to the change in temperature in the NCZ by conduction.

(2) $N1 = \frac{I_S \mu \hat{t}}{\alpha C_p T_0}$ = the magnitude of the contribution to the change in the NCZ by radiation

(3) $N2 = \frac{I_S \hat{t}}{\rho h_1 C_p T_0}$ = the magnitude of the contribution to the change in temperature in the UCZ due to radiation

(4) $N3 = \frac{k\hat{t}}{\rho h_1 C_p D}$ = the magnitude of the contribution to the change in temperature in the UCZ due to conduction

(5) $N4 = \frac{\hat{t} U_{LS}}{\rho h_1 C_p}$ = the magnitude of the contribution to the change in temperature in the UCZ due to losses through the surface

(6) $N5 = \dfrac{I_s \hat{t}}{T_0 \rho D_s C_p}$ = the magnitude of the contribution to the change in temperature in the LCZ due to radiation

(7) $N6 = \dfrac{k\hat{t}}{\rho D_s C_p D}$ = the magnitude of the contribution to the change in temperature in the LCZ due to conduction

(8) $N7 = \dfrac{U_{LG}\hat{t}}{\rho D_s C_p}$ = the magnitude of the contribution to the change in temperature in the LCZ due to losses to the ground

In this formulation, we will not consider the load term, as this study is concerned with the behavior of a solar pond with no heat load. For a typical solar pond of total depth 1.5 meters, the following values can be calculated for the dimensionless numbers :

$F_0 \cong 10^{-2}$
$N1 \cong 10^{-2}$
} NCZ

$N2 \cong 10^{2}$
$N3 \cong 10^{-1}$
$N4 \cong 10^{-1}$
} UCZ

$N5 \cong 1$
$N6 \cong 10^{-1}$
$N7 \cong 10^{-1}$
} LCZ

Since, in the NCZ, $F_0 \cong N1$, both the magnitude of N1 and F_0 must be respected. Since in the UCZ, $N2 \gg N3$ and $N2 \gg N4$, only N2 need be modelled. Similarly, in the LCZ, $N5 \gg N6$ and $N5 \gg N7$, so N6 and N7 can be sacrificed. Thus, four numbers must be respected in any experimental model : F_0, N1, N2 and N5.

2.4 Discretization of the equations

The non-dimensional equations 5-7 must be discretized for solution on the VAX computer. A Crank-Nicholsen scheme (implicit/explicit) was used. Using a forward time discretization and centered space discretization equation 5 becomes :

$$\frac{\theta_i^{n+1} - \theta_i^{n}}{\Delta\tau} = \frac{1}{2}\left[\frac{\theta_{i+1}^{n+1} - 2\theta_i^{n+1} + \theta_{i-1}^{n+1}}{\Delta Z^2}\right]$$

$$+ \frac{1}{2}\left[\frac{\theta_{i+1}^{n} - 2\theta_i^{n} + \theta_{i-1}^{n}}{\Delta Z^2}\right] + \left[\frac{D^2 I_h \mu \sec\theta_r}{kT_0}\right]_i \qquad (8)$$

Using a forward discretization in both time and space, equation 6 becomes :

$$\frac{\theta_1^{n+1} - \theta_1^{n}}{\Delta\tau} = \frac{1}{2}\frac{D}{h_1}\left[\frac{\theta_2^{n+1} - \theta_1^{n+1}}{\Delta Z}\right] + \frac{1}{2}\frac{D}{h_1}\left[\frac{\theta_2^{n} - \theta_1^{n}}{\Delta Z}\right]$$

$$+ \frac{D^2 I_s}{kT_0 h_1}\left|1-(1-F)\exp\{-\mu(h_1-\delta)\sec\theta_r\}\right|$$

$$+ \left[\frac{U_{LS} D^2}{kh_1}\theta_a\right] - \frac{1}{2}\frac{U_{LS} D^2}{kh}\theta_1^{n+1} - \frac{1}{2}\frac{U_{LS} D^2}{kh}\theta_1^{n} \qquad (9)$$

Using a forward time discretization and a backward space discretization, equation 7 becomes :

$$\frac{\theta_N^{n+1} - \theta_N^{n}}{\Delta\tau} = -\frac{1}{2}\frac{D}{D_s}\left(\frac{\theta_N^{n+1} - \theta_{N-1}^{n+1}}{\Delta Z}\right) - \frac{1}{2}\frac{D}{D_s}\left(\frac{\theta_N^{n} - \theta_{N-1}^{n}}{\Delta Z}\right)$$

$$+ \left[\frac{D^2(1-F)I_s}{kT_0D_s}\exp\left(-\mu(D-\delta)\sec\theta_r\right)\right] + \left(\frac{U_{LG}D^2\theta_{GR}}{k\ D_s}\right)$$

$$- \frac{1}{2}\frac{U_{LG}D^2}{kD_s}\theta_N^{n+1} - \frac{1}{2}\frac{U_{LG}D^2}{kD_s}\theta_N^{n} \qquad (10)$$

(Note that the heat withdrawal term has been dropped)

Equations 8, 9 and 10 can be programmed in Fortran to set up a tridiagonal matrix to solve for θ in a time-marching style (see Appendix 1 for the program listing). The Crank-Nicholsen scheme is unconditionally stable.

2.5 Temperature behavior

As the pond is heated at a constant heat input one would expect an exponential increase in temperature. When cycling occurs, the average heat input (average with respect to time) is decreased and thus the maximum temperature would be less that that with the same constant heat. Unequal cycling, with the time 'on' greater than the time 'off' would result in an intermediate maximum temperature.

3. EXPERIMENT

3.1 Apparatus

3.1.1 The pond

The model used for these experiments had a square surface area of 0.8281 m^2. The metal tank was lined on the inside wall with 4 cm of glass bead insulation (see Appendix 2). A pond depth of 30 cm was used with a mylar sheet floating on the surface. The purpose of the surface sheet was to prevent excessive losses due to evaporation. A photograph of the pond appears in figure 5.

3.1.2 The sun

Four halogen lamps were used to supply artificial sunlight to the pond. They were situated at a height that provided energy to the pond somewhat uniformly and of magnitude (at pond surface) of 550 W/m^2. Figure 6 shows the radiation isolines at the pond surface. The standard deviation of the data was 45.7 W/m^2, which is 8.2% of the average. For the cycling phase the "sun" was controlled by a microprocessor clock.

3.1.3 Temperature measurements

The temperature of the pond was measured by twelve Copper-Constantan thermocouples at the positions shown in Table 1. The temperature measurement chain is shown schematically in figure 7. A mechanical scanning device, the "clop-clop", was implemented to scan the thermocouples every 14 minutes. An electronic T-reference was used that also provided amplification for the signal to be received by the data logger. The data logger recorded the amplified signal on magnetic tape to be later processed by the PDP computer.

3.1.4 Salt concentration measurements

A probe, operating on optical principles, was developed to measure the concentration of $MgCl_2$ in the pond. A schematic of the measurement chain is shown in figure 8. A laser beam is directed into a 1 mm plastic optical fiber by a focusing device (see Fig. 9 for detail). The optical fiber then makes a U-turn. This U-turn is exposed to the solution in which the concentration is to be measured. As the laser beam hits the fiber wall, some of the light is refracted into the solution and some is reflected back into the fiber. The amount of light that is refracted into the solution is a function of the index of refraction of the solution which, in turn, is a function of salt concentration. Thus, a measure of the light intensity change through the bend is a measure of the salt concentration. To measure the intensity of light leaving the solution, a photo-resistor is used in the receiving network as shown in figure 10, and the output is read in volts. Seven probe shapes were tested (Fig. 11). The final shape chosen was probe number 7, whose calibration curve is shown in figure 12.

3.2 The procedure

3.2.1 Filling

The pond was filled using a port at the bottom of the tank. It was filled in layers, adding 40 ℓ fresh water first. Then 40 ℓ of 0.05 $\frac{gMgCl_2}{m\ell\ soln}$ solution was added, very slowly, so as not to mix the two layers. The concentrations were increased, as shown in figure 13, until the last layer of 0.3 $\frac{gMgCl_2}{m\ell\ soln}$ was added. The last layer was 12 cm deep to induce an effective LCZ. During filling, a concentration scan was performed to monitor the filling method.

3.2.2 Heating

The lights were turned on and the pond was heated for 75 hours. Data was taken intermittently during this period. Concentration scans were performed during the test and at its completion.

3.2.3 Cooling

After 75 hours of heating, the lights were shut off and the pond was allowed to cool for 70 hours. During the cooling phase temperature data was taken automatically every 14 minutes. At the end of the test, a concentration scan was made.

3.2.4 Day/night cycling

To study the cycling in the steady-state mode, the pond was first heated for several days until a surface temperature of about 40°C was reached. Then the controlling clock was set for 4.8 hours on, 4.8 hours off. A run of 16 hours was taken. Then the clock was set for 4.8 hours on, 2.93 hours off, and 60 hours of data were recorded. During all cycling phases, temperature data was taken automatically every 14 minutes on magnetic tape. At the completion of the cycling tests, a concentration scan was made.

3.3 Uncertainty analysis

3.3.1 Temperature measurements

3.3.1.1 Estimation of uncertainty

The temperatures were computed using the following formula :

$$T = -\frac{\sqrt{B^2-4AC}}{2A}$$

where :

$B = 8.03 \pm 0.01$

$A = 0.00641 \pm 0.00001$

$C = -DIG \pm 10$

(where DIG = the numerical value recorded on tape).

Thus, the uncertainty can be estimated using the following formula :

$$\delta T = \left[\left(\frac{\partial T}{\partial B} \delta B \right)^2 + \left(\frac{\partial T}{\partial A} \delta A \right)^2 + \left(\frac{\partial T}{\partial C} \delta C \right)^2 + \left(\frac{\partial T}{\partial DIG} \delta DIG \right)^2 \right]^{1/2}$$

For $T = 60°$, DIG = 500 and

$\delta T = 2°$

Thus, the uncertainty is $\sim$ 6%.

3.3.1.2 Radiation effects

The most important thermocouple error would most likely be from radiation. Figure 14 compares two sets of data taken at the same time. One was taken with the lights off and the other with the lights on to observe the radiation effects on the thermocouple measurements. It can be clearly seen that the effects of radiation are felt only at the first thermocouple near the surface. From these data it was decided not to include a correction for radiation effects.

3.3.2 Concentration measurements

The final probe tested has a repeatability of ± 0.015 volts. The calibration procedure has a great influence on the uncertainty. A linear formula is used for the temperature variation with volts.

$$C = mV + b$$

If the standard solutions are accurate to ± 5%, one can assume that m and b are accurate to about 5% also.

$m = - 0.212 \pm 0.010$

$b = \quad 0.239 \pm 0.012$

The uncertainty in C can then be calculated using :

$$\delta C = \left[\left(\frac{\partial C}{\partial m} \delta m \right)^2 + \left(\frac{\partial C}{\partial b} \delta b \right)^2 + \left(\frac{\partial C}{\partial V} \delta V \right)^2 \right]^{1/2}$$

Using this formula for

$C = 0.22$

$V = 4.16$

one obtains :

$\delta C = 0.05$ g/mℓ

or

$$\frac{0.05}{0.22} = 22\%$$

4. THE NUMERICAL MODEL

Equations 8, 9 and 10 (presented in section 2.4) were programmed, in FORTRAN, to be run on the VAX computer. First the equations were solved with no radiation in the program DECAY (see Appendix I). Then, in the program HEAT (Appendix I), the radiation effects were added. Then, the two programs were combined in SWITCH (Appendix I), to enable the day/night cycling to be simulated.

Runs were made that compared with the experimental heating, cooling and cycling. For the experimental comparison, the following parameters were used :

h_1 = 0.4 cm

D = 18 cm

D_s = 12 cm

μ = 0.1 m^{-1}

I_S = 550 W/m^2

$\Delta\tau$ = 0.00397

ΔZ = 0.1

U_{LS} = 0

$$U_{LG} = \begin{cases} 1.125\ W/m^2{}^\circ C & \text{lights "off"} \\ 0 & \text{lights "on"} \end{cases}$$

5. ANALYSIS OF RESULTS*

5.1 Experimental

5.1.1 Heating

5.1.1.1 Data

The series of profiles shown in figure 15 are selected from the data taken during the heating phase. Curve 1 represents the initial conditions of the pond, that is, nearly uniform temperature. The uppermost data point of each curve is 30 cm (pond surface) and the next point is at 27 cm (see Table 1). Thus, one can say from data presented here, that the UCZ is less than 3 cm thick. That is,

$0 < h_1 < 3$ cm

The data shows nearly uniform temperatures for the bottom 12 cm. Thus,

$D_s \cong 12$ cm

A pronounced temperature gradient is formed during the first 8 hours of heating, representing exaggerated heat absorption in the first zone. In the subsequent curves, the gradient becomes less pronounced, as the heat is convected through to the lower regions.

Figures 16a,b,c represent graphs of the data taken during heating that express the temperature as a function of time of three of the 12 thermocouple positions. Each curve represents an exponential increase with time. One can see the time constant is smaller near the pond surface and larger near the

---

* The complete set of raw data is stored on floppy disk and is available on request.

pond bottom. In the series of figures the effect of radiation coming in at the window can be clearly seen. There are three "humps" in the data that can be observed at $t \approx 6$ hours, $t \approx 30$ hours and $t \approx 55$ hours. These times correspond to late afternoon from 15 to 17h on each of the three testing days.

Figure 17 is the same time history for the average temperature during heating. The three "humps" are clearly visible here also.

5.1.1.2 Heat storage during the heating phase

An analysis of the pond heat storage during the heating phase can be made from the data shown in figure 17. The heat input was calculated by the known radiation at the pond surface. The energy stored in the pond was calculated by

heat stored = $mC_p\Delta T(t)$

where :

m = mass of pond = 293 kg

C_p = heat capacity of pond = 3634 J/kg°C

$\Delta T(t)$ = temperature difference from t = 0 to t.

In such a manner, figure 18 was generated. The minimum storage appears to be about 30%.

5.1.1.3 Global heat loss coefficient

A global heat balance on the pond yields :

$$mC_p \frac{dT}{dt} = I_s S - HS(T-T_a) \qquad (11)$$

where :

S = pond surface area = [m]

H = global heat loss coefficient [=] $W/m^2°C$

Using equation (11), one can solve for $H(T-T_a)$. The variation of $H\Delta T$ is shown in figure 19. As expected, $H\Delta T$ increases with time, that is, as the average temperature increases.

5.1.2 Cooling

Temperature profiles taken during the cooling phase are shown in figure 20. Curve 1 is the initial condition, the heated tank. In the first 9 hours, a drastic change takes place as the temperature gradient changes sense. Heat is lost quickly at the pond surface. After 54 hours of cooling (curve 7), there is still heat storage in the LCZ.

The time variations of the temperature at the twelve positions in the tank are shown in figures 21a-l. The outside radiation effects in the afternoon can again be clearly seen. The greatest effect of this is at the surface, smoothing out in the pond middle, and being felt again, but to a lesser degree, at the pond bottom. This indicates that absorption occurs at the top and at the bottom, the greater amount being absorbed at the top. As in the heating phase, the time constant is smallest at the pond surface. Figure 22 shows the average temperature variation with time during the cooling phase.

5.1.3 Cycling

5.1.3.1 Equal intervals

Figures 23a-c show the temperature variation with time of three of the twelve thermocouple positions during the cycling experiment. Figure 23a at the pond surface, shows a cyclic wave with a 10 hour period and large amplitude. This represents the strong effects of the radiation at the surface. As one moves further into the pond the cyclic variation decays until it is no longer seen at all. At the bottom of the NCZ the temperature is nearly constant with time, revealing the very stable nature of the pond at this point. Near the pond bottom,

a 10 hour cycle is again observed, but with a magnitude less than that at the top. This indicates that the absorption at the bottom is less than that at the top.

5.1.3.2 Unequal intervals

Figures 24a-l show the results of cycling tests run in the form of 5 hours on and 3 hours off. The same type of behaviour as described in section 5.1.3.1 appears in these figures.

The experiments were run by heating the tank, then performing the 5 on/5 off cycling beginning with the hot tank. Then the 5 on/3 off cycling was begun immediately after. Thus, one would expect to see the temperatures decrease as the maximum overall temperature decreases (see § 2.5), then decrease again as the average heat input is again decreased. The series of data taken did exhibit this behaviour, but the temperature changes were very small and occurred over long periods of time. Thus, it is not possible to illustrate this behaviour with the data shown here.

5.2 Numerical

5.2.1 Heating

Figures 25a-c show comparisons of the numerical results with the experimental data for three times in the heating phase; 5 hours, 24 hours and 48 hours. Although the shape of the curves agree in all cases, the actual temperature difference between experimental and numerical increases with time. The differences are due to the simplifications in the numerical model in describing the absorption of light in the pond. Also, it is expected that the experimental model would reach higher temperatures than predicted, as the additional radiation received through the window was not included in the numerical study.

5.2.2 Cooling

Figs. 26a,b,c show similar results for the cooling phase. The same comments apply to these as those made in section 5.2.1. There is, as shown in figure 28, a difference in slope at the pond bottom. From this one can conclude that the bottom losses are not correctly modelled.

5.2.3 Cycling

The results from the cycling experiments appear graphically in Figs.27a,b. Note that the greatest difference between the two models occurs at the pond surface. This supports the conclusion that the difference results from :

(1) Pond properties not modelled - especially the plastic cover.

(2) Radiation input from the windows.

(3) Simplified absorption model.

5.3 Concentration measurements

Figure 28a is a concentration profile taken during the filling of the pond. One can see the distinct layers, that is, the evidence that, during filling, the layers did not become mixed.

Figure 28b shows the concentration profile during the tests, verifying the stability of the pond.

Figure 28c shows the concentration profile after completion of all the tests. A gradient is still present, verifying the stability of the pond, but there is clear evidence of the upward diffusion of salt. There was initially 68.4 kg of salt added to the pond. Taking the area under the curve of figure 28c to compute the amount of salt yields 63.7 kg salt remaining in the pond. This represents a 7% salt loss.

Some salt was definitely lost from the solution by deposits on the tank bottom, and also through small leaks in the pond near the thermocouples. But the concentration measurements are highly uncertain and thus no quantitative analysis can be made concerning the salt loss.

6. CONCLUSIONS

Both the experimental model and the numerical model exhibited behavior characteristic of solar ponds. That is, the stable region is at the bottom of the NCZ with absorption in the upper and lower convecting zones. There is heat storage at the bottom evidenced in both.

The numerical model was found to be very sensitive to the depths of the three zones, which are chosen a priori. It is also very sensitive to the model used for absorption in the various layers. That is, to effectively use the model, one must know how radiation will be absorbed in the pond being modelled.

The experimental model acted in quite a "one-dimensional" way, as supported by the agreement between the numerical model and the experimental data. To ensure the same absorption characteristics as in a full-size pond, one need only respect the agreement of water quality and construction materials, if actual sunlight is used.

The problem becomes more difficult, however, when artificial light is used. The spectrum of the artificial light is not exactly the same as the spectrum of sunlight and thus the absorption characteristics are also different.

Finally, from the modelling attempted in this work, one can conclude that the modelling of solar ponds both experimentally and numerically is not only possible but feasible and should be investigated further.

7. RECOMMENDATIONS FOR FUTURE WORK

7.1 Numerical model

The numerical model could be improved by better modelling the pond loss (i.e., temperature-dependent heat loss coefficients). The validity of the analysis of the important dimensionless parameters could be checked using the numerical model.

It would be interesting to compare the results of the model with full-scale field tests.

7.2 Experimental

A longer test, with different cycling times, could be run to observe the phenomena described by section 2.5.

The experimental data could be compared with full-scale field tests.

If artificial light is to be used, an in-depth study of the absorption characteristics of the light in comparison with sunlight should be made.

The concentration probe, as described in section 3.1.4 could be further improved to reduce experimental uncertainty and make it easier to use.

REFERENCES

1. TABOR, H.: Review article - Solar ponds.
Solar Energy, Vol. 27, No. 3, 1981, pp 181-194.

2. NIELSEN, C.E.: Conditions for absolute stability of salt gradient solar ponds.
Department of Physics, The Ohio State University.

3. WILKINS, E. & PINDER, K.: Experiments with a model solar pond.

4. BRIARD, E. & PERRIOT, P.: Etude et experimentation d'un bassin solaire.
Institut des Sciences de l'Ingénieur,
Université de Nancy I., Juin 1981.

5. HAWLADER, M.N.A. & BRINKWOR, T.B.J.: An analysis of the non-convecting solar pond.
Solar Energy, Vol. 27, No. 3, 1981, pp 195-204.

6. SHAH, S.A.; SHORT, T.H.E.; FYNN, R.P.: Modeling and testing a salt gradient solar pond in Northeast Ohio.
Solar Energy, Vol. 27, No. 5, 1981, pp 393-401.

7. AKBARZADEH, A. & AHMADI, G.: Computer simulation of the performance of a solar pond in the southern part of Iran.
Solar Energy, Vol. 24, No. 2, 1980, pp 143-151.

8. HULL, J.R.: Computer simulation of solar pond thermal behaviour .
Solar Energy, Vol. 25, No. 1, 1980, pp 33-40.

9. WEINBERGER, H.: The physics of the solar pond.
Solar Energy, Vol. 8, No. 1, 1964, p 45.

10. BACHMAN, R.A. & GOLDMAN, C.R.: Hypolimnetic heating in Castle Lake, California.
Limnology & Oceanography, Vol. 10, 1965, p 2.

11. NIELSEN, C.E.: Experience with a proto type solar pond for solar heating.
Proc. Conf. Sharing the Sun,
Vol. 5, 1976, pp 169-182.

Thermocouple number	Distance from pond bottom (cm)
1	3
2	6
3	9
4	11.5
5	13
6	14.5
7	16
8	18
9	21
10	24
11	27
12	30

TABLE 1

APPENDIX 1 - PROGRAM LISTINGS

(a) Numerical - cooling

(b) Numerical - heating

(c) Numerical - cycling

(d) Program to solve tridiagonal matrix

(e) Plot - temperature vs height

(f) Plot - temperature vs time

(a)

```
DECAY.FOR;3                    17-JUN-1982 16:41:53.34          PAGE 1

  100           DIMENSION A(50),B(50),C(50),D(50),PHI(50),X(50),TEMP(50)
  200           DIMENSION A1(100),B1(100),C1(100),D1(100),F(100)
  300           TYPE 11
  400    11     FORMAT(1X,'ENTER NUMBER OF SEGMENTS')
  500           READ(5,12)N
  600    12     FORMAT(I3)
  700           TYPE 13
  800    13            FORMAT(1X,'ENTER NUMBER OF TIME STEPS')
  900           READ(5,12)ITMAX
 1000           TYPE 14
 1100    14     FORMAT(1X,'ENTER DELTA T')
 1200           READ(5,15)DELT
 1300    15     FORMAT(F10.5)
 1400           TYPE 16
 1500    16     FORMAT(1X,'ENTER DELTA X')
 1600           READ(5,15)DELX
 1700           TYPE 30
 1800     30    FORMAT(1X,'ENTER FRACTION OF RADIATION REFLECTED FROM BO
 1900        E  TTOM')
 2000           READ(5,15)FRAC
 2100           DO 3000 I=2,N
 2200           X(I)=X(I-1)+DELX
 2300   3000    CONTINUE
 2400           X(1)=0
 2500           TYPE 1001
 2600    1001   FORMAT(1X,'ENTER REFEPENCE TEMPERATURE')
 2700           READ(5,15)TZERO
 2800   C       CALCULATE Q AND P
 2900           TYPE 22
 3000      22   FORMAT(1X,'ENTER DEPTH OF UCZ IN CM')
 3100           READ(5,15)XTOP
 3200           TYPE 24
 3300      24   FORMAT(1X,'ENTER DEPTH OF NCZ IN CM')
 3400           READ(5,15)DEPTH
 3500           TYPE 23
 3600      23   FORMAT(1X,'ENTER DEPTH OF LCZ IN CM')
 3700           READ(5,15)XBOT
 3800           Q=(DEPTH+XTOP)/XTOP
 3900           P=-(DEPTH+XTOP)/XBOT
 4000   C       CALCULATE INITIAL SOLUTION
 4100           TYPE 25
 4200      25   FORMAT(1X,'ENTER INITIAL CONDITIONS IN NON-DIM FORM')
 4300           DO 700 IK=1,N
 4400           READ(5,15)PHI(IK)
 4500    700   CONTINUE
 4600           DO 2000 I=1,N
 4700           TEMP(I)=PHI(I)*TZERO
 4800           X(I)=FLOAT(I-1)*DELX
 4900   2000    CONTINUE
 5000   C       PRINT INITIAL SOLUTION
 5100           WRITE(50,20)
 5200           DO 600 II=1,N
 5300           WRITE(50,21)X(II),PHI(II),TEMP(II)
 5400    600    CONTINUE
 5500           TMAX=FLOAT(ITMAX)*DELT
 5600   C       CALCULATE A(I),B(I),C(I)
 5700   C       TC IS THE THERMAL CONDUCTIVITY OF THE POND IN W/MK
 5800           TC=0.596
 5900   C       HR IS THE TOP LOSS COEFFICIENT IN W/M2K
 6000   C       HI IS THE RADIATION IN W/M2
 6100           HI=0
 6400   C       UMU IS THE EFFECTIVE EXTINCTION COEFFICIENT IN 1/M
 6500           UMU=.1
 6600   C       HIR IS THE REFLECTED RADIATION
 6700           HIR=.6*FRAC*HI
 6800           HR=TC*100./DEPTH
 6900   C       PHIAMB IS THE AMBIENT TEMPERATURE
 7000           PHIAMB=19./TZERO
 7100           CONE=-HR*(DEPTH+XTOP)**2/(TC*XTOP*100.)
 7200           A1(1)=(-Q*DELT)/(2.*DELX)
 7300   C       UB IS THE BOTTOM LOSS COEFFICIENT IN W/M2K
 7400           UB=1.125
 7500           CTWO=-UB*(XTOP+DEPTH)**2/(TC*XBOT*100.)
 7600           B1(1)=1.+(Q*DELT)/(2.*DELX)-CONE*DELT/2.
 7700           B1(N)=1.-(P*DELT)/(2.*DELX)-CTWO*DELT/2.
 7800           C1(1)=0.
 7900           C1(N)=(P*DELT)/(2.*DELX)
 8000           A1(N)=0.
 8100           DO 100 I=2,N-1
 8200           Q=1.
 8300           A1(I)=(-Q*DELT)/(2.*DELX**2)
 8400           B1(I)=1.+(Q*DELT)/(DELX**2)
 8500           C1(I)=A1(I)
```

```
 100    CONTINUE
C       TIME LOOP:
        ITAU=0
        DO 200 J=1,ITMAX
        T=T+DELT
        ITAU=ITAU+1
C       CALCULATE DI
C       CALCULATE B,F,AND G
        B=BB*(DEPTH+XTOP)**2*PHIAMB/(TC*XTOP*100.)+(DEPTH+XTOP)**
     A  2*(1.-(.6*EXP(-UMU*(XTOP-6.)/100.)))*HI/(TC*TZERO*XTOP*100.)
     G  +HIR*(1.-.6*EXP(-UMU*((DEPTH+XBOT-6.)/100.)))*(DEPTH+XTOP
     I  )**2/(TC*T
     H  ZERO*XTOP*100.)
        DO 800 IK=1,N
        DI(IK)=HI*.6*EXP(-UMU*(FLOAT(IK-1)*(DEPTH+XTOP)-6.)/100.)
     M  +HIR*.6*EXP(-UMU*((1-FLOAT(IK-1))*(DEPTH+XTOP)+XBOT-6.)/
     N  100.)
        F(IK)=(DEPTH+XTOP)**2*DI(IK)*UMU/(TC*TZERO*100**2)
C       WRITE(70,26)F(IK)
 800    CONTINUE
  26    FORMAT(1X,'F=',F10.5)
C       PHIG IS THE TEMPERATURE OF THE GROUND
        PHIG=15./TZERO
        G=UB*(DEPTH+XTOP)**2*PHIG/(TC*XBOT*100.)+(DEPTH+XTOP)**
     B  2*.6*HI*EXP(-UMU*(DEPTH+XTOP-6.)/100.)/(TC*TZERO*XBOT*100.)
     K  +(DEPTH+XTOP)**2*.6*PHIAMB*HIR*EXP(-UMU*(XBOT-6.)/100.)/(
     L  TC*TZERO*XBOT*100.)
        D(1)=(Q*DELT*PHI(2))/(2.*DELX)+(1.-(Q*DELT)/(2.*DELX)*PHI(
     A  1))+(DELT/2.)*(H+H)+CONE*PHI(1)*DELT/2.
C       WRITE(70,27)D(1)
  27    FORMAT(1X,'D1=',F10.5)
        D(N)=((P*DELT)/(2.*DELX)+1.)*PHI(N)-((P*DELT)/(2.*DELX))*P
     B  HI(N-1)+(DELT/2.)*(G+G)+CTWO*PHI(N)*DELT/2.
C       WRITE(70,28)D(N)
  28    FORMAT(1X,'DN=',F10.5)
        DO 300 I=2,N-1
        D(I)=(Q*DELT*PHI(I+1))/(2.*DELX**2)+(1.-(Q*DELT)/(DELX
     D  **2))*PHI(I)+((Q*DELT)/(2.*(DELX**2)))*PHI(I-1)+(DELT/2.
     E  )*(F(I)+F(I))
C       WRITE(70,29)D(1)
  29    FORMAT(1X,'D=',F10.5)
 300    CONTINUE
C       CALCULATE SOLUTION AT TIME T
        DO 301 JJ=1,N
        A(JJ)=A1(JJ)
        B(JJ)=B1(JJ)
        C(JJ)=C1(JJ)
 301    CONTINUE
        CALL TRID(A,B,C,D,N,PHI)
        DO 2002 I=1,N
        TEMP(I)=PHI(I)*TZERO
2002    CONTINUE
C       PRINT NEW SOLUTION
        IF(ITAU.NE.4)GO TO 55
        WRITE(50,19)T
  19    FORMAT(1X,'T=',F10.5)
        WRITE(50,20)
  20    FORMAT(1X,8X,'X',12X,'SOLUTION',8X,'TEMPERATURE')
        DO 500 K=1,N
        WRITE(50,21)X(K),PHI(K),TEMP(K)
        ITAU=0
 500    CONTINUE
  55    CONTINUE
 200    CONTINUE
  21    FORMAT(2X,F10.5,8X,F10.5,8X,F10.5)
        STOP
        END
```

(b)


```
HEAT.FOR;5                    17-JUN-1982 16:42:19.85          PAGE 1

  100           DIMENSION A(50),B(50),C(50),L(50),PHI(50),X(50),TEMP(50)
  200           DIMENSION A1(100),B1(100),C1(100),L1(100),F(100)
  300           TYPE 11
  400    11     FORMAT(1X,'ENTER NUMBER OF SEGMENTS')
  500           READ(5,12)N
  600    12     FORMAT(I3)
  700           TYPE 13
  800    13           FORMAT(1X,'ENTER NUMBER OF TIME STEPS')
  900           READ(5,12)ITMAX
 1000           TYPE 14
 1100    14     FORMAT(1X,'ENTER DELTA T')
 1200           READ(5,15)DELT
 1300    15     FORMAT(F10.5)
 1400           TYPE 16
 1500    16     FORMAT(1X,'ENTER DELTA X')
 1600           READ(5,15)DELX
 1700           TYPE 30
 1800     30    FORMAT(1X,'ENTER FRACTION OF RADIATION REFLECTED FROM BO
 1900        E  TTOM')
 2000           READ(5,15)FRAC
 2100           DO 3000 I=2,N
 2200           X(I)=X(I-1)+DELX
 2300    3000   CONTINUE
 2400           X(1)=0
 2500           TYPE 1001
 2600    1001   FORMAT(1X,'ENTER REFERENCE TEMPERATURE')
 2700           READ(5,15)TZERO
 2800   C       CALCULATE Q AND P
 2900           TYPE 22
 3000     22    FORMAT(1X,'ENTER DEPTH OF UCZ IN CM')
 3100           READ(5,15)XTOP
 3200           TYPE 24
 3300     24    FORMAT(1X,'ENTER DEPTH OF NCZ IN CM')
 3400           READ(5,15)DEPTH
 3500           TYPE 23
 3600     23    FORMAT(1X,'ENTER DEPTH OF LCZ IN CM')
 3700           READ(5,15)XBOT
 3800           Q=(DEPTH+XTOP)/XTOP
 3900           P=-(DEPTH+XTOP)/XBOT
 4000   C       CALCULATE INITIAL SOLUTION
 4100           TYPE 25
 4200     25    FORMAT(1X,'ENTER INITIAL CONDITIONS IN NON-DIM FORM')
 4300           DO 700 IK=1,N
 4400           READ(5,15)PHI(IK)
 4500    700   CONTINUE
 4600           DO 2000 I=1,N
 4700           TEMP(I)=PHI(I)*TZERO
 4800           X(I)=FLOAT(I-1)*DELX
 4900    20     CONTINUE
 5000   C       PRINT INITIAL SOLUTION
 5100           WRITE(50,20)
 5200           DO 600 II=1,N
 5300           WRITE(50,21)X(II),PHI(II),TEMP(II)
 5400    600    CONTINUE
 5500           TMAX=FLOAT(ITMAX)*DELT
 5600   C       CALCULATE A(I),B(I),C(I)
 5700   C       TC IS THE THERMAL CONDUCTIVITY OF THE POND IN W/MK
 5800           TC=0.6
 5900   C       HR IS THE TOP LOSS COEFFICIENT IN W/M2K
 6000   C       HI IS THE RADIATION IN W/M2
 6100           TYPE 31
 6200     31    FORMAT(1X,'ENTER INCIDENT RADIATION')
 6300           READ(5,15)HI
 6400   C       UMU IS THE EFFECTIVE EXTINCTION COEFFICIENT IN 1/M
 6500           UMU=.1
 6600   C       HIR IS THE REFLECTED RADIATION
 6700           HIR=.6*FRAC*HI
 6800           HR=0.
 6900   C       PHIAMB IS THE AMBIENT TEMPERATURE
 7000           PHIAMB=35./TZERO
 7100           CONE=-HR*(DEPTH+XTOP)**2/(TC*XTOP*100.)
 7200           A1(1)=(-Q*DELT)/(2.*DELX)
 7300   C       UB IS THE BOTTOM LOSS COEFFICIENT IN W/M2K
 7400           UB=0.
 7500           CTWO=-UB*(XTOP+DEPTH)**2/(TC*XBOT*100.)
 7600           B1(1)=1.+(Q*DELT)/(2.*DELX)-CONE*DELT/2.
 7700           B1(N)=1.-(P*DELT)/(2.*DELX)-CTWO*DELT/2.
 7800           C1(1)=0.
 7900           C1(N)=(P*DELT)/(2.*DELX)
 8000           A1(N)=0.
 8100           DO 100 I=2,N-1
 8200           Q=1.
 8300           A1(I)=(-Q*DELT)/(2.*DELX**2)
```

```
8400              B1(I)=1.+(Q*DELT)/(DELX**2)
8500              C1(I)=A1(I)
8600        100   CONTINUE
8700        C     TIME LOOP:
8750              ITAU=0
8800              DO 200 J=1,ITMAX
8900              T=T+DELT
8950              ITAU=ITAU+1
9000        C     CALCULATE DI
9100        C     CALCULATE H,F,AND G
9200              H=HR*(DEPTH+XTOP)**2*PHIAIR/(TC*XTOP*100.)+(DEPTH+XTOP)**
9300             A 2*HI/(TC*TZERO*XTOP*100.)
9400        C     G  +HIR*(EXP(-UMU*((DEPTH+XBOT)/100.)))*(DEPTH+XTOP
9500        C     I )**2/(TC*I
9600        C     H ZERO*XTOP*100.)
9650        C       H=0.
9700              DO 800 IK=1,N
9800              DI(IK)=H1*EXP(-UMU*(FLOAT(IK-1)*(DEPTH+XTOP))/100.)
9900             M +HIR*EXP(-UMU*((1-FLOAT(IK-1))*(DEPTH+XTOP)+XBOT)/
10000            N 100.)
10100             F(IK)=(DEPTH+XTOP)**2*DI(IK)*UMU*DELX/(TC*TZERO*100**2)
10200       C      WRITE(70,26)F(IK)
10300          800 CONTINUE
10400           26 FORMAT(1X,'F=',F10.5)
10500       C      PHIG IS THE TEMPERATURE OF THE GROUND
10600              PHIG=20./TZERO
10700             G=UB*(DEPTH+XTOP)**2*PHIG/(TC*XBOT*100.)
10800            Z  +(DEPTH+XTOP)**2*H1*(DEPTH+XTOP)*(1.-EXP(-UMU*(DEPTH+XTOP)/100
10850            Y  )/(TC*TZERO*XBOT*100.)
10900
11100             D(1)=(Q*DELT*PHI(2))/(2.*DELX)+(1.-(Q*DELT)/(2.*DELX)*PHI(
11200           A  1))+(DELT/2.)*(H+H)+CONE*PHI(1)*DELT/2.
11300       C      WRITE(70,27)D(1)
11400          27 FORMAT(1X,'D1=',F10.5)
11500             D(N)=((P*DELT)/(2.*DELX)+1.)*PHI(N)-((P*DELT)/(2.*DELX))*P
11600           B  HI(N-1)+(DELT/2.)*(G+G)+CTWO*PHI(N)*DELT/2.
11700       C      WRITE(70,28)D(N)
11800          28 FORMAT(1X,'DN=',F10.5)
11900             DO 300 I=2,N-1
12000             D(I)=(Q*DELT*PHI(I+1))/(2.*DELX**2)+(1.-(Q*DELT)/(DELX
12100           D **2))*PHI(I)+((Q*DELT)/(2.*(DELX**2)))+PHI(I-1)+(DELT/2.
12200           E )*(F(I)+F(I))
12300       C      WRITE(70,29)D(I)
12400          29 FORMAT(1X,'D=',F10.5)
12500         300 CONTINUE
12600       C     CALCULATE SOLUTION AT TIME T
12700             DO 301 JJ=1,N
12800             A(JJ)=A1(JJ)
12900             B(JJ)=B1(JJ)
13000             C(JJ)=C1(JJ)
13100         301 CONTINUE
13200             CALL TRID(A,B,C,D,N,PHI)
13300             DO 2002 I=1,N
13400             TEMP(I)=PHI(I)*TZERO
13500        2002 CONTINUE
13550             IF(ITAU.NE.4)GO TO 55
13600       C     PRINT NEW SOLUTION
13700             WRITE(50,19)T
13800          19 FORMAT(1X,'T=',F10.5)
13900             WRITE(50,20)
14000          20 FORMAT(1X,8X,'X',12X,'SOLUTION',8X,'TEMPERATURE')
14100             DO 500 K=1,N
14200             WRITE(50,21)X(K),PHI(K),TEMP(K)
14300         500 CONTINUE
14350             ITAU=0.
14375          55 CONTINUE
14400         200 CONTINUE
14500          21 FORMAT(2X,F10.5,8X,F10.5,8X,F10.5)
14600             STOP
14700             END
```

(c)


```
SWITCH.FOR;15                    17-JUN-1982 16:42:47.01          PAGE 1

  100           DIMENSION A(50),B(50),C(50),D(50),PHI(50),X(50),TEMP(50)
  200           DIMENSION A1(100),B1(100),C1(100),D1(100),F(100)
  300           TYPE 11
  400    11     FORMAT(1X,'ENTER NUMBER OF SEGMENTS')
  500           READ(5,12)N
  600    12     FORMAT(I3)
  700           TYPE 13
  800    13           FORMAT(1X,'ENTER NUMBER OF TIME STEPS')
  900           READ(5,12)ITMAX
 1000           TYPE 14
 1100    14     FORMAT(1X,'ENTER DELTA T')
 1200           READ(5,15)DELT
 1300    15     FORMAT(F10.5)
 1400           TYPE 16
 1500    16     FORMAT(1X,'ENTER DELTA X')
 1600           READ(5,15)DELX
 1700           TYPE 30
 1800     30    FORMAT(1X,'ENTER FRACTION OF RADIATION REFLECTED FROM BO
 1900          E TTOM')
 2000           READ(5,15)FRAC
 2100           TYPE 32
 2200     32    FORMAT(1X,'ENTER TIME OF SUNLIGHT IN HOURS')
 2300           READ(5,15)ON
 2400           TYPE 33
 2500     33    FORMAT(1X,'ENTER TIME OF DARK IN HOURS')
 2600           READ(5,15)OFF
 2700           TYPE 99
 2800     99    FORMAT(1X,'ENTER AMBIENT TEMP DURING SUN')
 2950           READ(5,15)TSUN
 2875           TYPE 98
 2887     98    FORMAT(1X,' ENTER AMBIENT TEMP DURING DARK')
 2893           READ(5,15)TDARK
 2900           DO 3000 I=2,N
 3000           X(I)=X(I-1)+DELX
 3100   3000    CONTINUE
 3200           X(1)=0
 3300           TYPE 1001
 3400   1001    FORMAT(1X,'ENTER REFERENCE TEMPERATURE')
 3500           READ(5,15)TZERO
 3600   C       CALCULATE Q AND P
 3700           TYPE 22
 3800     22    FORMAT(1X,'ENTER DEPTH OF UCZ IN CM')
 3900           READ(5,15)XTOP
 4000           TYPE 24
 4100     24    FORMAT(1X,'ENTER DEPTH OF NCZ IN CM')
 4200           READ(5,15)DEPTH
 4300           TYPE 23
 4400     23    FORMAT(1X,'ENTER DEPTH OF LCZ IN CM')
 4500           READ(5,15)XBOT
 4600           Q=(DEPTH+XTOP)/XTOP
 4700           P=-(DEPTH+XTOP)/XBOT
 4725           TLIGHT=.0858*ON*60./(DEPTH+XTOP)**2
 4750           TDARK=.0858*OFF*60./(DEPTH+XTOP)**2-DELT
 4800   C       CALCULATE INITIAL SOLUTION
 4900           TYPE 25
 5000     25    FORMAT(1X,'ENTER INITIAL CONDITIONS IN NON-DIM FORM')
 5100           DO 700 IK=1,N
 5200           READ(5,15)PHI(IK)
 5300    700   CONTINUE
 5400           DO 2000 I=1,N
 5500           TEMP(I)=PHI(I)*TZERO
 5600           X(I)=FLOAT(I-1)*DELX
 5700   2000    CONTINUE
 5800   C       PRINT INITIAL SOLUTION
 5900           WRITE(50,20)
 6000           DO 600 II=1,N
 6100           WRITE(50,21)X(II),PHI(II),TEMP(II)
 6200    600    CONTINUE
 6300           IMAX=FLOAT(ITMAX)*DELT
 6400   C       CALCULATE A(I),B(I),C(I)
 6500   C       TC IS THE THERMAL CONDUCTIVITY OF THE POND IN W/MK
 6600           TC=0.596
 6700   C       HR IS THE TOP LOSS COEFFICIENT IN W/M2K
 6800   C       HI IS THE RADIATION IN W/M2
 6900           TYPE 31
 7000     31    FORMAT(1X,'ENTER INCIDENT RADIATION')
 7100           READ(5,15)HIMP
 7125           HI=HIMP
 7150           TAMB=TSUN
 7200   C       UMU IS THE EFFECTIVE EXTINCTION COEFFICIENT IN 1/M
 7300           UMU=.1
 7400   C       HIR IS THE REFLECTED RADIATION
 7500           HR=0.
```

```
      7800              CONF=-HR*(DEPTH+XTOP)**2/(TC*XTOP*100.)
      7900              A1(1)=(-U*DELT)/(2.*DELX)
      8000        C     UB IS THE BOTTOM LOSS COEFFICIENT IN W/M2K
      8100              UB=0.
      8500              C1(1)=0.
      8600              C1(N)=(P*DELT)/(2.*DELX)
      8700              A1(N)=0.
      8800              DO 100 I=2,N-1
      8900              U=1.
      9000              A1(I)=(-U*DELT)/(2.*DELX**2)
      9100              B1(I)=1.+(U*DELT)/(DELX**2)
      9125              CTWO=-UB*(XTOP+DEPTH)**2/(TC*XBOT*100.)
      9150              B1(1)=1.+(U*DELT)/(2.*DELX)-CONF*DELT/2.
      9175              B1(N)=1.-(P*DELT)/(2.*DELX)-CTWO*DELT/2.
      9200              C1(I)=A1(I)
      9300          100 CONTINUE
      9400              TIME=0.
      9500              T=0.
      9600        C     TIME LOOP:
      9650              ITAU=0
      9700              DO 200 J=1,ITMAX
      9800              T=T+DELT
      9850              ITAU=ITAU+1
      9900              TIME=TIME+DELT
     10000              IF(TIME.LT.TLIGHT)GO TO 101
     10100              IF(TIME.GE.(TLIGHT+TDARK))TIME=0.
     10225              UB=1.125
     10237              HI=0.
     10243              IF(TIME.EQ.0.)HI=HINF
     10250              TAMB=TDARK
     10251        C     PHIAMB IS THE AMBIENT TEMPERATURE
     10252              PHIAMB=TAMB/TZERO
     10300        C     CALCULATE DI
     10400        C     CALCULATE H,F,AND G
     10500              HIP=.6*FRAC*HI
     10600          101  H=HR*(DEPTH+XTOP)**2*PHIAMB/(TC*XTOP*100.)+(DEPTH+XTOP)**
     10700             A 2*HI/(TC*TZERO*XTOP*100.)
     10800             G +HIP*(1.-.6*EXP(-UMU*((DEPTH+XBOT-6.)/100.)))*(DEPTH+XTOP
     10900             I )**2/(TC*T
     11000             H ZERO*XTOP*100.)
     11100              DO 800 IK=1,N
     11200              DI(IK)=HI*EXP(-UMU*(FLOAT(IK-1)*(DEPTH+XTOP))/100.)
     11300             M +HIP*.6*EXP(-UMU*((1-FLOAT(IK-1))*(DEPTH+XTOP)+XBOT-6.)/
     11400             N 100.)
     11500              F(IK)=(DEPTH+XTOP)**2*DI(IK)*UMU*DELX/(TC*TZERO*100**2)
     11600        C     WRITE(70,26)F(IK)
     11700          800 CONTINUE
     11800           26 FORMAT(1X,'F=',F10.5)
     11900        C     PHIG IS THE TEMPERATURE OF THE GROUND
     12000              PHIG=15./TZERO
     12100              G=UB*(DEPTH+XTOP)**2*PHIG/(TC*XBOT*100.)+(DEPTH+XTOP)**
     12200             B 2*HI*(1.-EXP(-UMU*(DEPTH+XTOP)/100.))/(TC*TZERO*XBOT*100.)
     12300             K +(DEPTH+XTOP)**2*.6*PHIAMB*HIP*EXP(-UMU*(XBOT-6.)/100.)/(
     12400             L TC*TZERO*XBOT*100.)
     12500              D(1)=(U*DELT*PHI(2))/(2.*DELX)+(1.-(U*DELT)/(2.*DELX)*PHI(
     12600             A 1))+(DELT/2.)*(H+H)+CONF*PHI(1)*DELT/2.
     12700        C     WRITE(70,27)D(1)
     12800           27 FORMAT(1X,'D1=',F10.5)
     12900              D(N)=((P*DELT)/(2.*DELX)+1.)*PHI(N)-((P*DELT)/(2.*DELX))*P
     13000             B HI(N-1)+(DELT/2.)*(G+G)+CTWO*PHI(N)*DELT/2.
     13100        C     WRITE(70,28)D(N)
     13200           28 FORMAT(1X,'DN=',F10.5)
     13300              DO 300 I=2,N-1
     13400              D(I)=(U*DELT*PHI(I+1))/(2.*DELX**2)+(1.-(U*DELT)/(DELX
     13500             D **2))*PHI(I)+((U*DELT)/(2.*(DELX**2)))*PHI(I-1)+(DELT/2.
     13600             E )*(F(I)+F(I))
     13700        C     WRITE(70,29)D(I)
     13800           29 FORMAT(1X,'D=',F10.5)
     13900          300 CONTINUE
     14000        C     CALCULATE SOLUTION AT TIME T
     14100              DO 301 JJ=1,N
     14200              A(JJ)=A1(JJ)
     14300              B(JJ)=B1(JJ)
     14400              C(JJ)=C1(JJ)
     14500          301 CONTINUE
     14600              CALL TRID(A,B,C,D,N,PHI)
     14700              DO 2002 I=1,N
     14800              TEMP(I)=PHI(I)*TZERO
     14900         2002 CONTINUE
     14950        C           IF(ITAU.NE.4)GO TO 55
     15000        C     PRINT NEW SOLUTION
     15100              WRITE(50,19)T
     15200           19 FORMAT(1X,'T=',F10.5)
     15300              WRITE(50,20)
     15400           20 FORMAT(1X,8X,'X',12X,'SOLUTION',8X,'TEMPERATURE')
     15500              DO 500 K=1,N
     15600              WRITE(50,21)X(K),PHI(K),TEMP(K)
     15700          500 CONTINUE
```

```
 15750                 ITAU=0
 15775       C 55      CONTINUE
 15800         200     CONTINUE
 15900          21     FORMAT(2X,F10.5,8X,F10.5,8X,F10.5)
 16000                 STOP
 16100                 END
```

(d)

```
TRID.FOR;2                          2-AUG-1982 13:08:39.17          PAGE 1

  100                 SUBROUTINE TRID(A,B,C,D,J,PHI)
  600     C
 3100     C
 3150                 DIMENSION A(1),B(1),C(1),D(1),PHI(1)
 3200     C           SOLVE FOR THE SOLUTION VECTOR BY DOUBLE SWEEP ALGORITHM
 3300     C           FIRST SWEEP - ELIMINATE LOWER DIAGONAL
 3400                 DO 1 I=2,J
 3500                 B(I)=B(I)-C(I)*A(I-1)/B(I-1)
 3600                 D(I)=D(I)-C(I)*D(I-1)/B(I-1)
 3700                 C(I)=0.
 3800       1         CONTINUE
 3900     C           SECOND SWEEP - DETERMINE SOLUTION VECTOR
 4000                 PHI(N)=D(N)/B(N)
 4100                 DO 2 I=1,N-1
 4200                 J=N-I
 4300       2         PHI(J)=(D(J)-A(J)*PHI(J+1))/B(J)
 4400     C           SOLUTION COMPLETE
 4500                 RETURN
 4600                 END
```

(e)

```
      PROGRAM BROWN
      LOGICAL*1 YES
      DIMENSION IVEC(1),JVEC(4),T(17),X(17),TN(15)
      DATA X /3.,6.,9.,11.5,13.,14.5,16.,18.,21.,24.,27.,30.,
     1       33.,36.,39.,42.,45./
C
      TYPE 1000
1000  FORMAT(' CALCULATIONS WITH OUTPUT LIST [1]'/
     .       ' PLOTTER [2] '/)
      ACCEPT 1010,IOPT
1010  FORMAT(I5)
      IF(IOPT.EQ.1) CALL ASSIGN (2,'BROWN.OUT')
      IF(IOPT.EQ.1) GO TO 5
      TYPE 1012
1012  FORMAT(' TOTAL NUMBER OF DATA POINTS ->  '$)
      ACCEPT 1010,NPTOT
      MODE=0
      TYPE 777
777   FORMAT('DO YOU WANT STARS?[Y/N]')
      IF(YES())MODE=7
5     IDEB=0
      IPLOT=0
      NIMA=0
      IF(IOPT.EQ.1) GO TO 6
      TYPE 1011
1011  FORMAT(' NUMBER OF POINTS TO SKIP -> '$)
      ACCEPT 1010,NSKIP
      IF(NSKIP.EQ.0) NSKIP=1
      NCURVE=NPTOT/NSKIP
      NPLOT=0
6     II=1
10    DO 25 I=II,4
      CALL GETVAL (0,IVEC,ISTAT)
      IF(ISTAT.LT.0) GO TO 999
      IF(IDEB.NE.0) GO TO 21
      TYPE 15
15    FORMAT(/' T-REFERENCE ->  '$)
      IDEB=1
      ACCEPT 20,TREF
20    FORMAT(F10.0)
21    JVEC(I)=IVEC(1)
25    CONTINUE
C
      IF(IOPT.EQ.1) TYPE 9000,JVEC
9000  FORMAT(1X,4I10)
C
C     AVE=(JVEC(1)+JVEC(2)+JVEC(3)+JVEC(4))/4
C
      DO 30 I=1,17
      CALL GETVAL (0,IVEC,ISTAT)
      T(I)=TREF+
     1 (-8.03+SQRT(64.48+0.02564*(FLOAT(IVEC(1)))))/0.01282
30    CONTINUE
C
      IPLOT=IPLOT+1
      IF(IOPT.EQ.2) GO TO 2000
      IF(NIMA.NE.0) GO TO 2001
      NIMA=1
      XMIN=T(1)
      XMAX=XMIN
2001  DO 2002 I=1,17
      IF(I.EQ.14.OR.I.EQ.16) GO TO 2002
      XMIN=AMIN1(XMIN,T(I))
```

```
      XMAX=AMAX1(XMAX,T(I))
2002  CONTINUE
      WRITE (2,35) T
35    FORMAT(1X,10F8.1)
      WRITE (2,40)
40    FORMAT(1H )
C
2000  CONTINUE
      IF(IOPT.EQ.1) GO TO 3000
      IF(NSKIP.EQ.1) GO TO 2003
      IF(MOD(IPLOT,NSKIP).NE.1) GO TO 3000
2003  IT=0
      DO 2010 I=1,17
      IF(I.EQ.14.OR.I.EQ.16) GO TO 2010
      IT=IT+1
      TN(IT)=T(I)
2010  CONTINUE
      CALL LILI (15,TN,X,1,MODE,NCURVE,3,1,1)
C     IPLOT=0
      NPLOT=NPLOT+1
C
3000  DO 50 I=1,27
      CALL GETVAL (0,IVEC,ISTAT)
      IF(IOPT.EQ.1) GO TO 3001
      IF(NPLOT.EQ.NCURVE) GO TO 52
3001  IF(ISTAT.LT.0) GO TO 999
50    CONTINUE
51    CALL GETVAL (0,IVEC,ISTAT)
      IF(ISTAT.LT.0) GO TO 999
      IF(IABS(IVEC(1)).GT.1000) GO TO 51
      JVEC(1)=IVEC(1)
      II=2
      GO TO 10
C
52    IF(ISTAT.LT.0) GO TO 999
      CALL GETVAL (0,IVEC,ISTAT)
      GO TO 52
999   IDEB=0
      TYPE 55
55    FORMAT(' NEXT RUN [Y/N]  :  '$)
      IF(YES()) GO TO 5
      IF(IOPT.NE.1) GO TO 9999
      WRITE(2,35) XMIN,XMAX
      CLOSE (UNIT=2,DISP='PRINT')
9999  STOP
      END
```

(f)

```
      PROGRAM BROWN2
      LOGICAL*1 YES
      DIMENSION IVEC(1),JVEC(4),T(17),X(1000),TN(1000)
C
      TYPE 1012
1012  FORMAT(' TOTAL NUMBER OF DATA POINTS ->  '$)
      ACCEPT 202 NPTOT
C     IDEB=1
      IT=0
      ACCUNT=0
      DO 7 I=1,1000
C     X(I)= 23333+FLOAT(I-1)
C     II=1
10    DO 25 I=II,4
      CALL GETVAL (0,IVEC,ISTAT)
      IF(ISTAT.LT.0) GO TO 999
      IF(IDEB.NE.0) GO TO 21
      TYPE 15
15    FORMAT(/,' T-REFERENCE ->  '$)
      IDEB=1
      ACCEPT 20,TREF
20    FORMAT(F10.0)
      TYPE 201
201   FORMAT(' PROBE NUMBER ,ENTER 100 FOR AVERAGE,->  '$)
      ACCEPT 202,NPROBE
202   FORMAT(I3)
21    JVEC(I)=IVEC(1)
25    CONTINUE
C
      AVE=(JVEC(1)+JVEC(2)+JVEC(3)+JVEC(4))/4
C
      DO 30 I=1,17
      CALL GETVAL (0,IVEC,ISTAT)
      T(I)=TREF+
     1  (-8.03+SQRT(64.48+0.02564*(FLOAT(IVEC(1))-AVE))/0.01282
30    CONTINUE
C
      IT=IT+1
      IF(NPROBE.EQ.100)GO TO 500
      TN(IT)=T(NPROBE)
      GO TO 3000
500   SUM=0
      DO 70 J=1,17
      SUM=SUM+T(J)
70    CONTINUE
      SUM = SUM-T(14)-T(16)
      TN(IT)=SUM/15
C
3000  DO 50 I=1,27
      CALL GETVAL (0,IVEC,ISTAT)
3001  IF(ISTAT.LT.0) GO TO 999
50    CONTINUE
51    CALL GETVAL (0,IVEC,ISTAT)
      IF(ISTAT.LT.0) GO TO 999
      IF(IABS(IVEC(1)).GT.1000) GO TO 51
      JVEC(1)=IVEC(1)
      II=2
      GO TO 10
C
32    IF(ISTAT.LT.0) GO TO 999
      CALL GETVAL (0,IVEC,ISTAT)
      GO TO 32
999   IDEB=1
```

```
      CALL LILI (NPTOT,X,TN,1,0,NCURVE,3,1,1)
      TYPE 55
55    FORMAT(' NEXT RUN [Y/N]  :  '$)
      IF(YES()) GO TO 5
9999  STOP
      END
```

APPENDIX 2 - APPARATUS INFORMATION

Insulation

PITTSBURGH CORNING EUROPE S.A.

FOAMGLAS®

PROPRIETES PHYSIQUES

Deux types :

1 - FOAMGLAS® T2 principalement destiné aux applications pour lesquelles la conductivité thermique représente le facteur prédominant.

2 - FOAMGLAS® S3, appliqué plus particulièrement lorsque les exigences en matière de résistance à la compression sont sévères.

Deux isolants FOAMGLAS® pourront donc être spécifiés pour les applications dans les domaines du bâtiment, de l'industrie et du froid.

COMPOSITION :	Verre cellulaire alumino-silicaté d'une composition spécialement étudiée, totalement inorganique, sans addition de liants
TEMPERATURE D'EMPLOI :	– 260 à + 430°C
POINT DE RAMOLLISSEMENT :	Point de ramollissement du verre : environ 730°C
ABSORPTION D'EAU : (à l'immersion)	Nulle à l'exception de la rétention momentanée de surface
HYGROSCOPICITE :	Nulle
PERMEABILITE A LA VAPEUR D'EAU :	Nulle, selon norme AFNOR-NFX 41.001 (Essai du C.S.T.B. - Paris)
FACTEUR DE RESISTANCE A LA DIFFUSION DE VAPEUR D'EAU :	$\mu : \infty$, Forschungsinstitut für Wärmeschutz, Allemagne (Dr. Cammerer)
CAPILLARITE :	Nulle
RESISTANCE AUX ACIDES :	Résiste à tous les acides communément employés ainsi qu'à leurs vapeurs
INCOMBUSTIBILITE :	Classé M.O.
STABILITE DIMENSIONNELLE :	Parfaite
ISOLEMENT ACOUSTIQUE BRUT AUX FREQUENCES AUDIBLES :	28 dB pour une épaisseur de 10 cm

FOAMGLAS® T2 FOAMGLAS® S3

	FOAMGLAS® T2		FOAMGLAS® S3	
Dimensions en mm. Longueur / Largeur	300 / 450		300 / 450	
	600 / 450		600 / 450	
Epaisseur	40, 45, 50, 60, 70, 80, 90, 100, 120, 130 50, 60, 70, 80, 90, 100, 120, 130		40, 50, 60, 100 50, 60, 100	
	marquage rouge		marquage bleu	
	M	**SI**	**M**	**SI**
MASSE VOLUMIQUE (tolérance ± 10%)	125 kg/m³	125 kg/m³	135 kg/m³	135 kg/m³
CONDUCTIVITE THERMIQUE (tolérance ± 5%)	à -20°C: 0,033 kcal/m.h.°C 0°C: 0,036 kcal/m.h.°C +20°C: 0,039 kcal/m.h.°C	à -20°C: 0,038 W/m K 0°C: 0,042 W/m K +20°C: 0,045 W/m K	à -20°C: 0,035 kcal/m.h.°C 0°C: 0,038 kcal/m.h.°C +20°C: 0,041 kcal/m.h.°C	à -20°C: 0,041 W/m K 0°C: 0,044 W/m K +20°C: 0,048 W/m K
*RESISTANCE A LA COMPRESSION (valeur moyenne)	5 kg/cm²	490 kPa	7 kg/cm²	680 kPa
RESISTANCE A LA FLEXION	4,5 kg/cm²	440 kPa	5,3 kg/cm²	520 kPa
MODULE D'ELASTICITE (A LA FLEXION)	10.000 kg/cm²	980 MPa	12.000 kg/cm²	1.180 MPa
COEFFICIENT DE DILATATION LINEAIRE	8,5 x 10^{-6}/°C	8,5 x 10^{-6}/K	8,5 x 10^{-6}/°C	8,5 x 10^{-6}/K
CHALEUR SPECIFIQUE	0,20 kcal/kg°C	0,84 kJ/kg K	0,20 kcal/kg°C	0,84 kJ/kg K
DIFFUSIVITE THERMIQUE A 0°C	4,0 x 10^{-3} cm²/sec.	4,0 x 10^{-7} m²/sec.	4,0 x 10^{-3} cm²/sec.	4,0 x 10^{-7} m²/sec.

Le coefficient de sécurité sera choisi par le bureau d'études en fonction de l'application. Une valeur de 3 est fréquemment adoptée. Sauf indications contraires, les propriétés du verre cellulaire FOAMGLAS® sont données à la température ambiante et correspondent aux méthodes d'essais ASTM N° C 303, C 240, C 165, C 177, C 203, C 355 et E 136.

Pour l'isolation des fonds de réservoirs, on se référera à la spécification i 22 - édition 1978.

FABRIQUÉ PAR

PITTSBURGH CORNING EUROPE S.A.

PITTSBURGH CORNING EUROPE S.A.
Avenue de Tervuren 36 - Boîte 19
B - 1040 BRUXELLES Belgique. Tél. (02) 735 90 36
Télex 22277 Picto B.

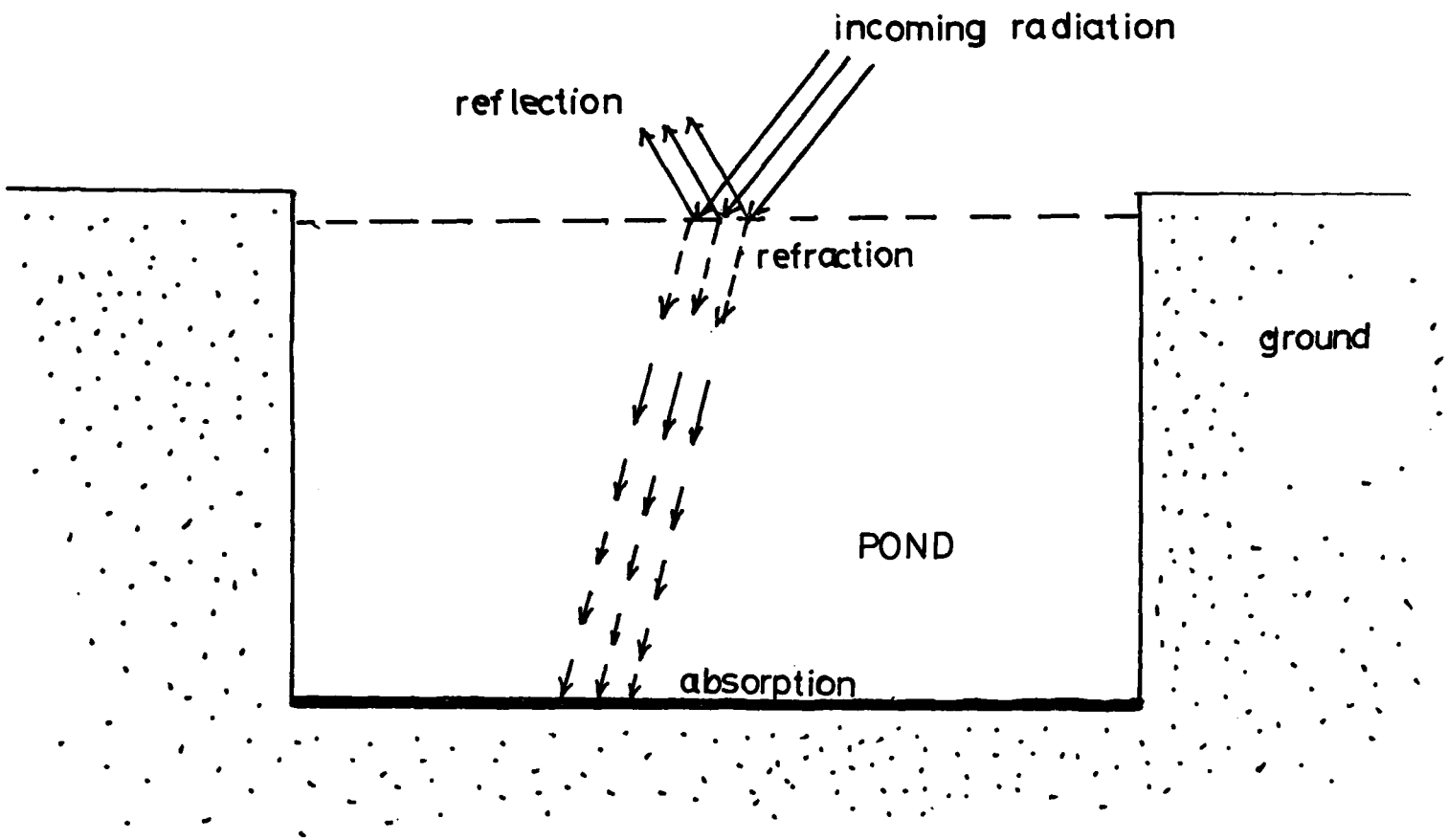

FIGURE 1
RADIATION PHENOMENA IN A SOLAR POND

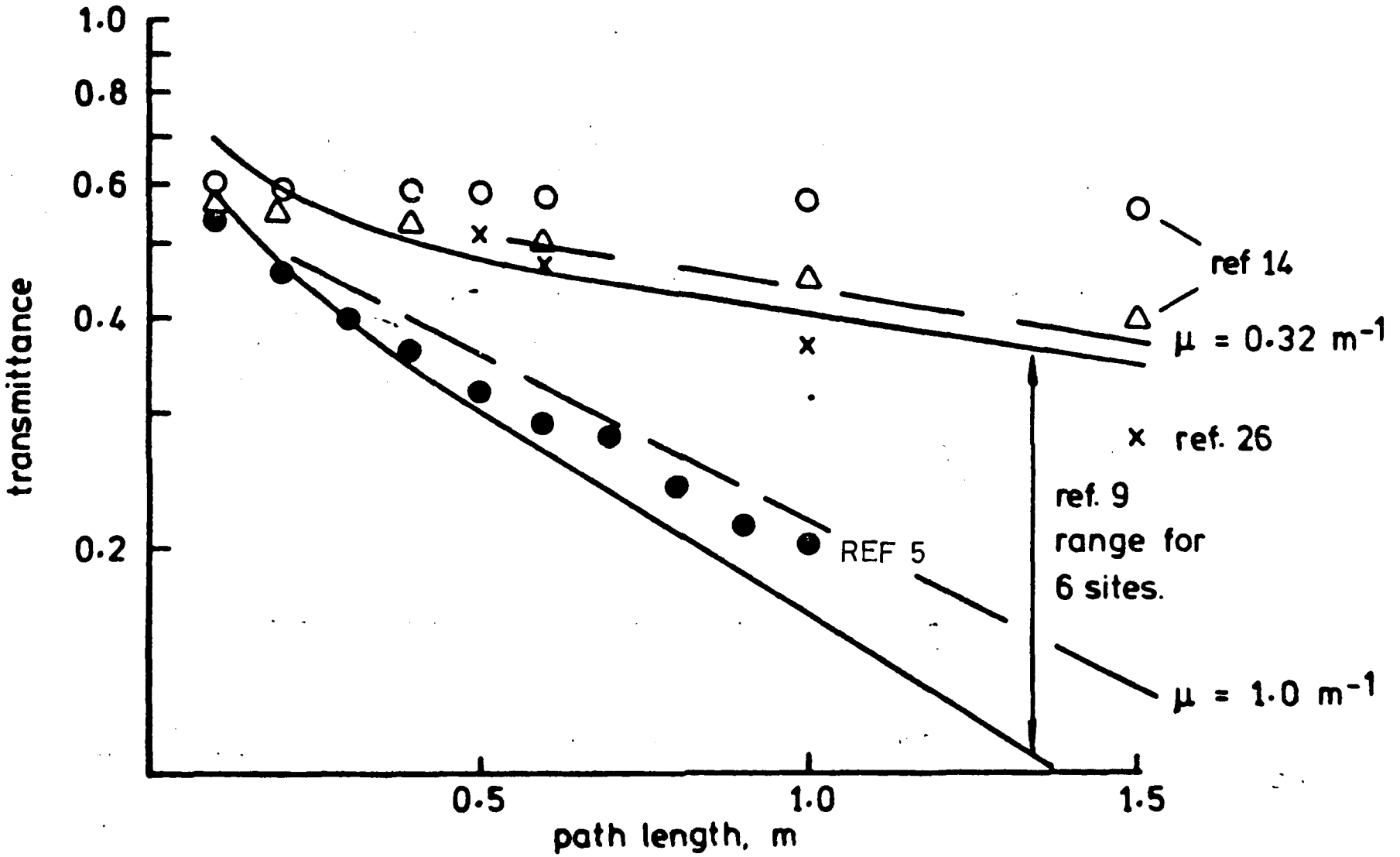

FIGURE 2
LIGHT ABSORPTION IN WATER

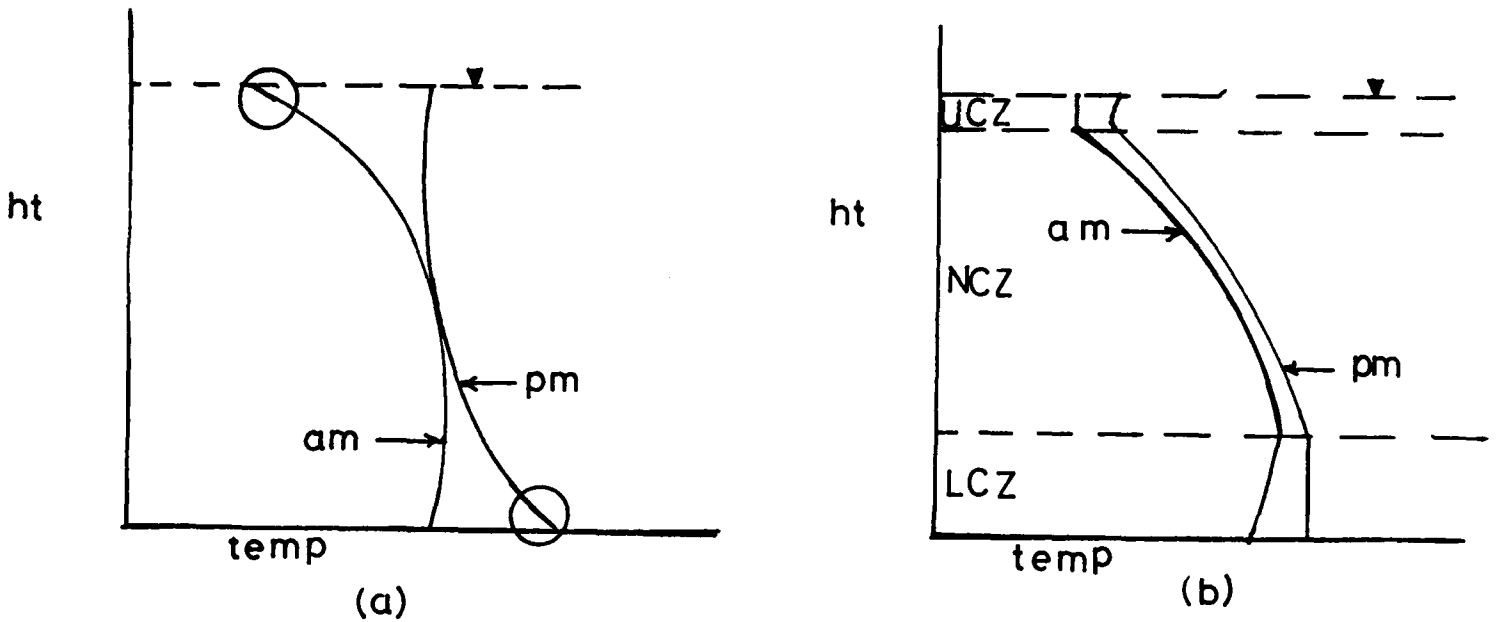

FIGURE 3
THE CONVECTIVE ZONES

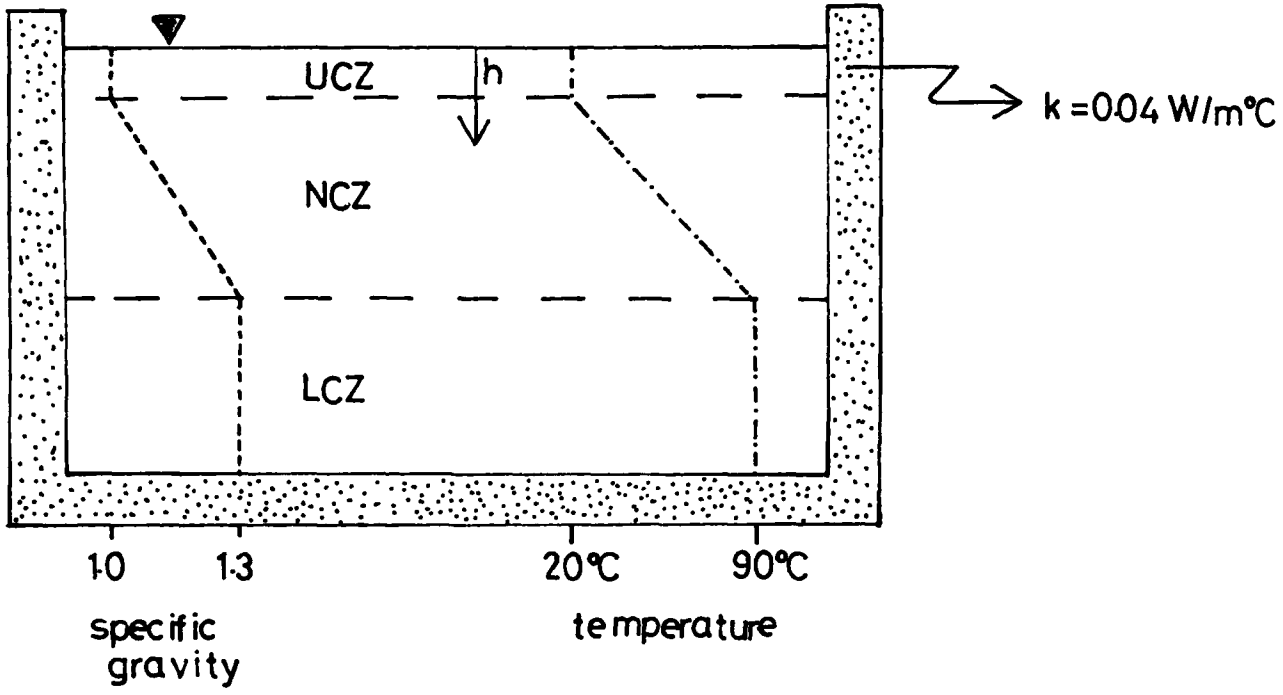

$$\frac{\partial \rho}{\partial h} = \left(\frac{\partial \rho}{\partial T}\right)_q \frac{\partial T}{\partial h} + \left(\frac{\partial \rho}{\partial q}\right)_T \frac{\partial q}{\partial h} > 0$$

THE GRADIENTS

FIGURE 4

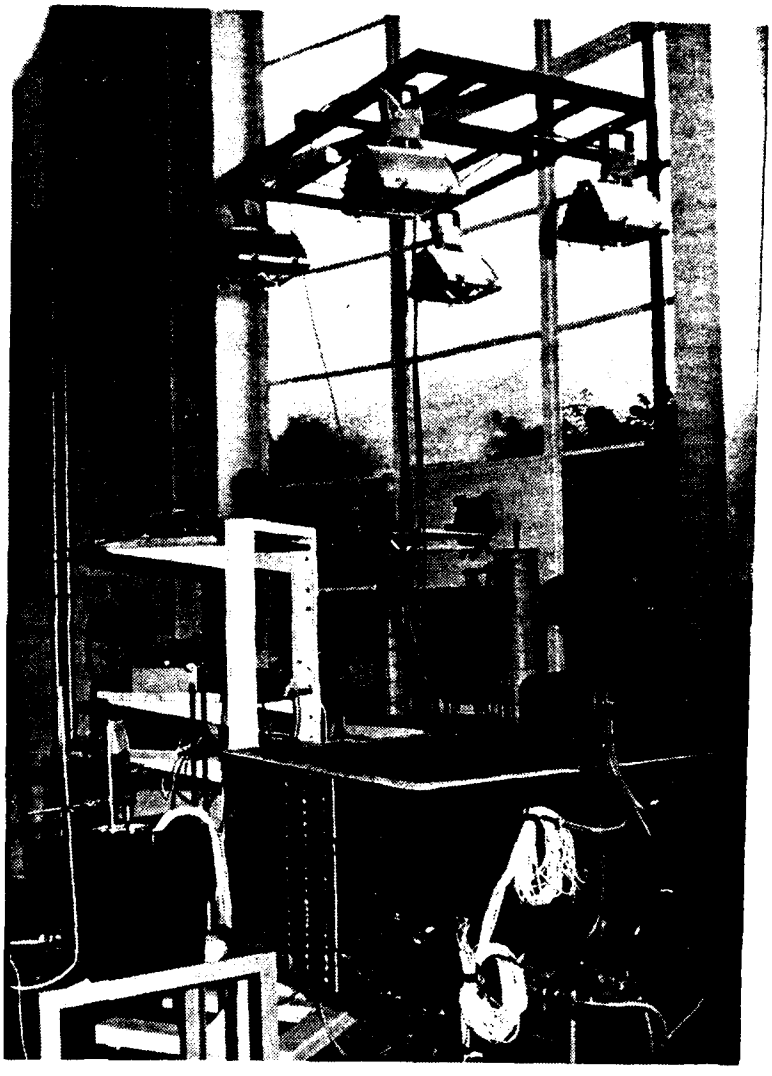

FIGURE 5 - POND STRUCTURE

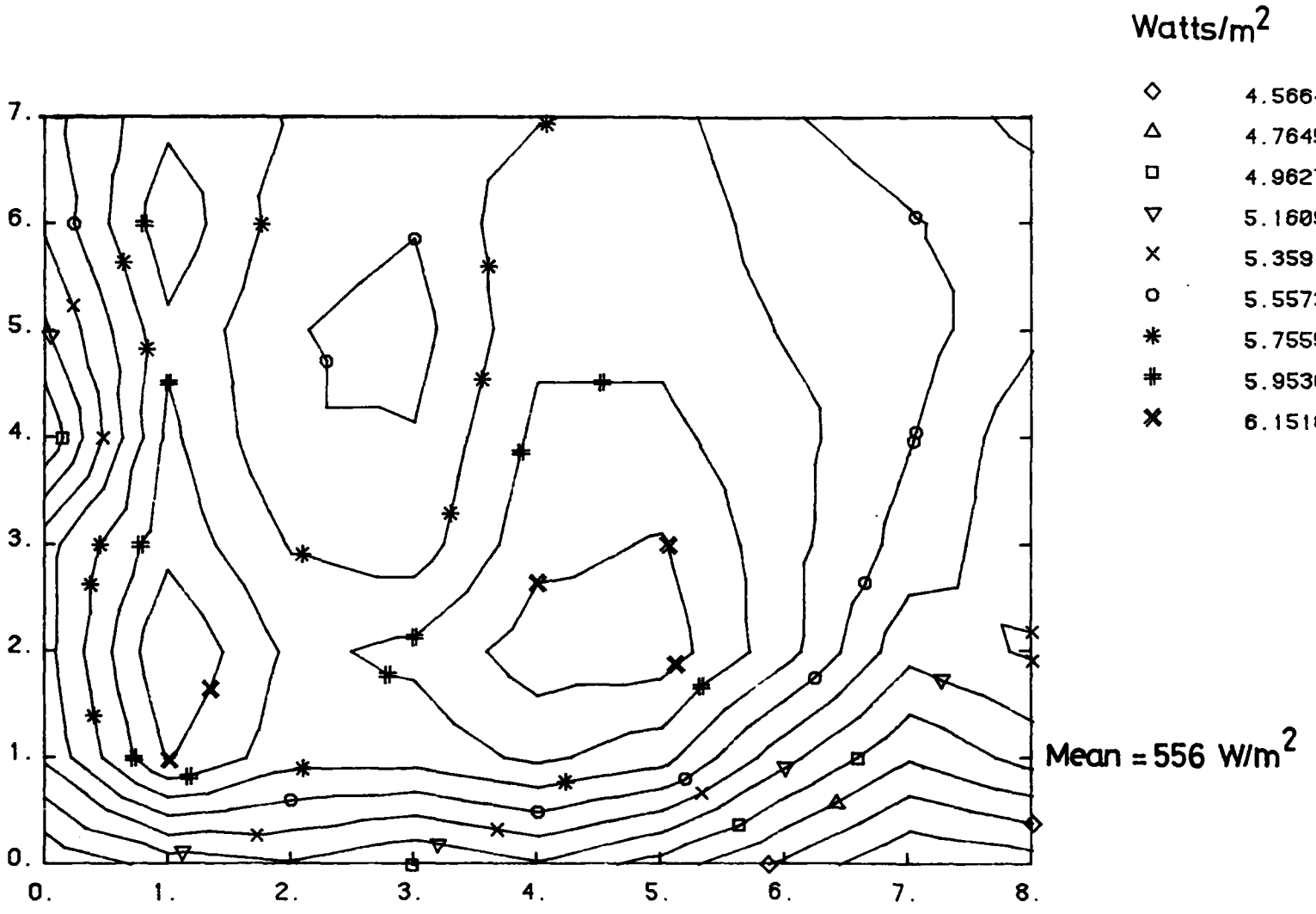

FIGURE 6 : RADIATION FIELD ISOLINES

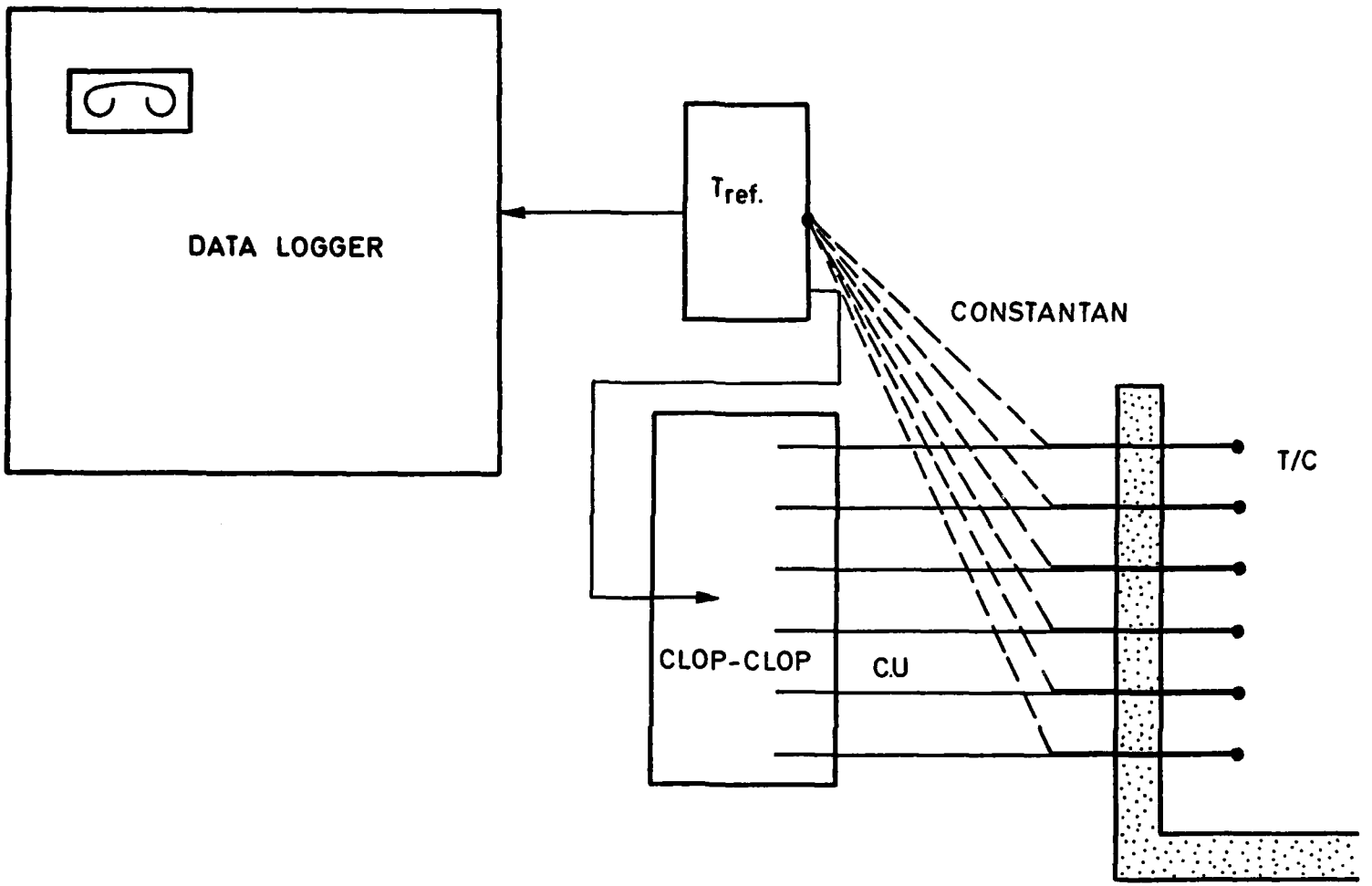

TEMPERATURE MEASUREMENT CHAIN
FIGURE 7

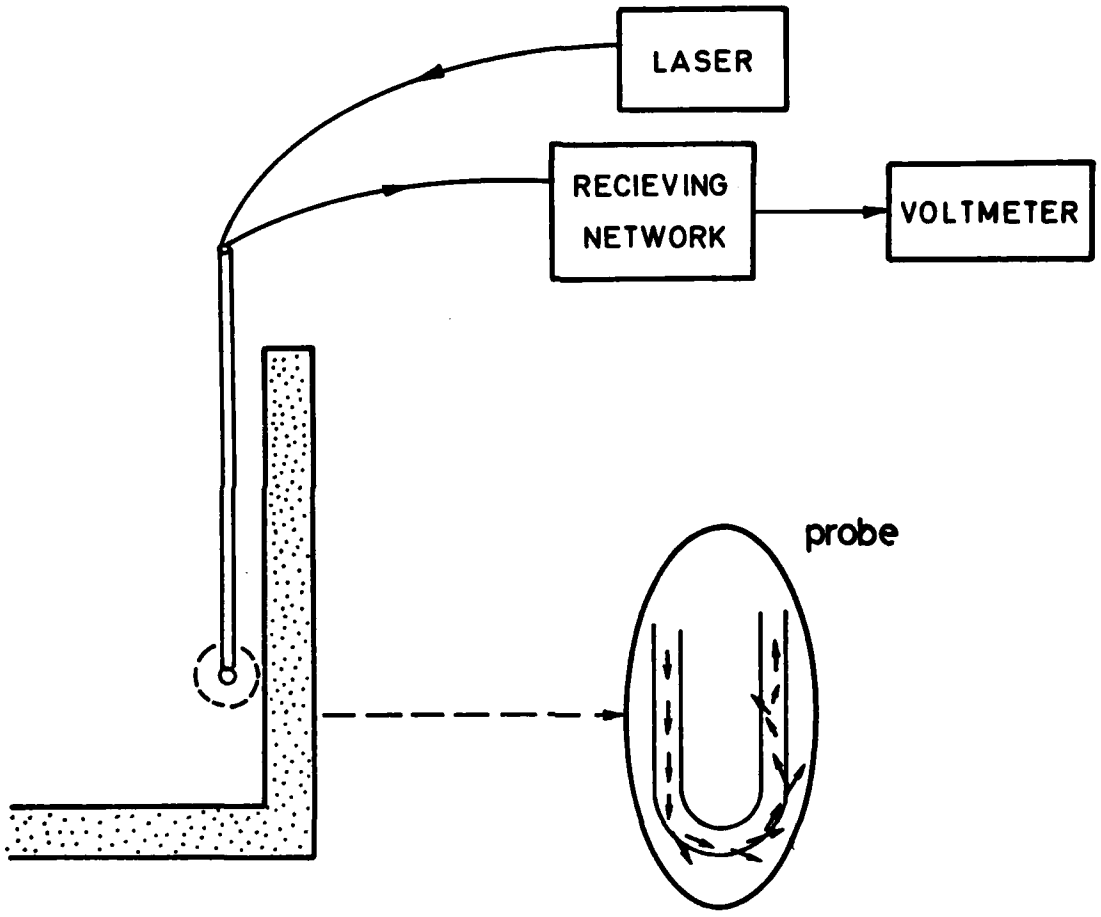

CONCENTRATION MEASUREMENT CHAIN

FIGURE 8

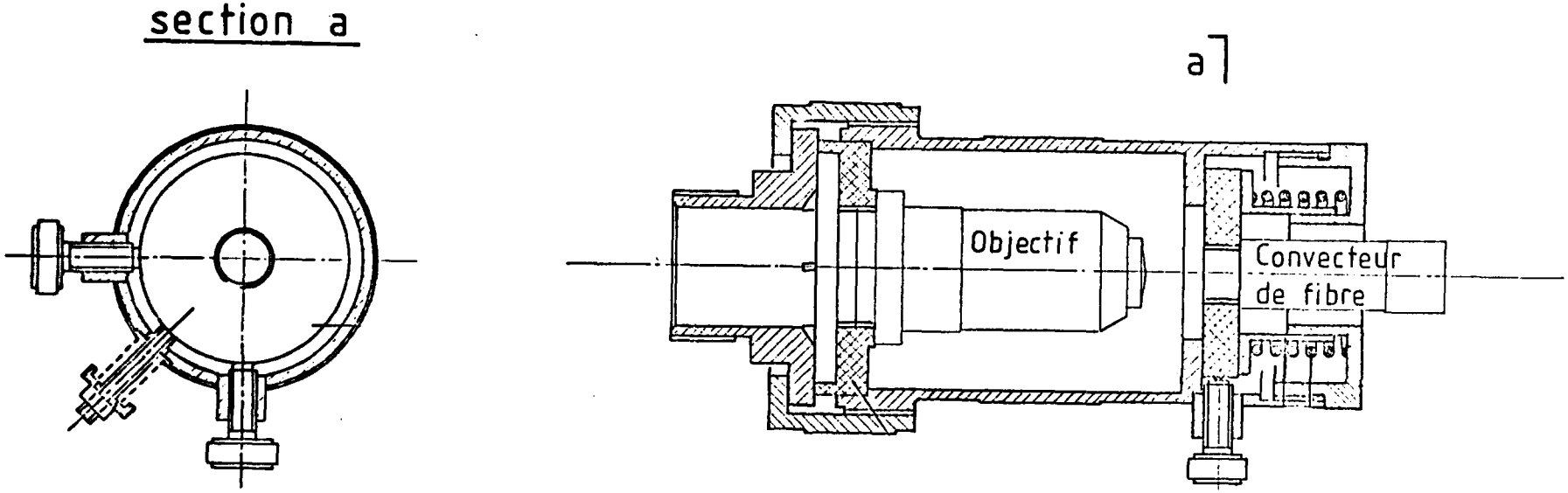

THE FOCUSING DEVICE

FIGURE 9

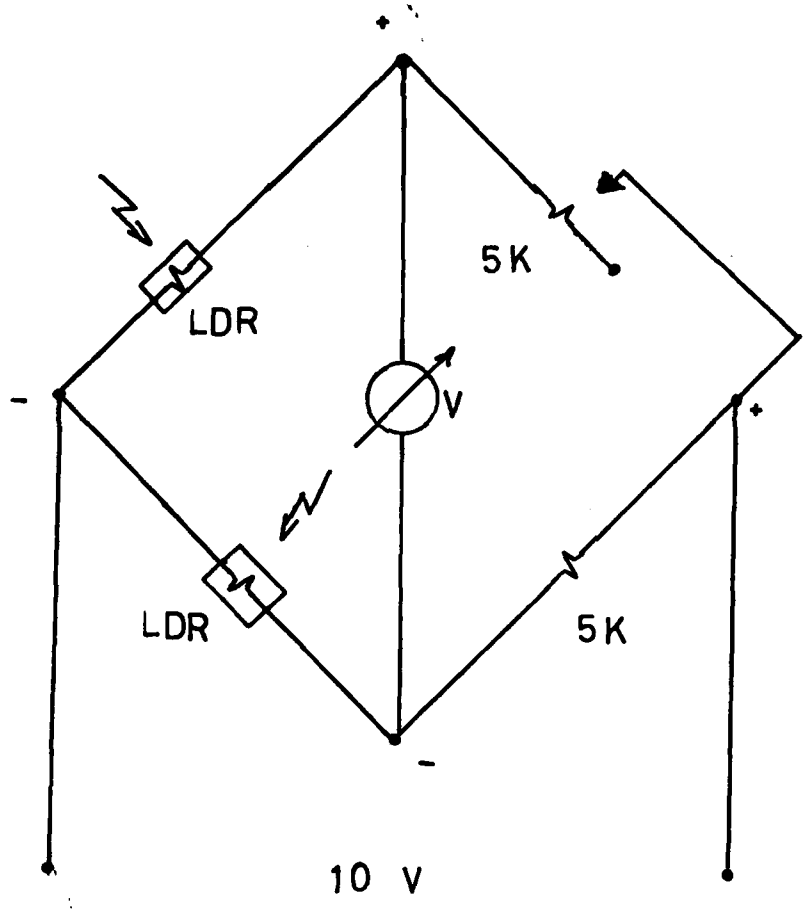

FIGURE 10

RECEIVING NETWORK

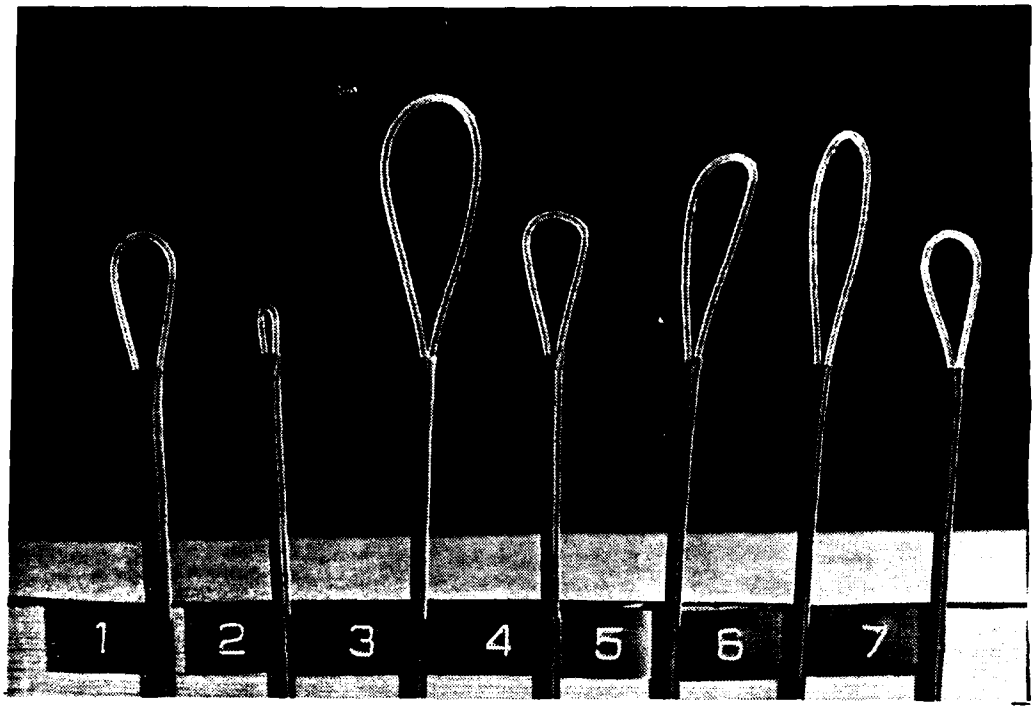

FIGURE 11 - PROBE TIPS

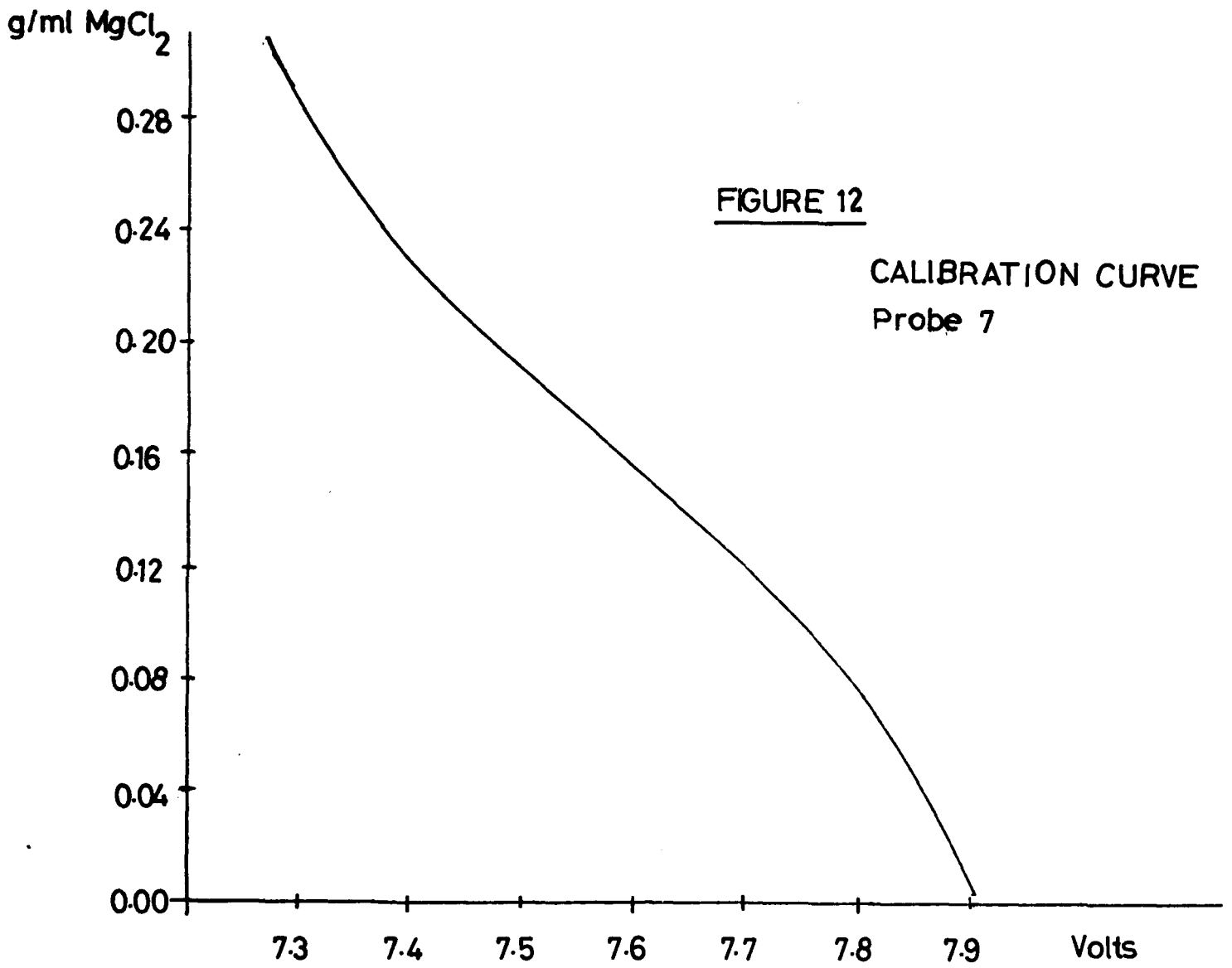

FIGURE 12

CALIBRATION CURVE
Probe 7

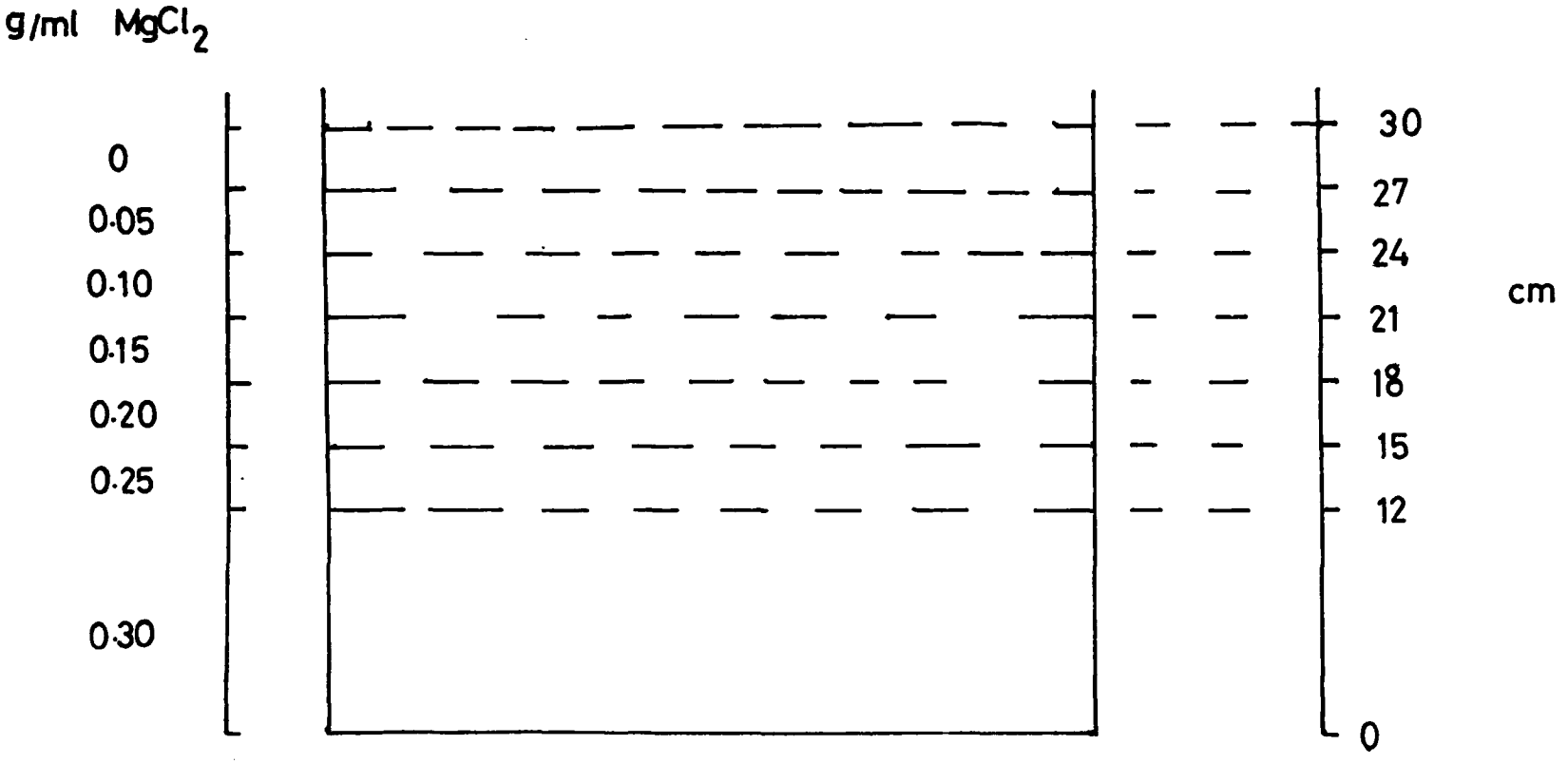

FIGURE 13

POND FILLING

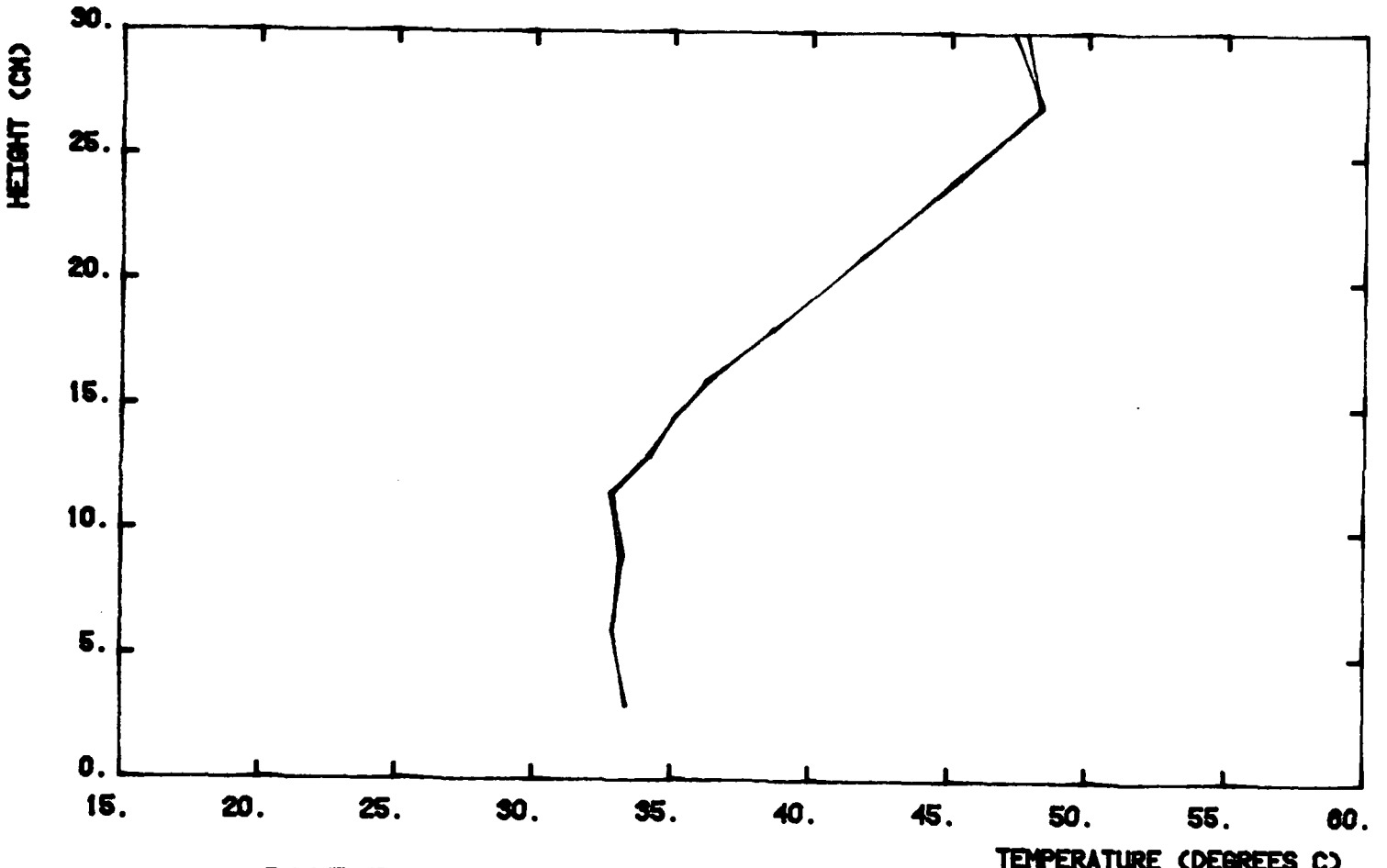

RADIATION EFFECT ON TEMPERATURE MEASUREMENTS

FIGURE 14

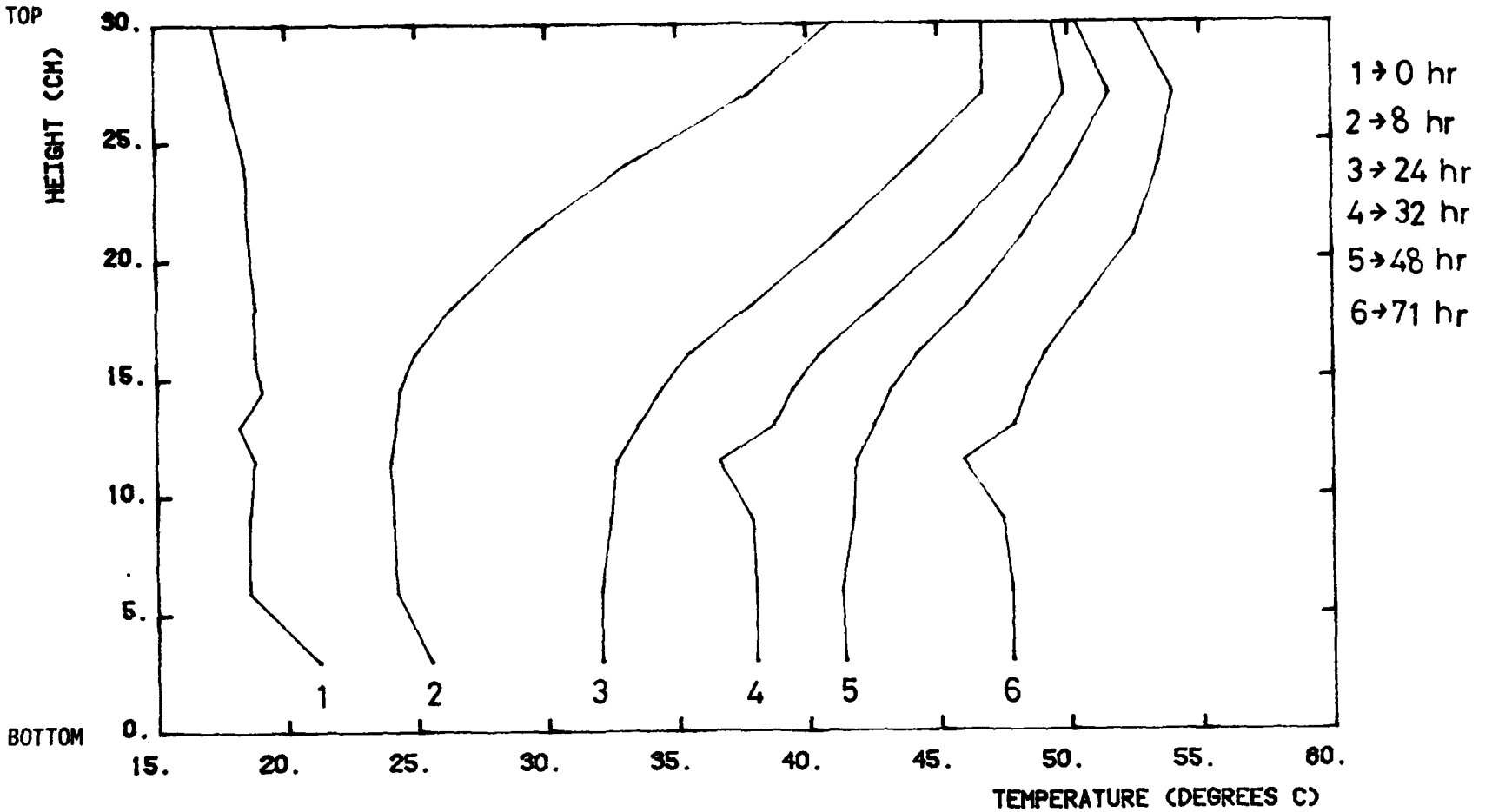

HEATING
EXPERIMENTAL DATA
FIGURE 15

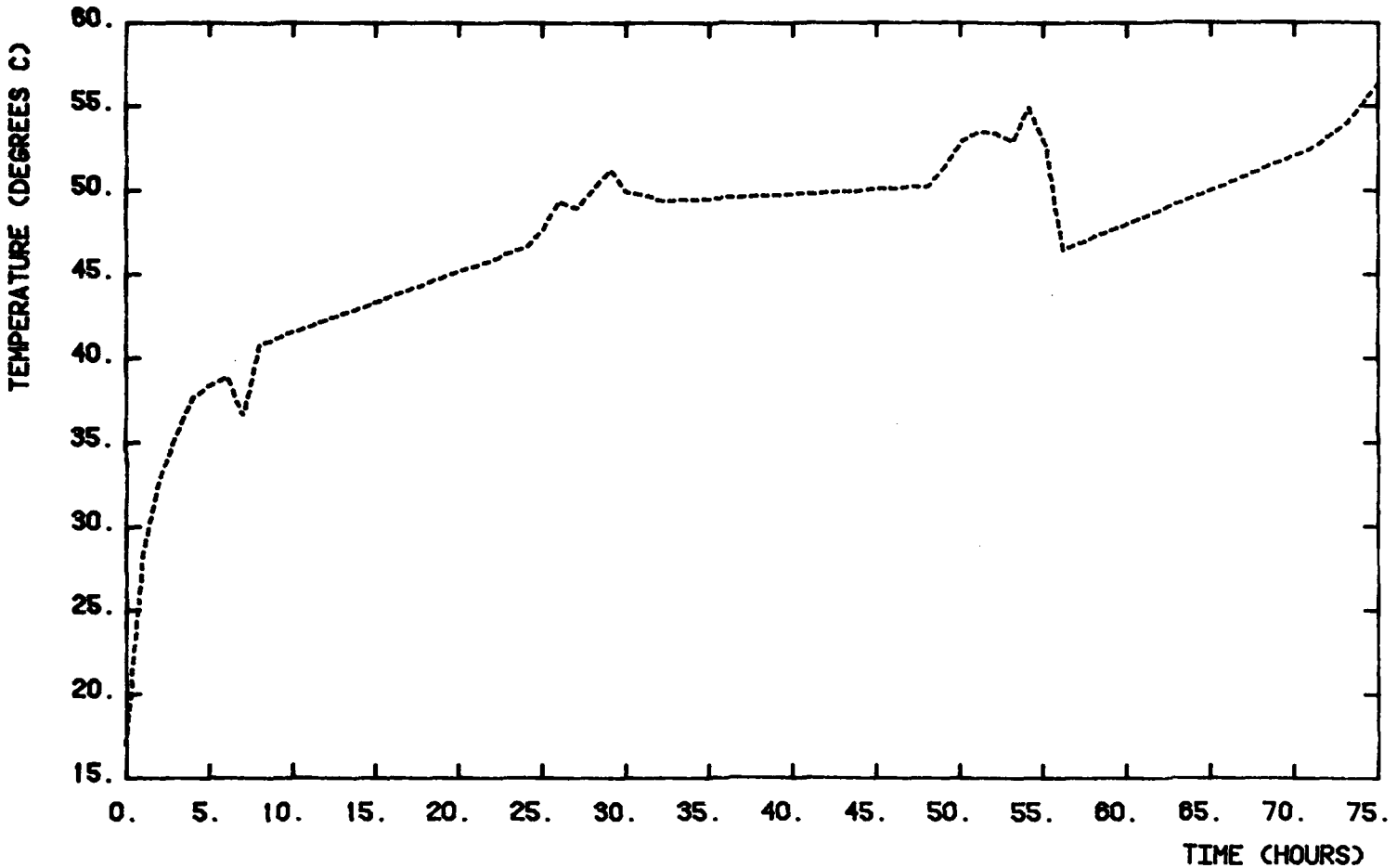

EXPERIMENTAL DATA - HEATING - HT.=30.CM

FIGURE 16a

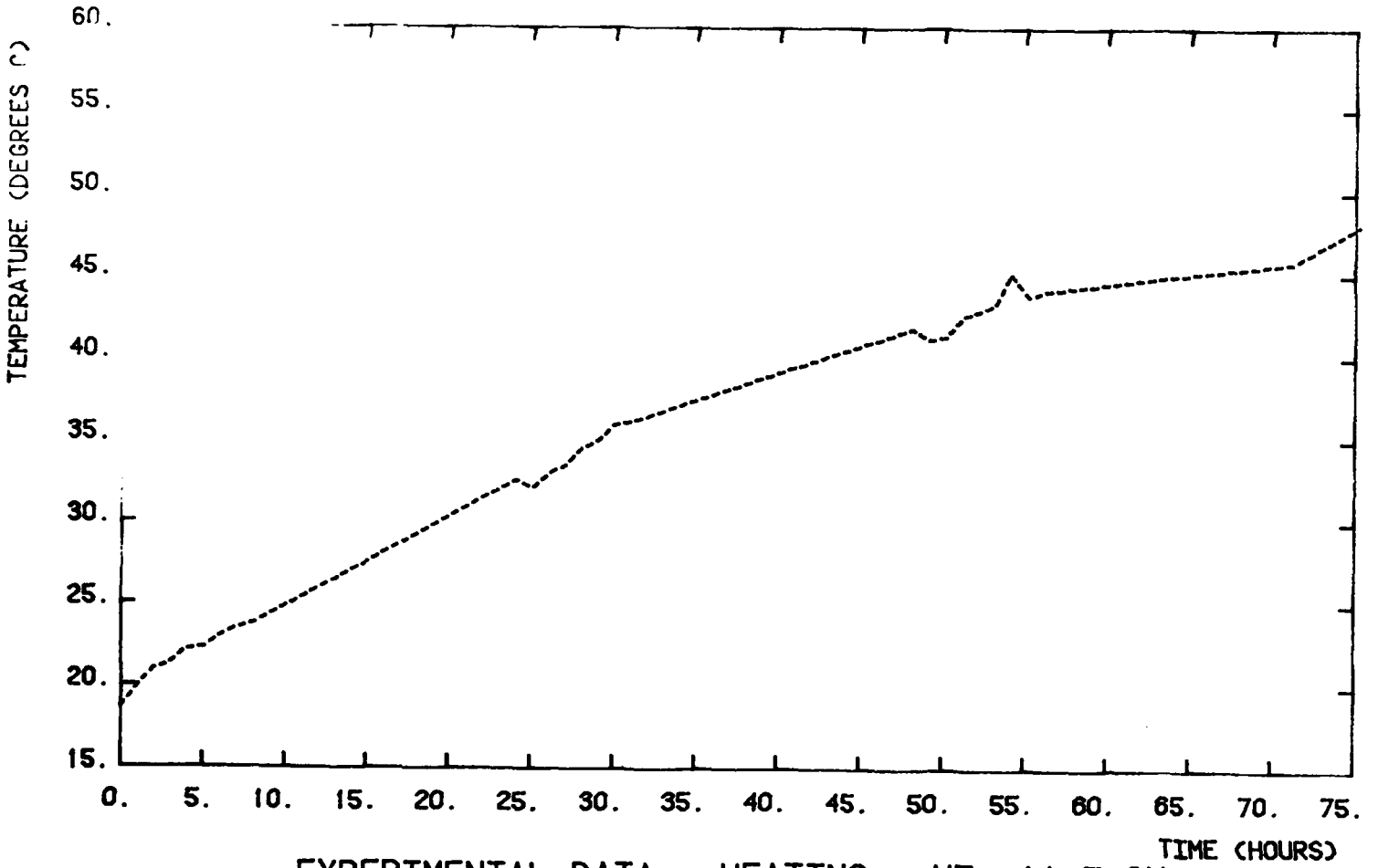

EXPERIMENTAL DATA - HEATING - HT.=11.5 CM

FIGURE 16b

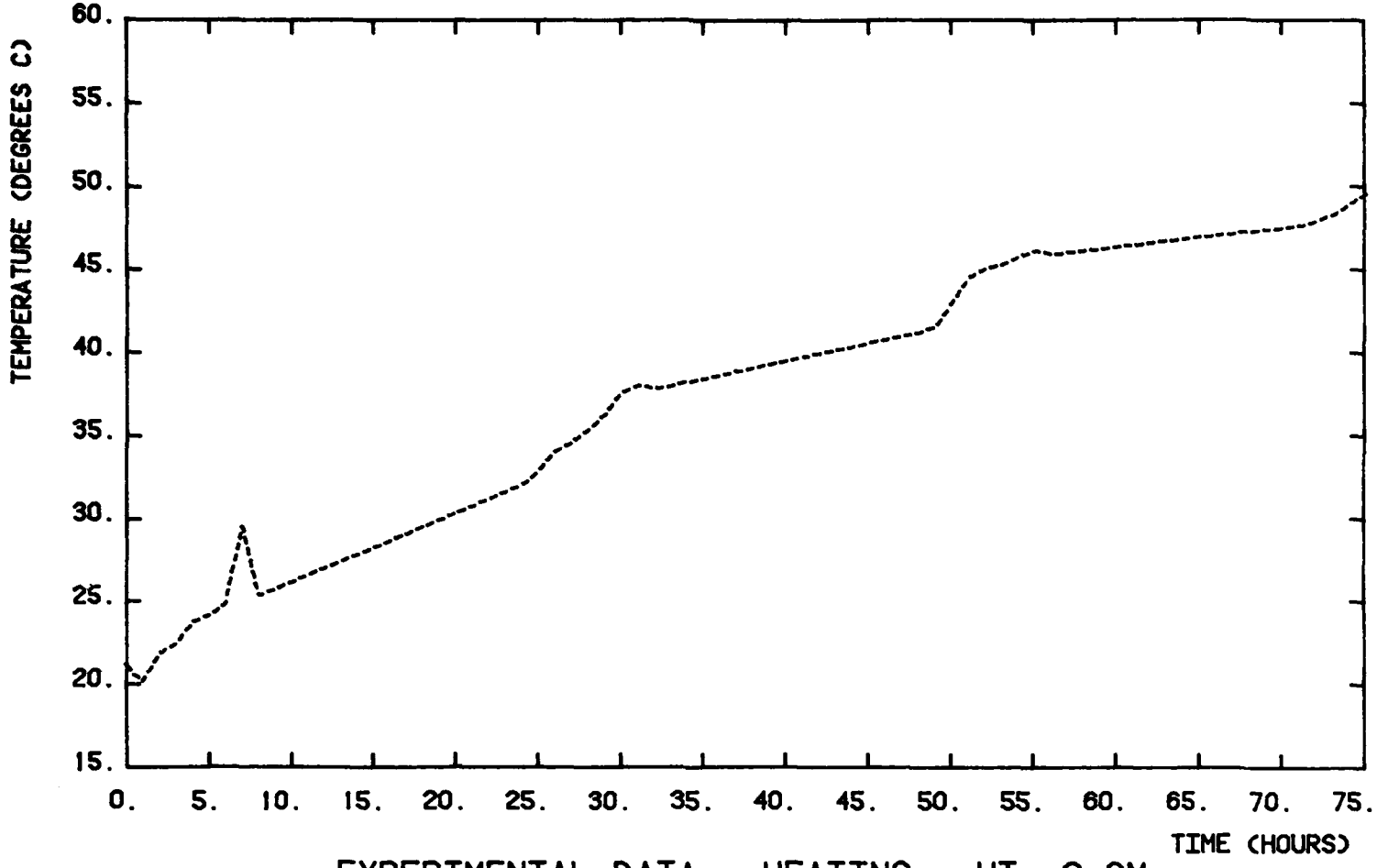

EXPERIMENTAL DATA - HEATING - HT.=3.CM

FIGURE 16c

FIGURE 17

AVERAGE TEMPERATURE DURING HEATING

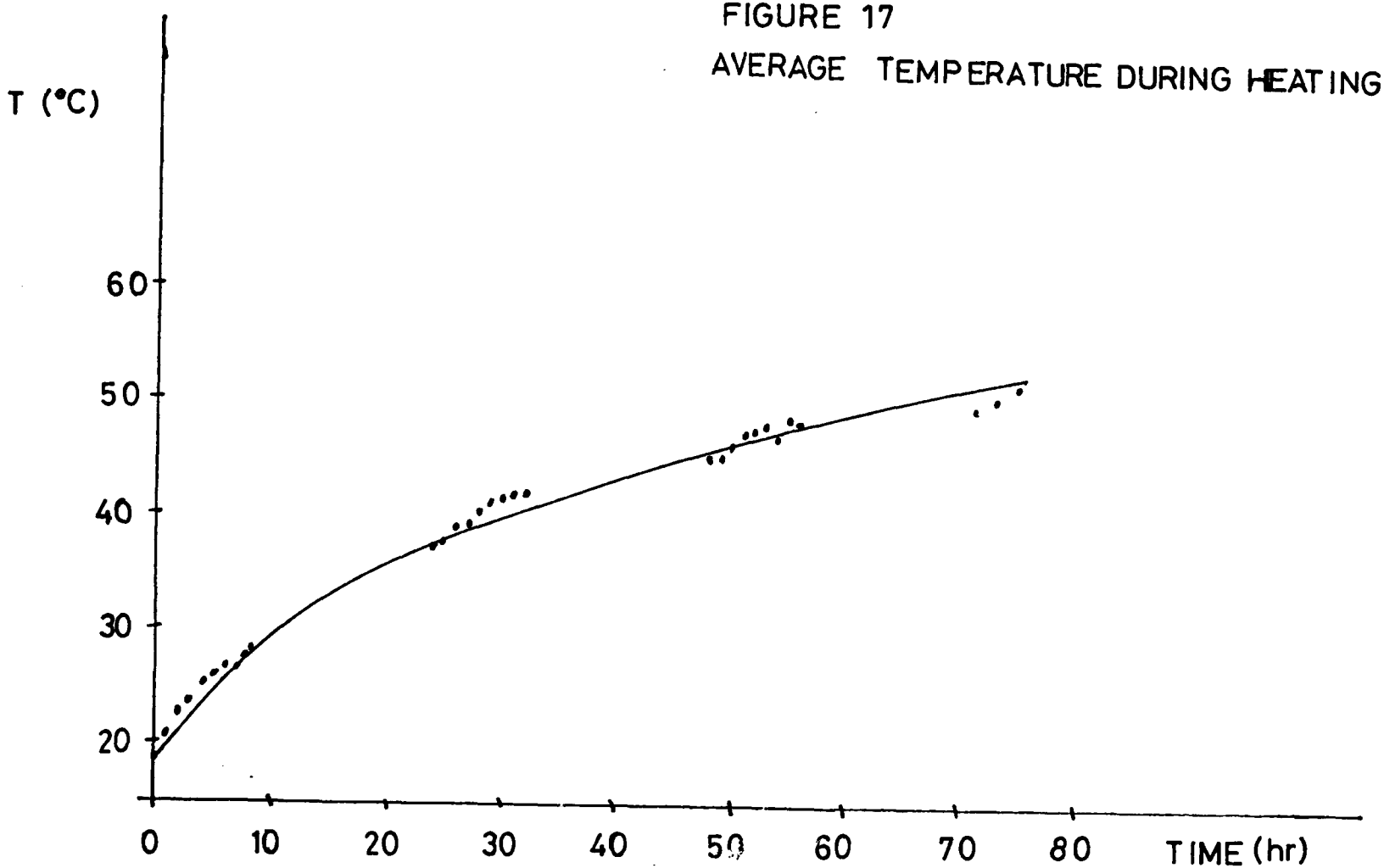

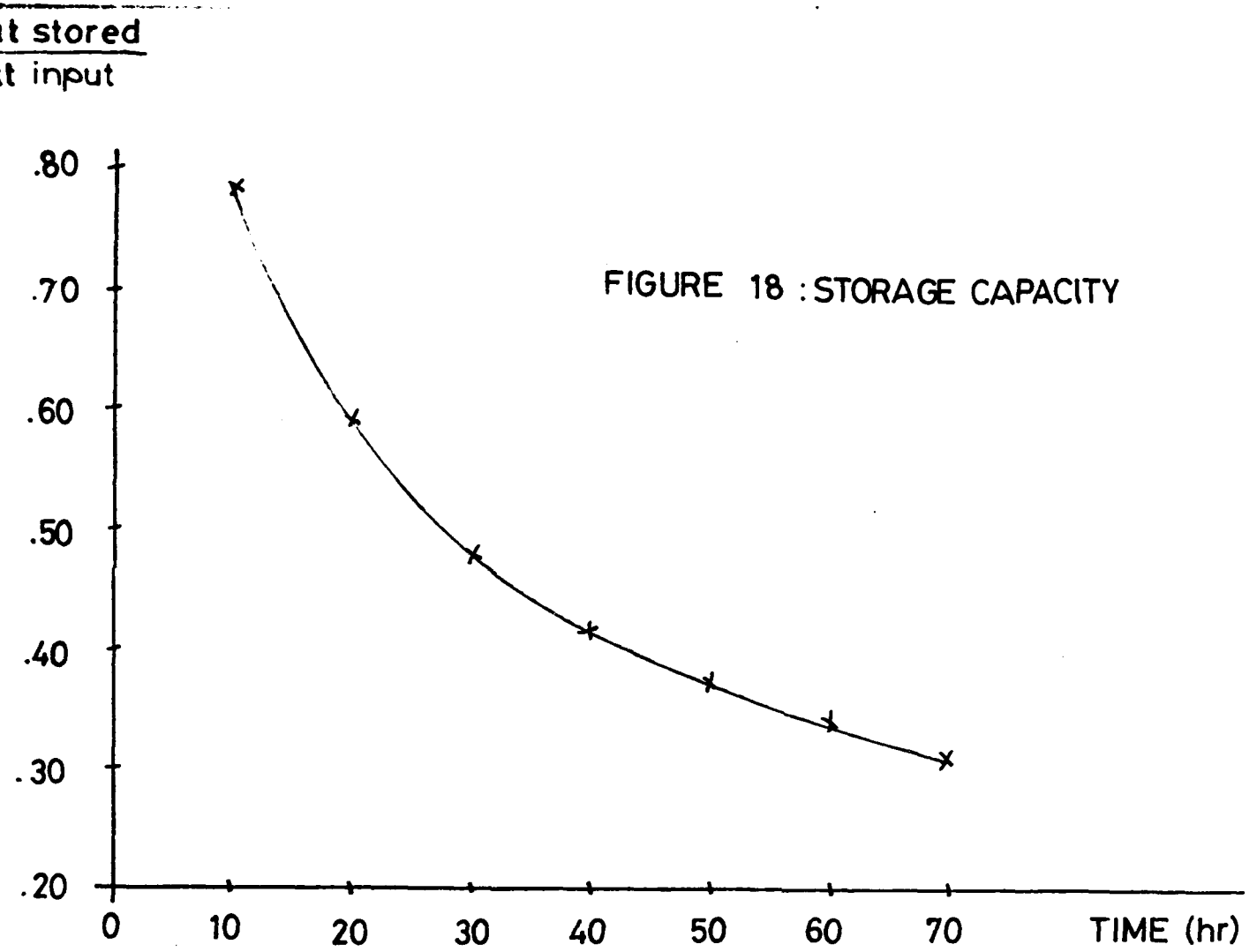

FIGURE 18 : STORAGE CAPACITY

FIGURE 19
OVERALL LOSS COEFFIENT DURING HEATING

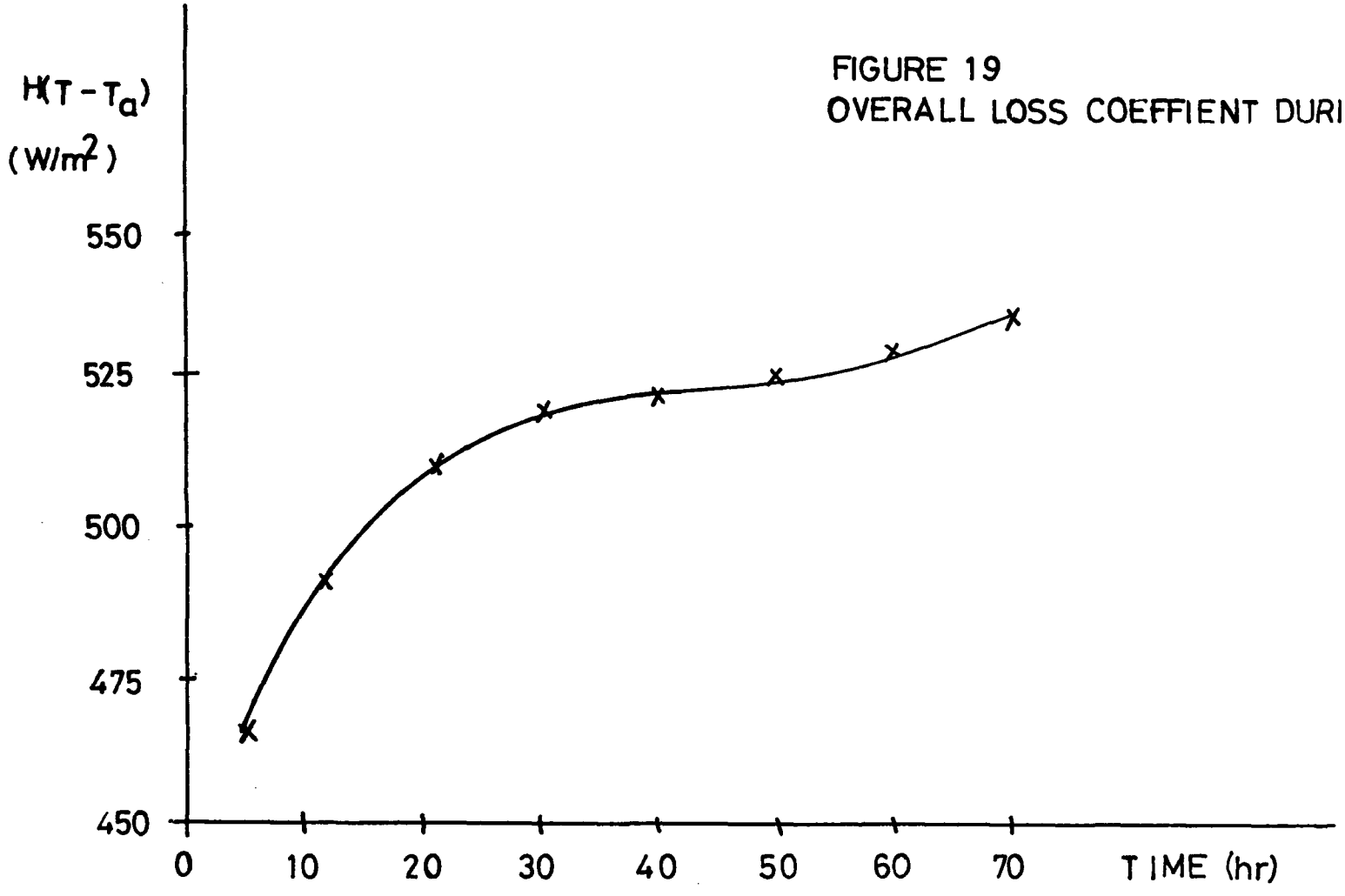

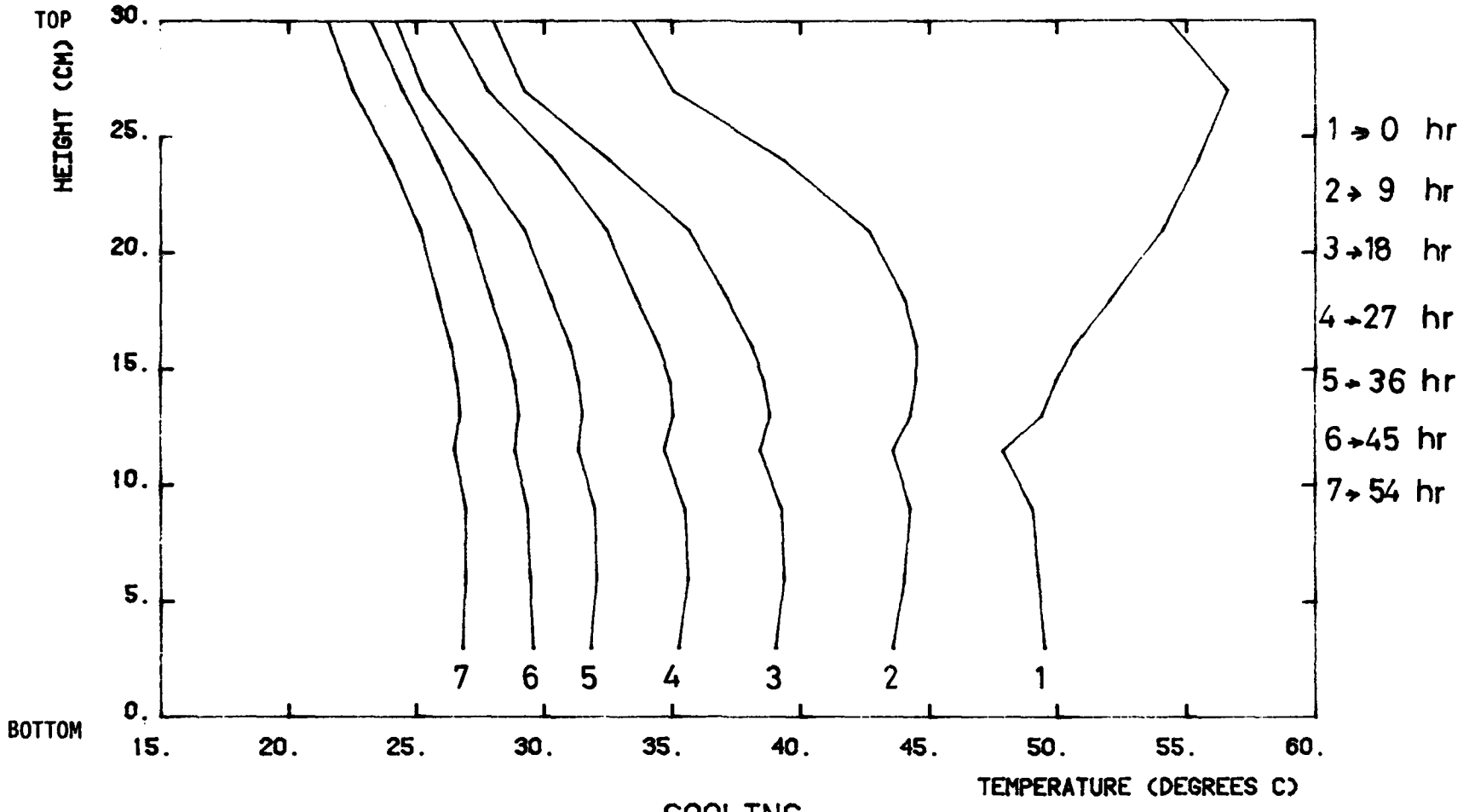

COOLING
EXPERIMENTAL DATA
FIGURE 20

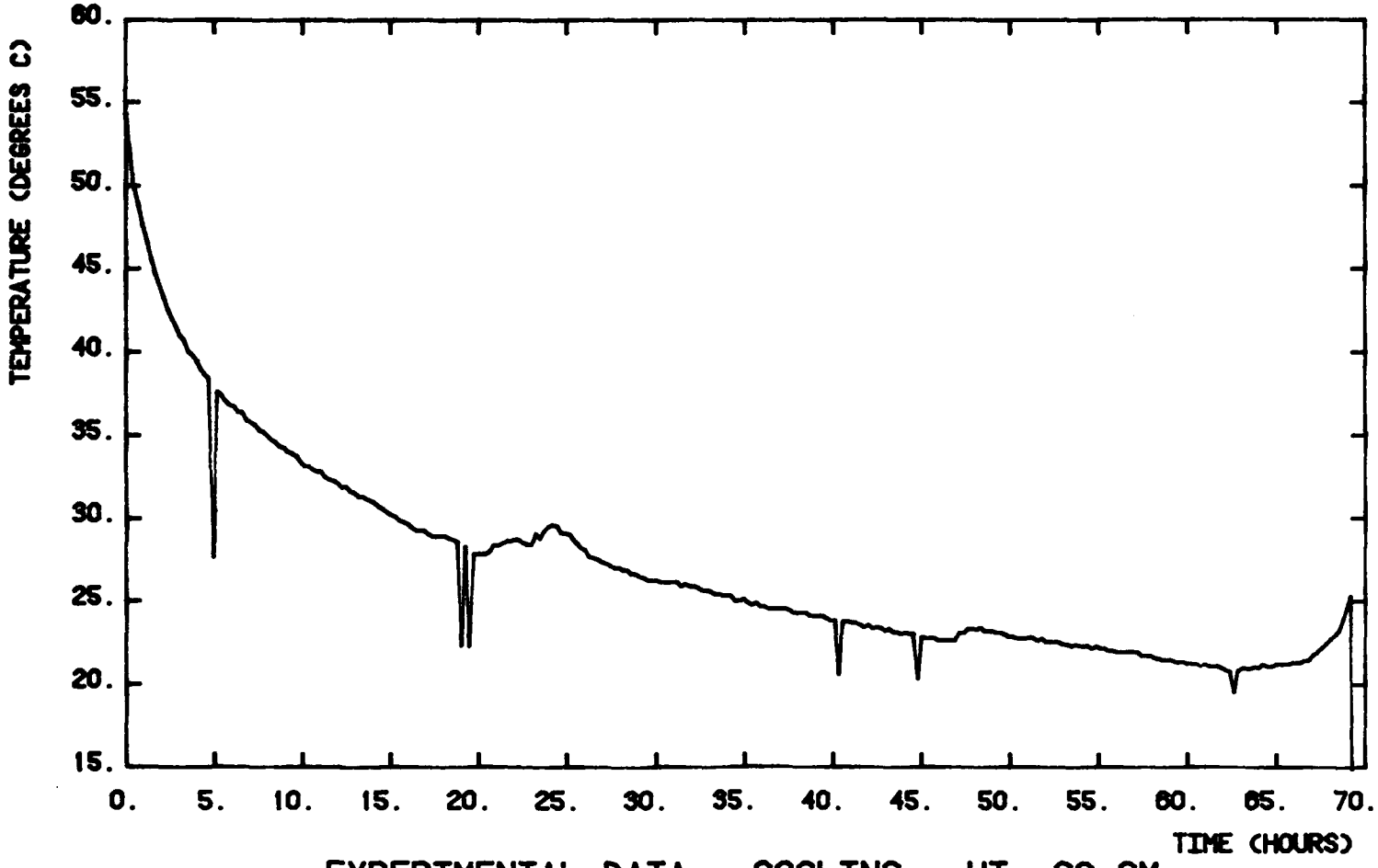

EXPERIMENTAL DATA - COOLING - HT.=30.CM

FIGURE 21a

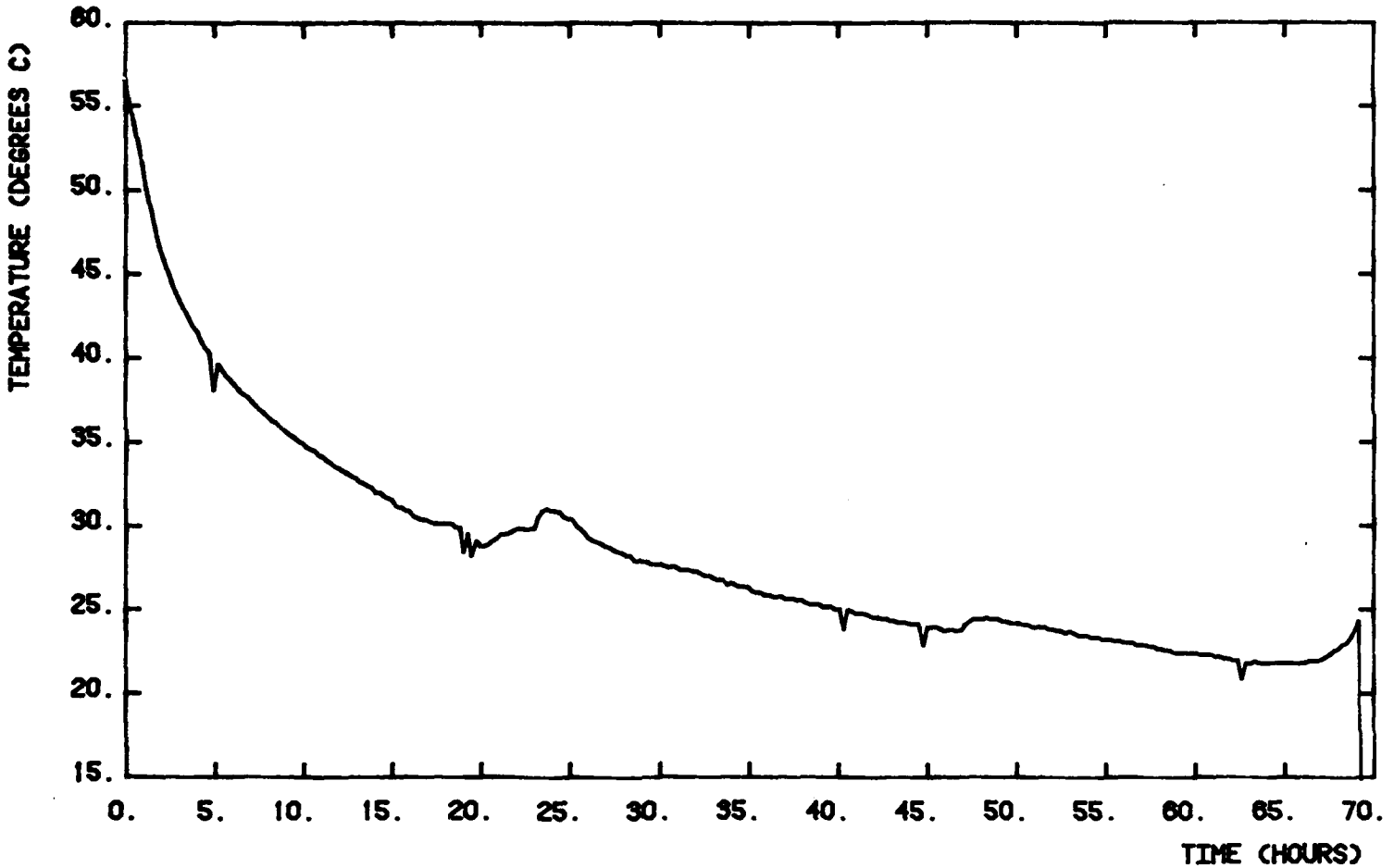

EXPERIMENTAL DATA - COOLING - HT.=27.CM

FIGURE 21b

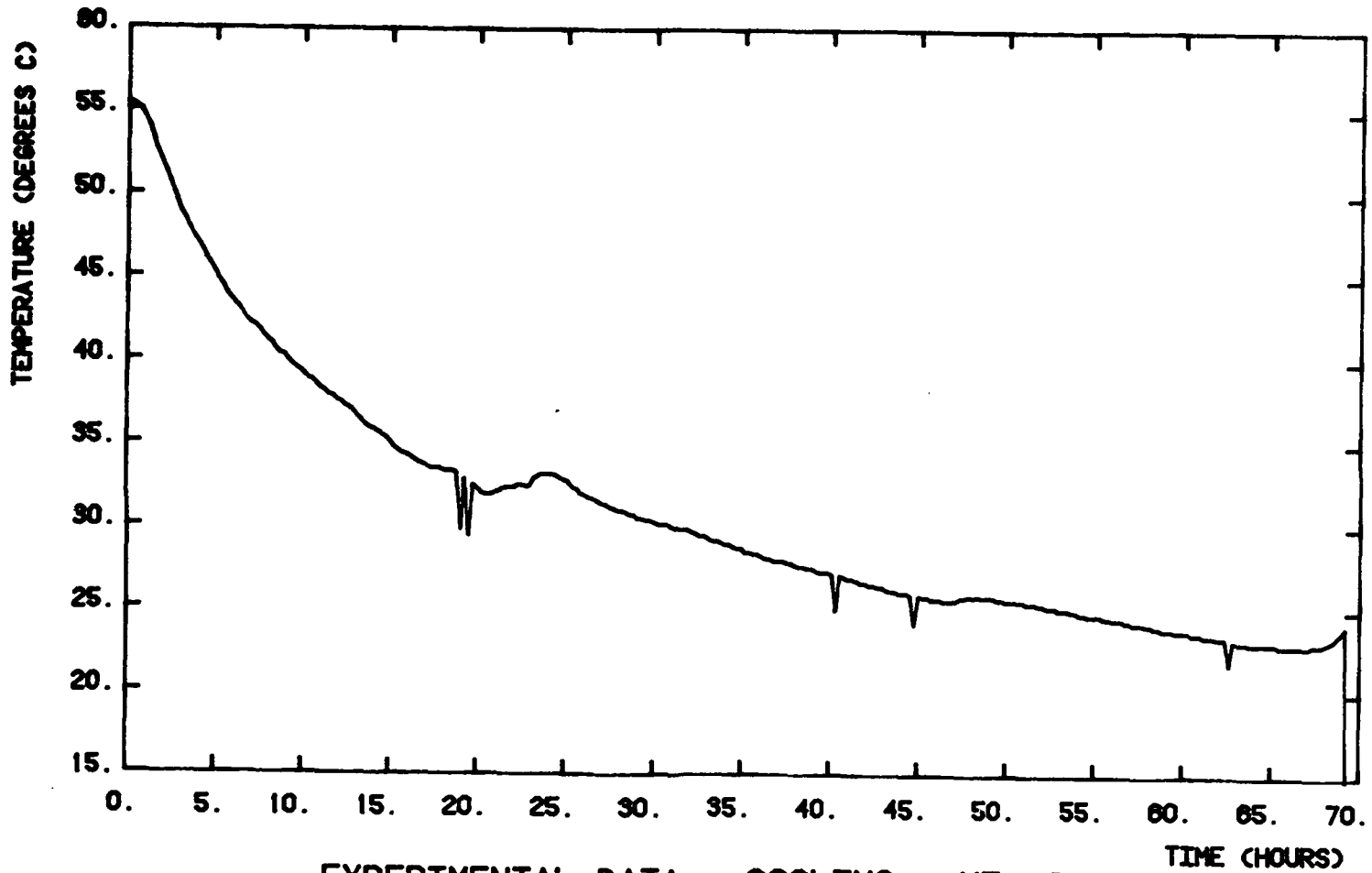

EXPERIMENTAL DATA - COOLING - HT.=24.CM

FIGURE 21c

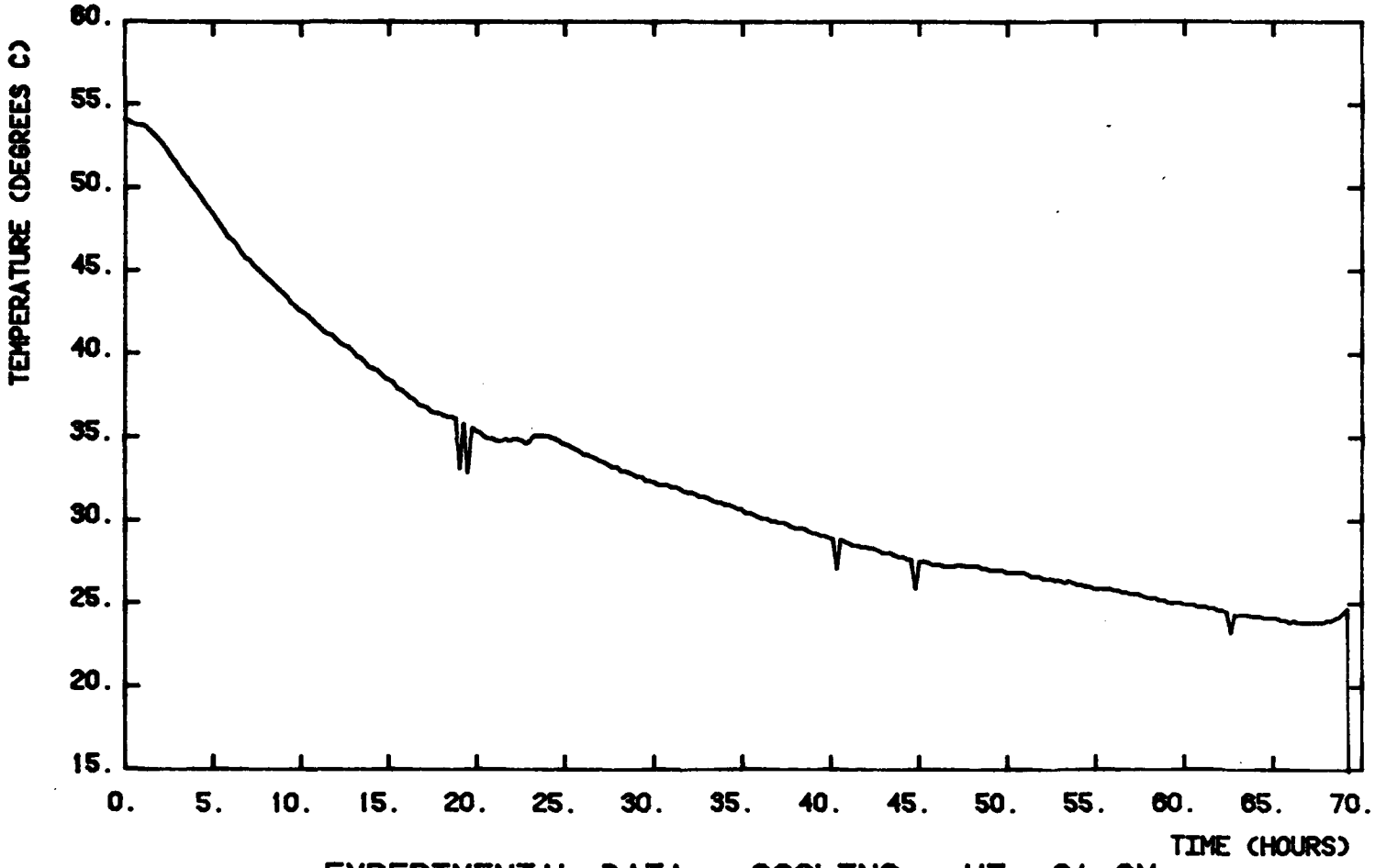

EXPERIMENTAL DATA - COOLING - HT.=21.CM

FIGURE 21d

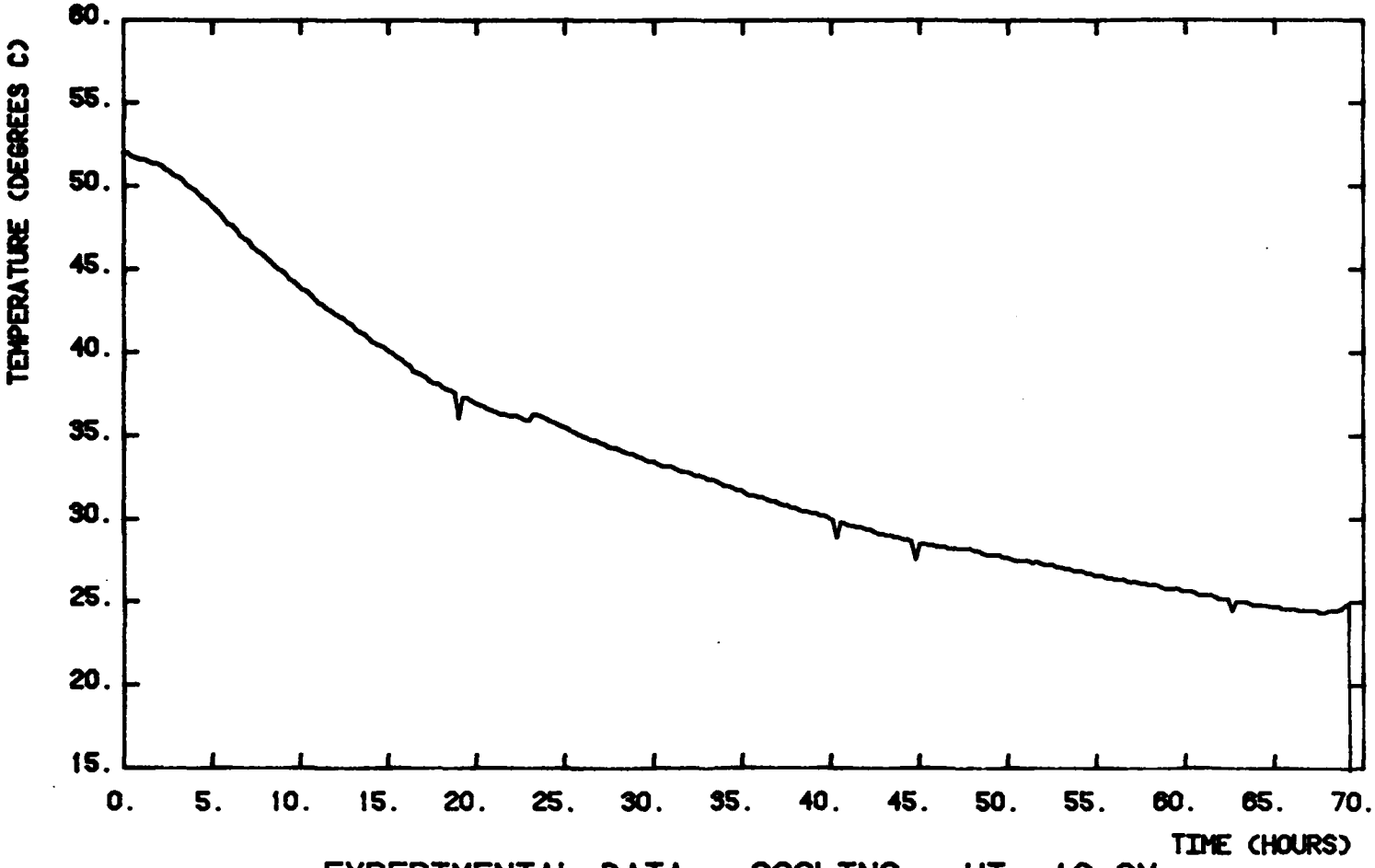

EXPERIMENTAL DATA - COOLING - HT.=18.CM

FIGURE 21e

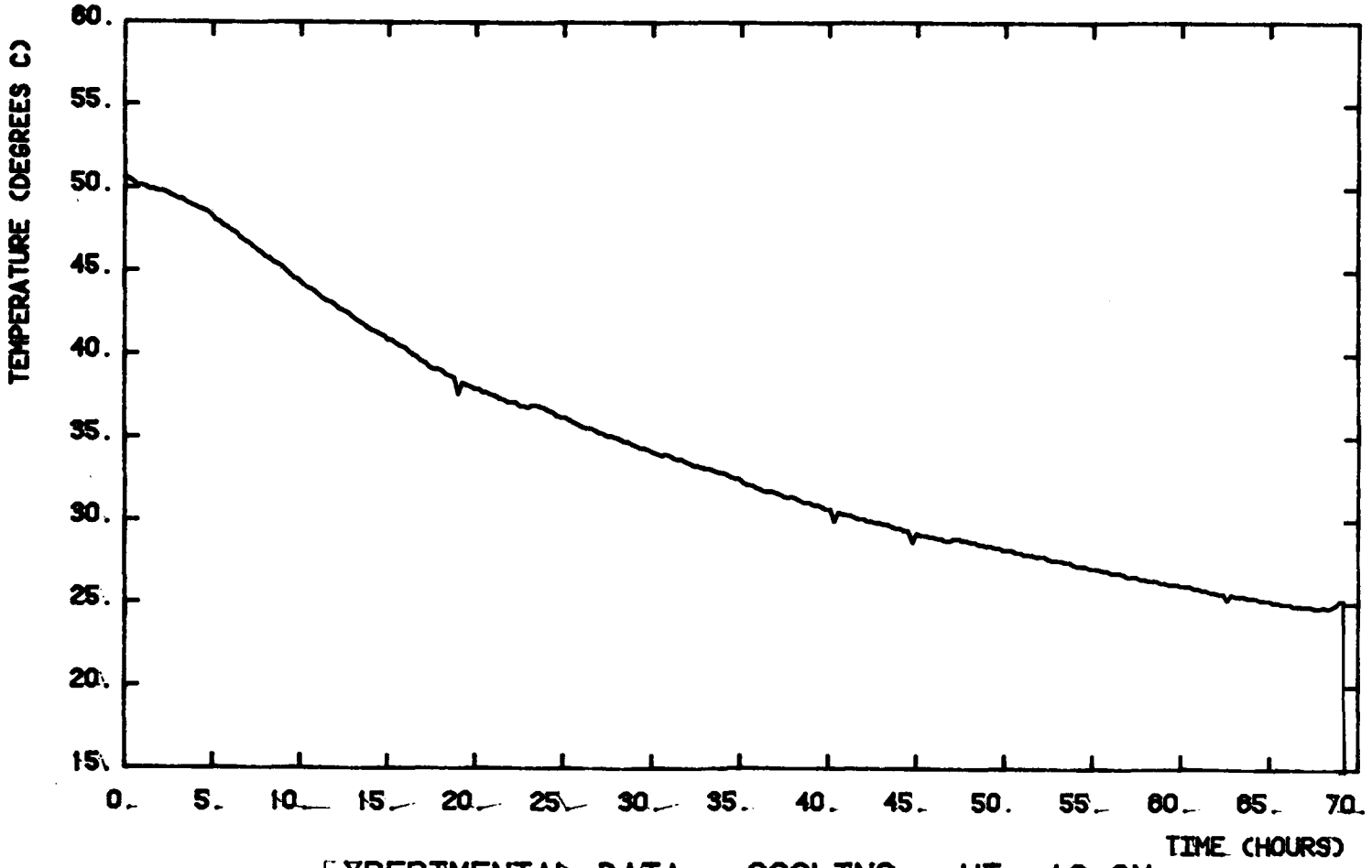

EXPERIMENTAL DATA – COOLING – HT.=16.CM

FIGURE 21f

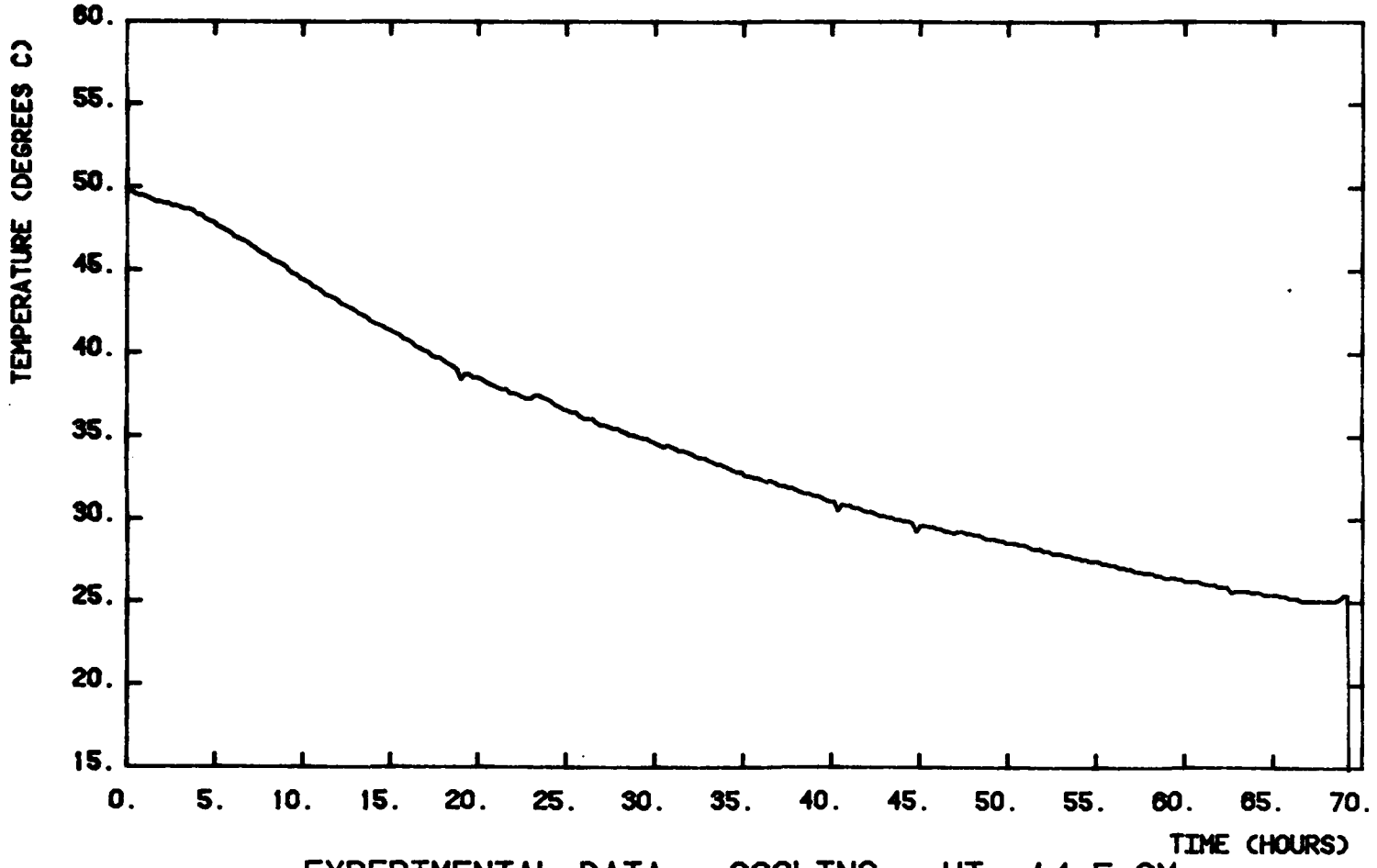

EXPERIMENTAL DATA - COOLING - HT.=14.5 CM

FIGURE 21g

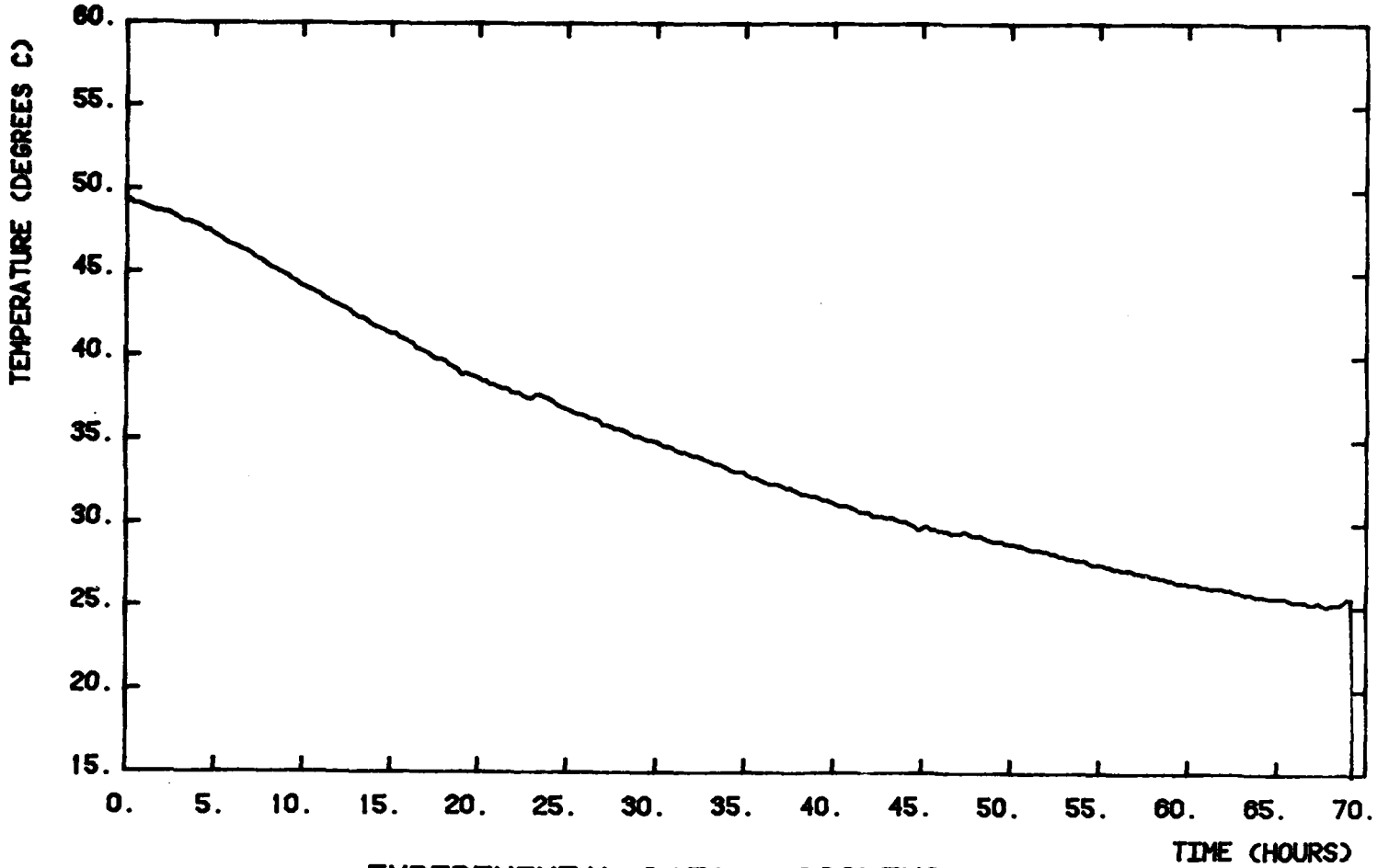

EXPERIMENTAL DATA - COOLING - 13.CM

FIGURE 21h

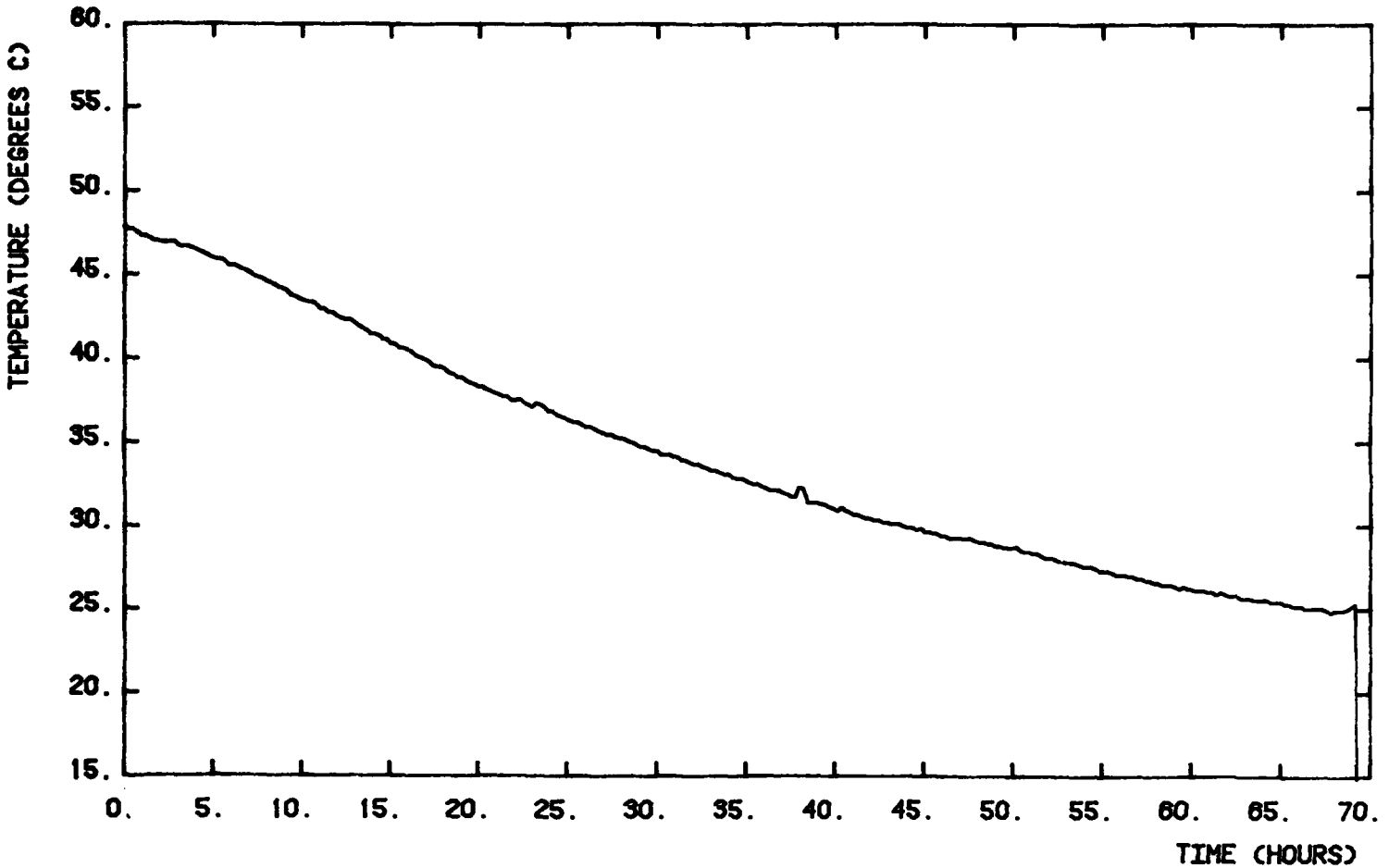

EXPERIMENTAL DATA - COOLING - HT.=11.5 CM

FIGURE 21i

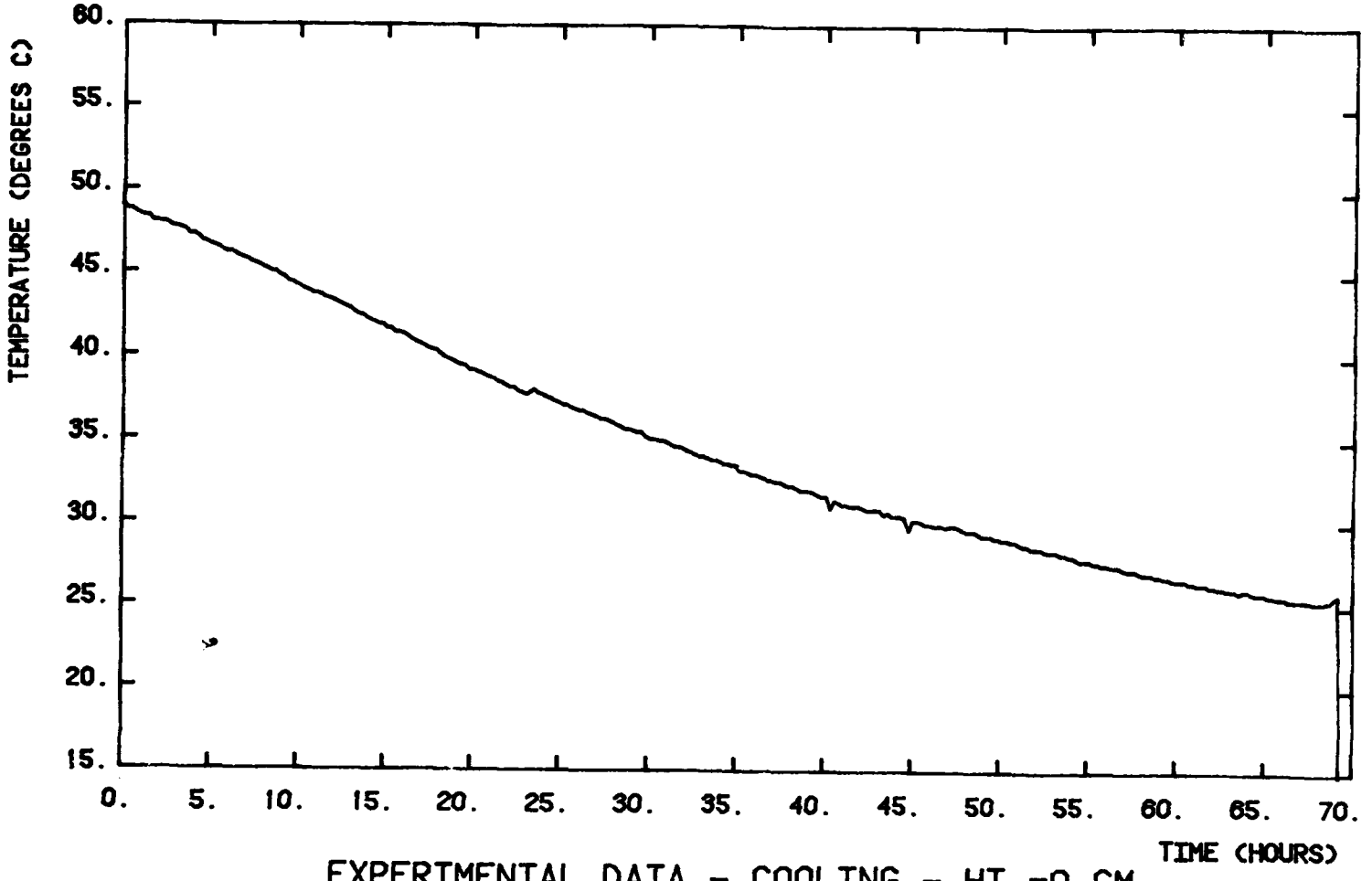

EXPERIMENTAL DATA - COOLING - HT.=9.CM

FIGURE 21j

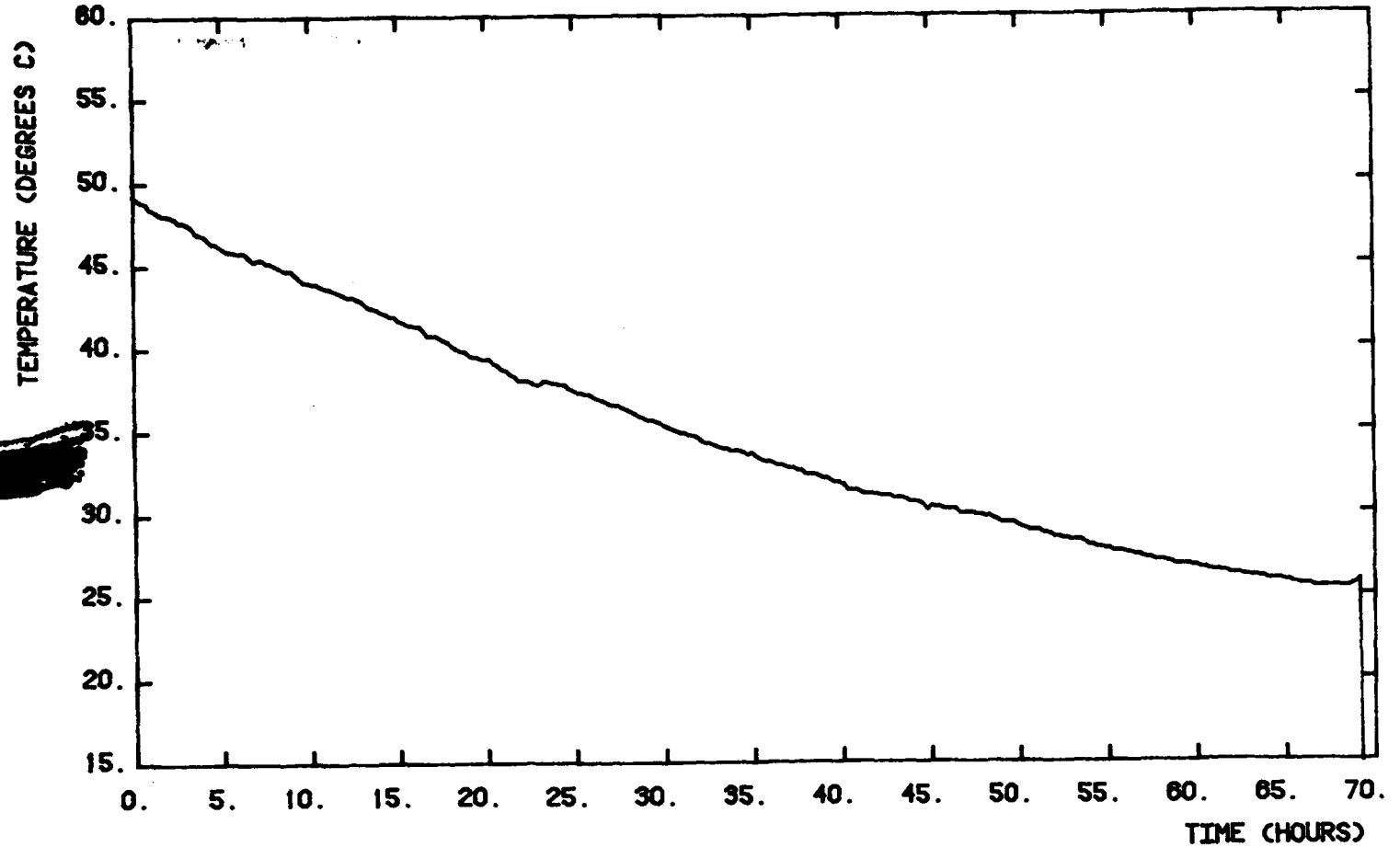

EXPERIMENTAL DATA - COOLING - HT.=6.CM

FIGURE 21k

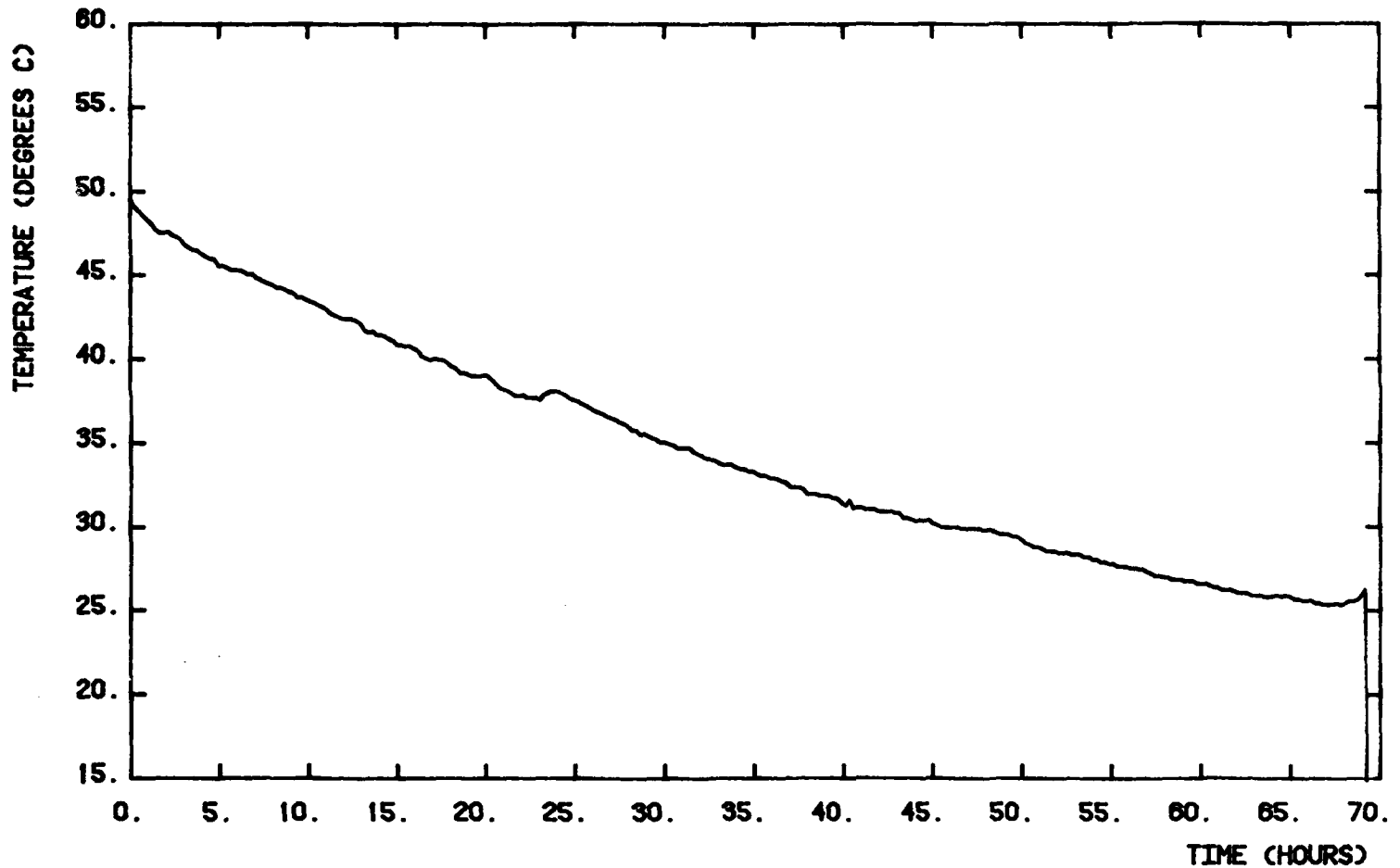

EXPERIMENTAL DATA - COOLING - HT.=3.CM

FIGURE 21l

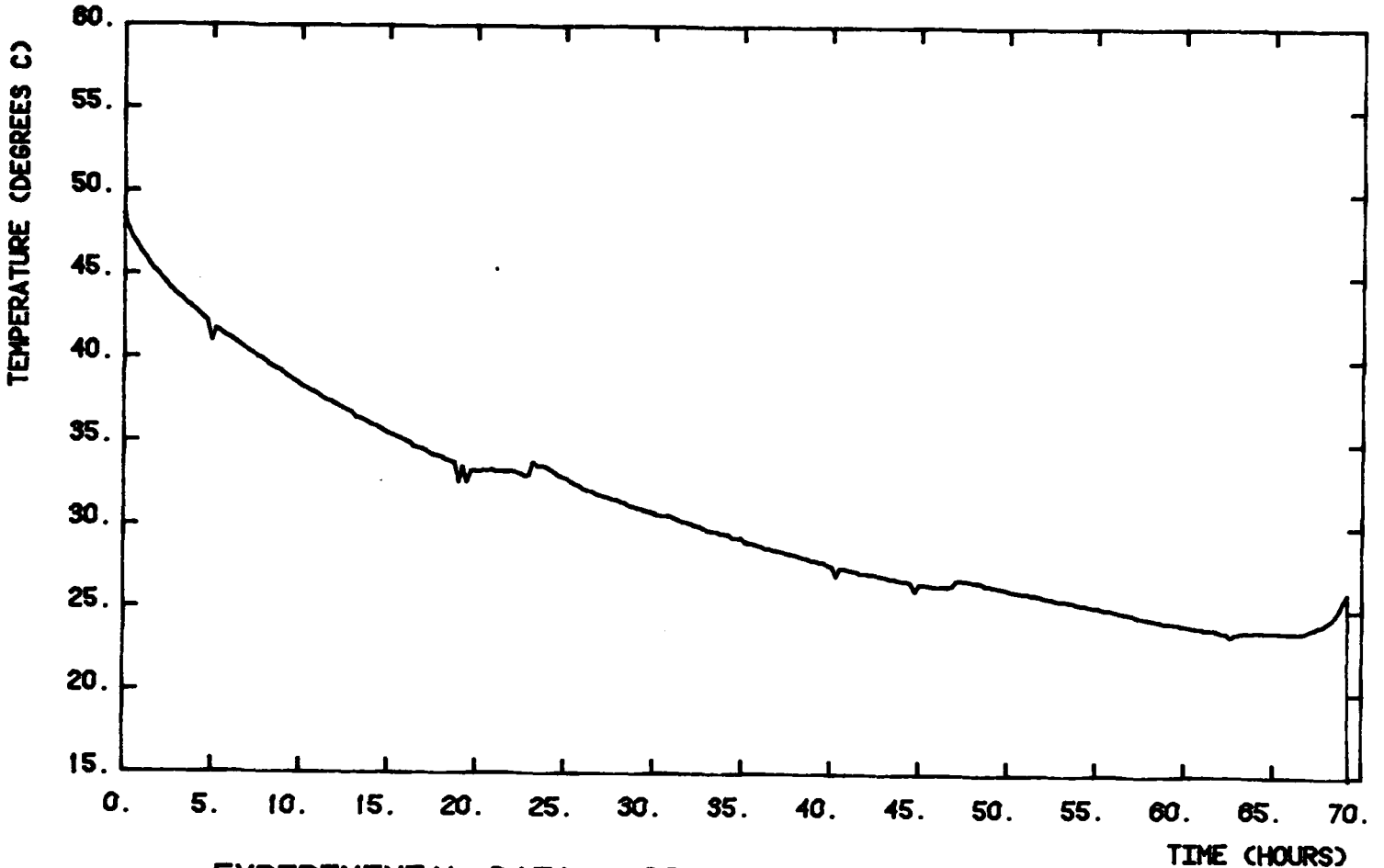

EXPERIMENTAL DATA - COOLING - AVERAGE TEMPERATURE

FIGURE 22

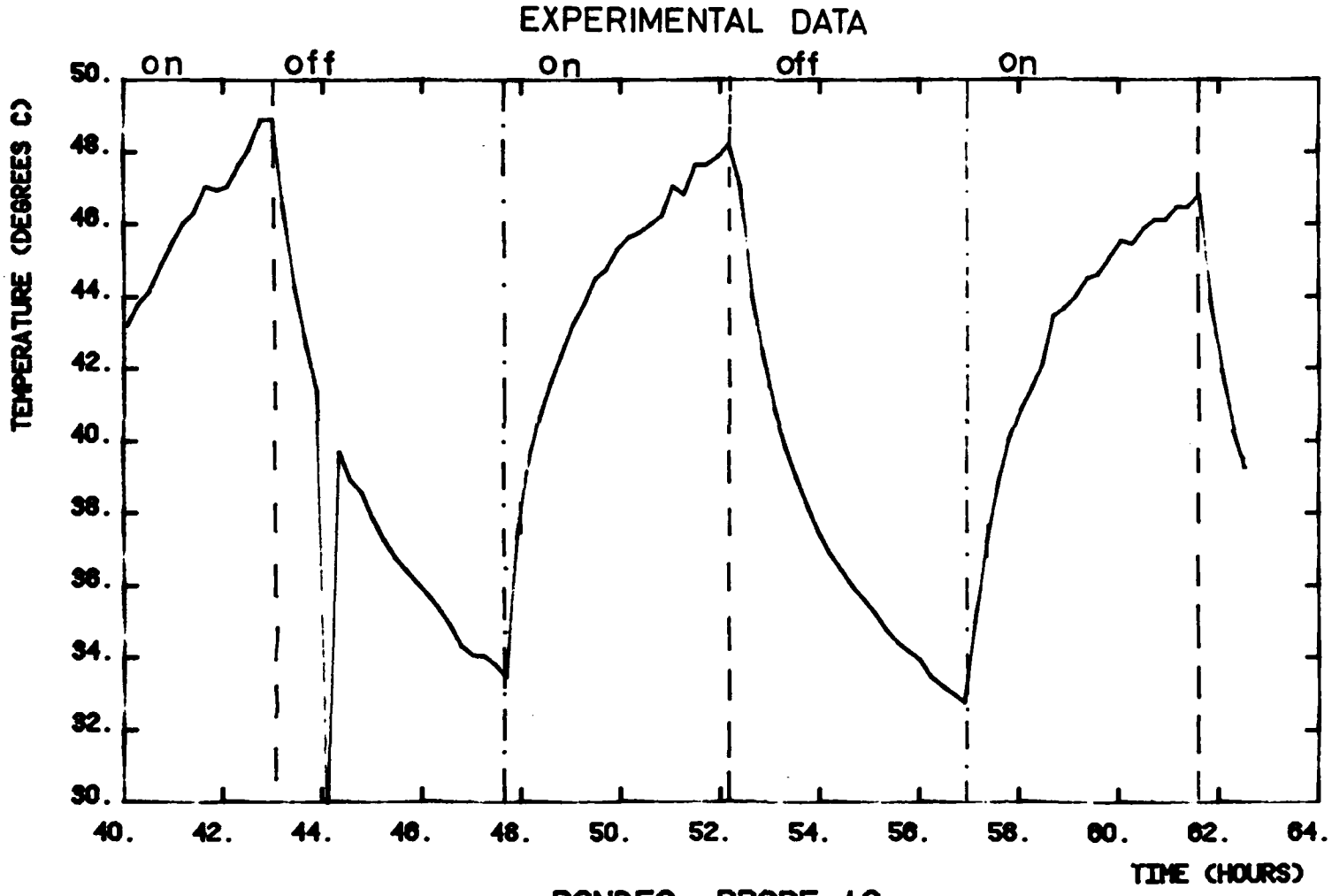

POND58, PROBE 12

POND SURFACE

FIGURE 23a

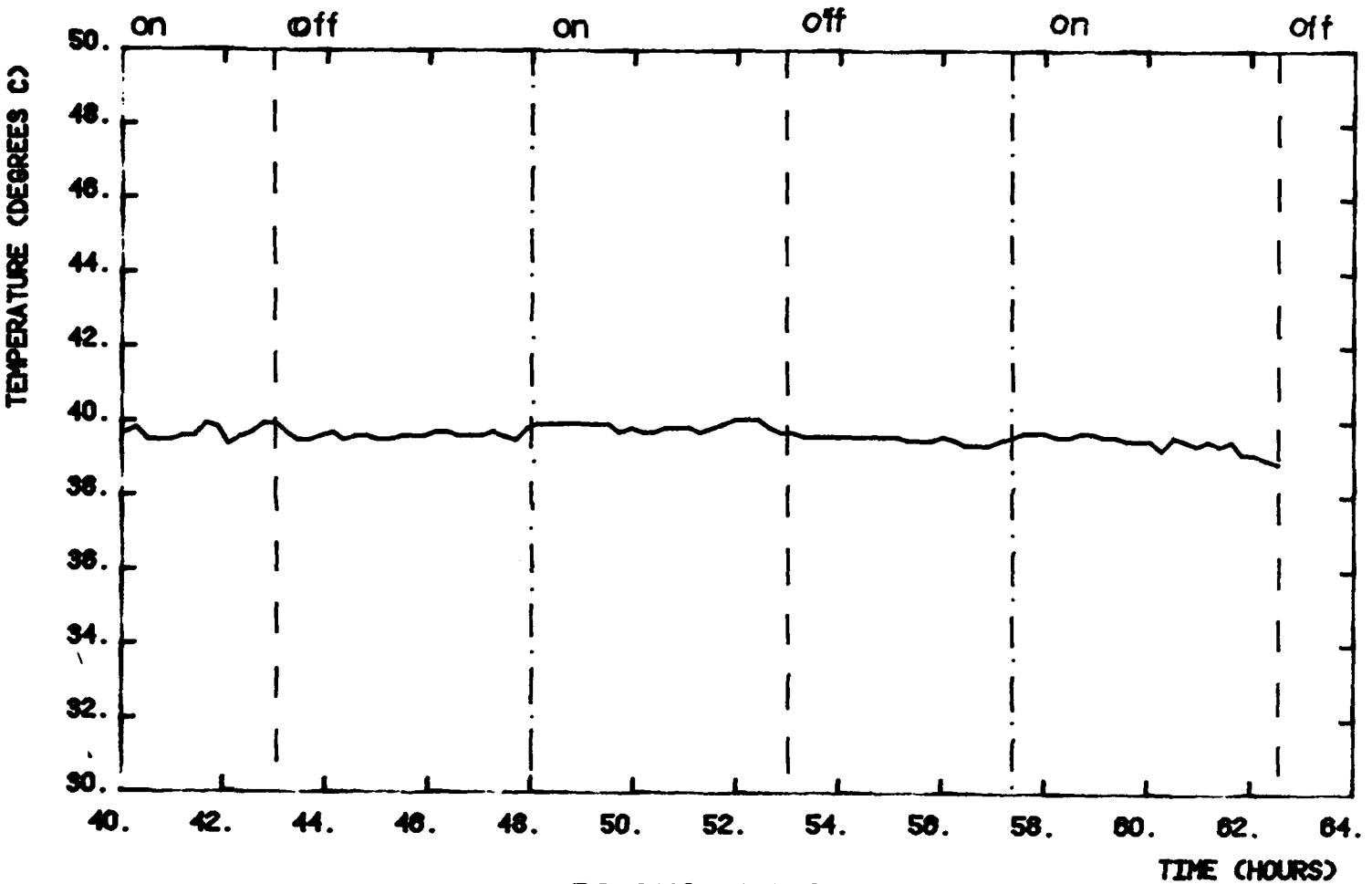

POND58, PROBE 6

BOTTOM OF NCZ

FIGURE 23b

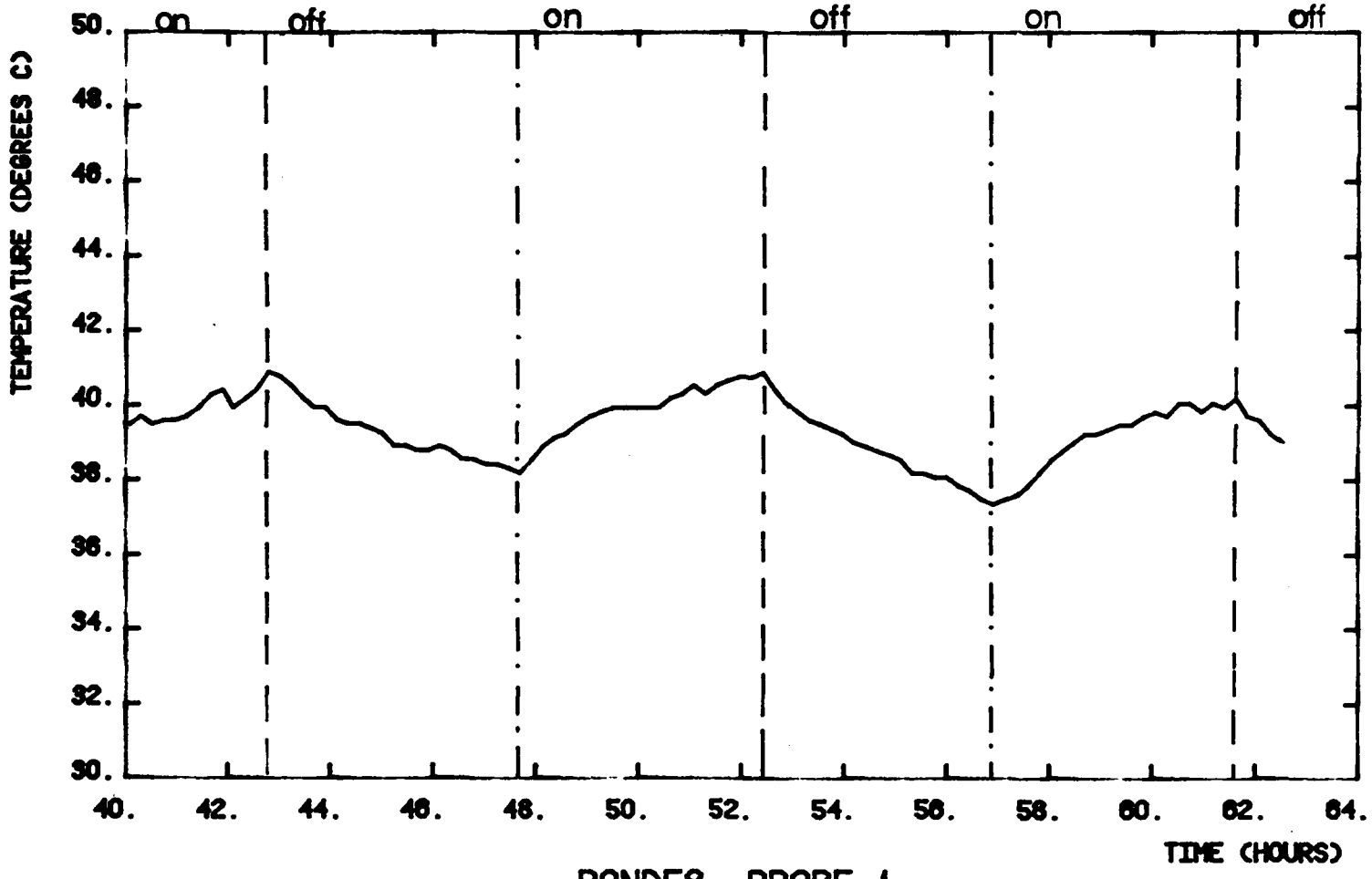

POND58, PROBE 1

POND BOTTOM

FIGURE 23c

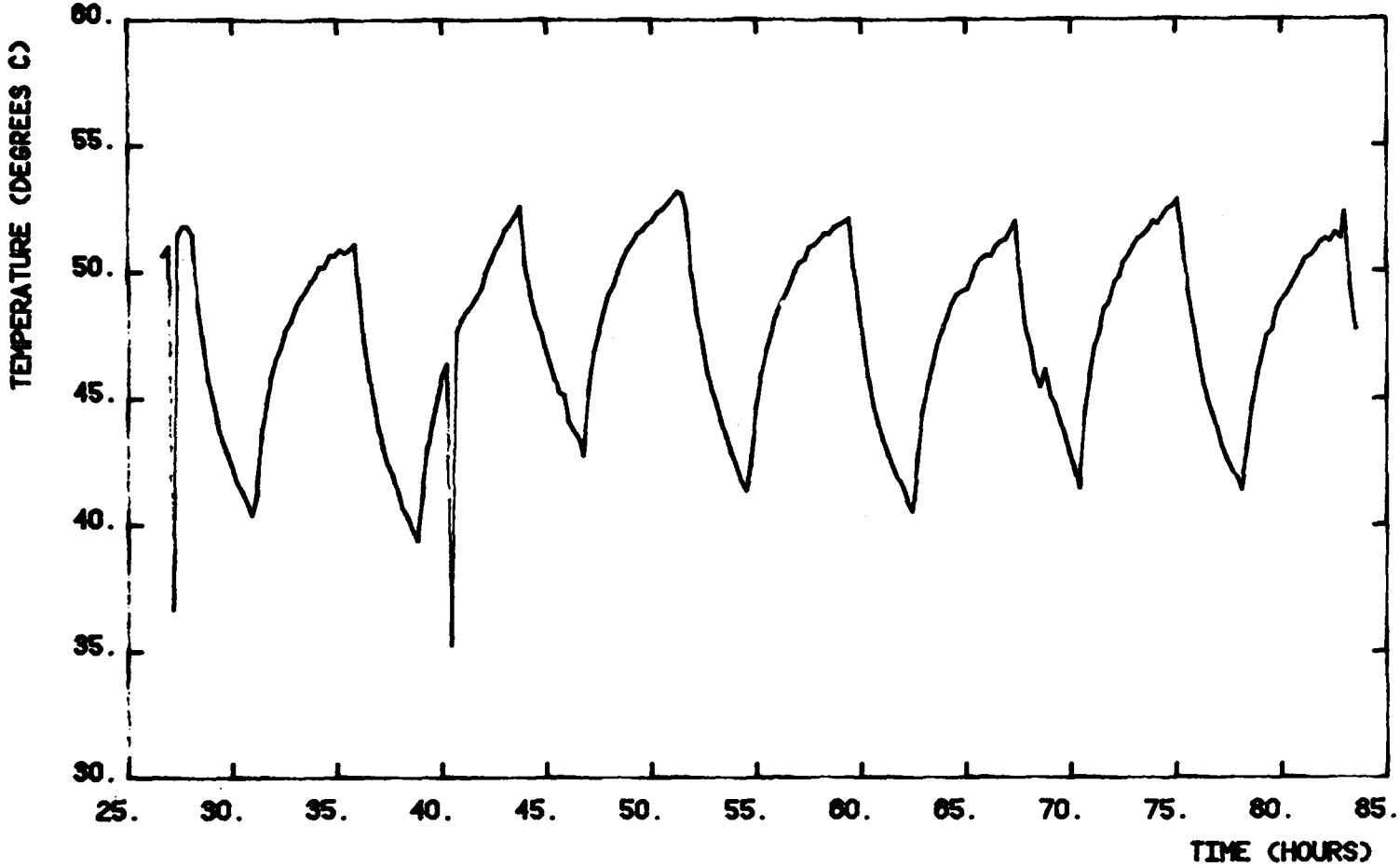

POND80, PROBE 12 (HT.=30.CM)

FIGURE 24a

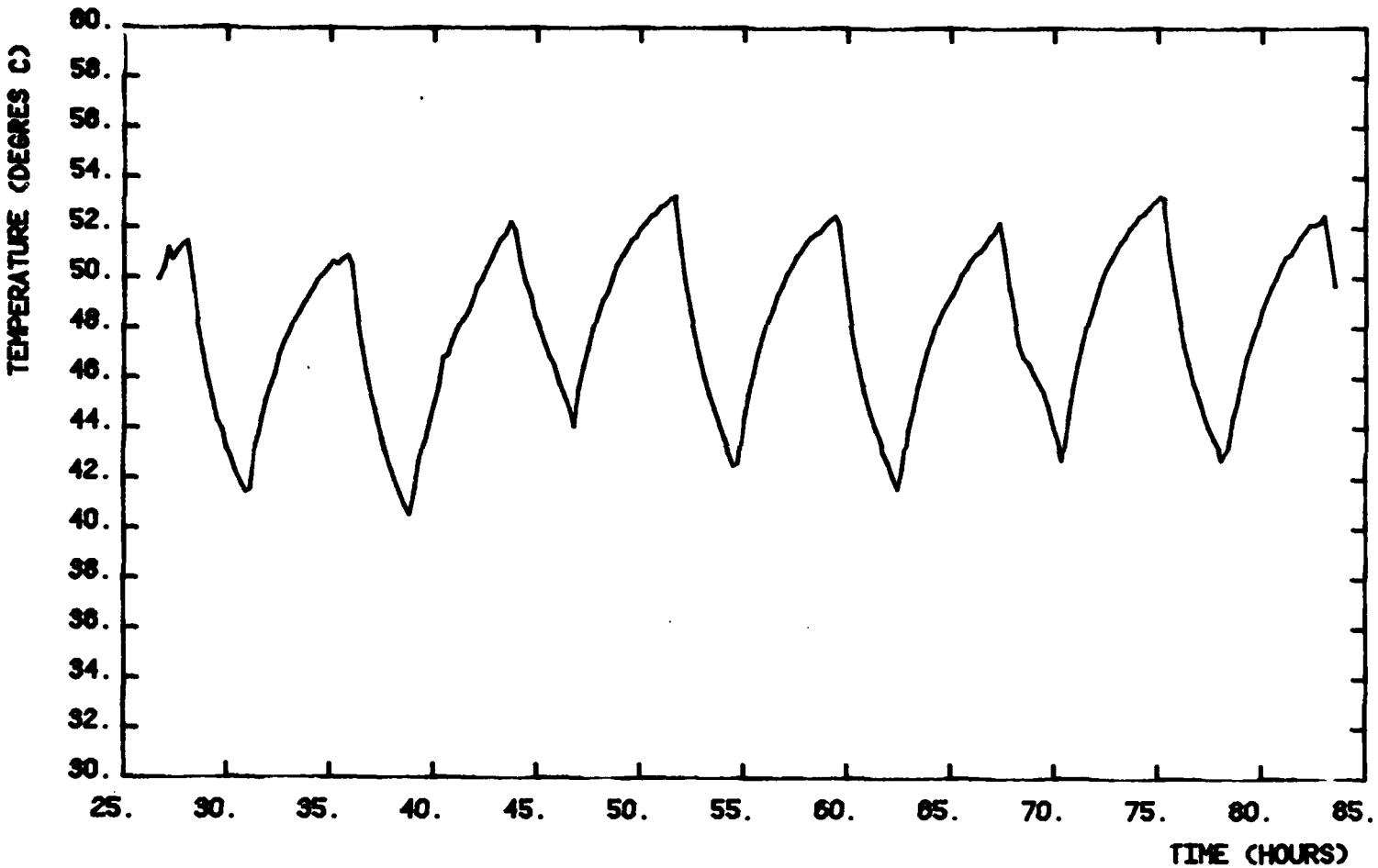

POND80, PROBE 11 (HT.=27.CM)

FIGURE 24b

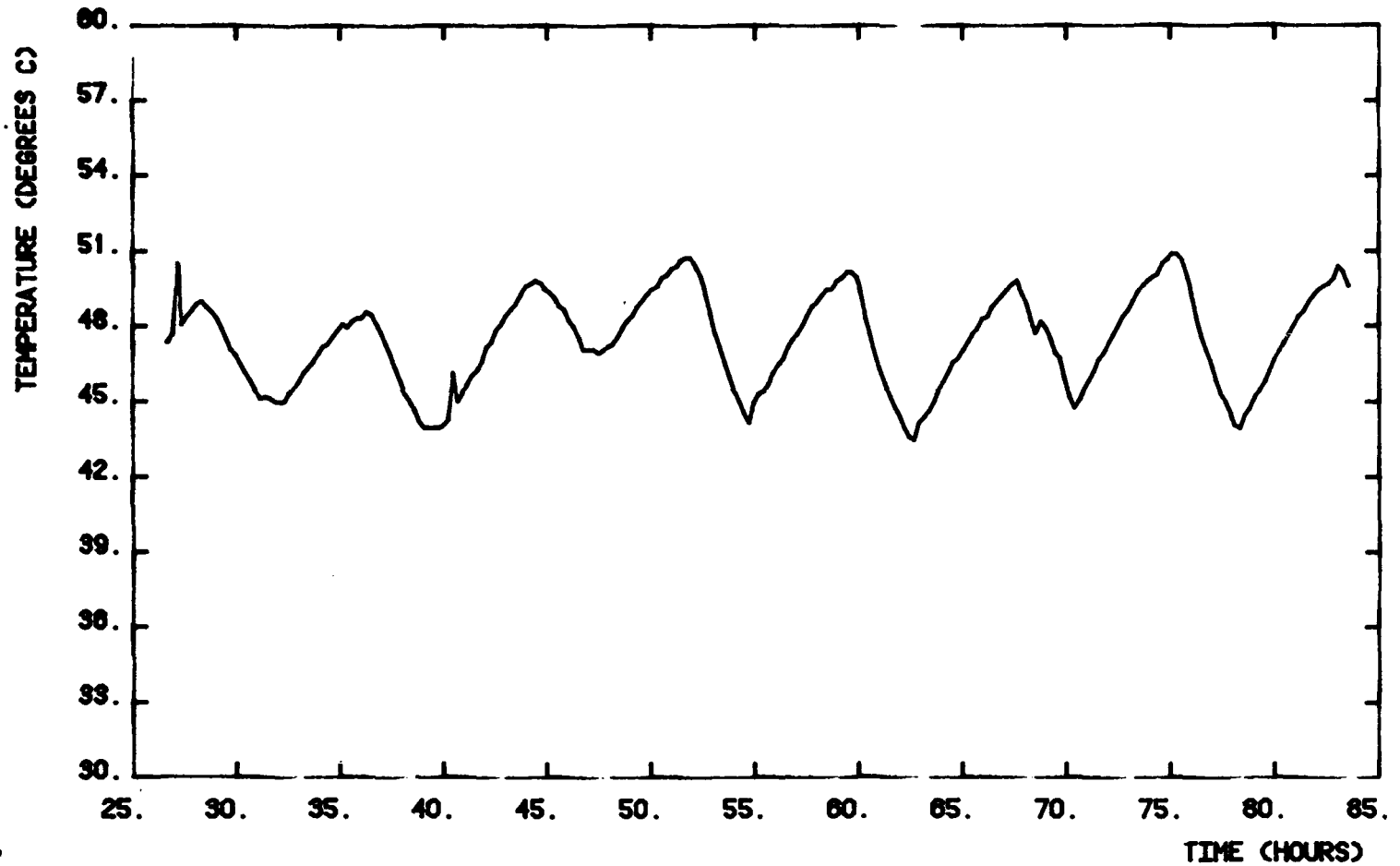

POND80. PROBE 10 (HT.=24.CM)

FIGURE 24c

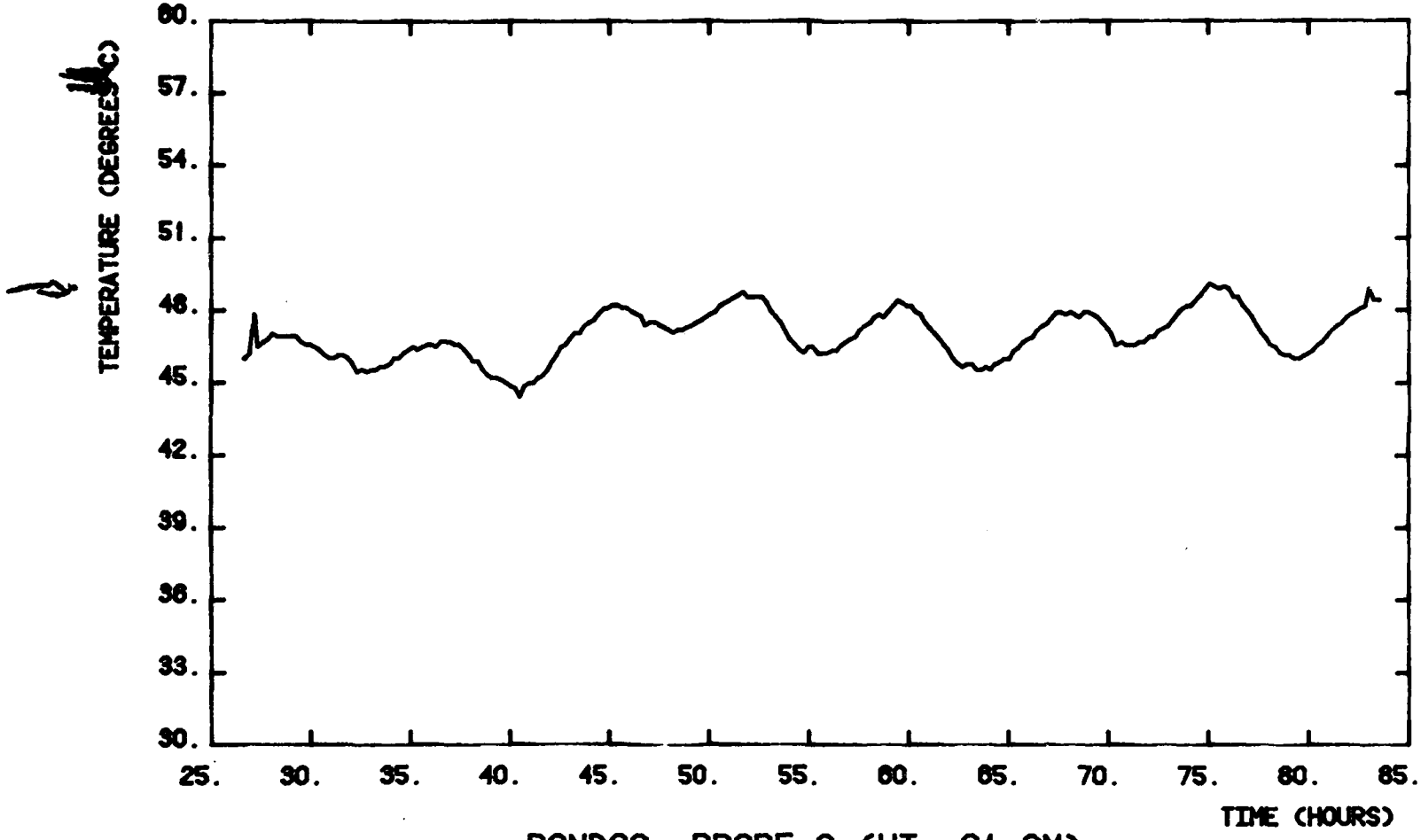

POND80, PROBE 9 (HT.=21.CM)

FIGURE 24d

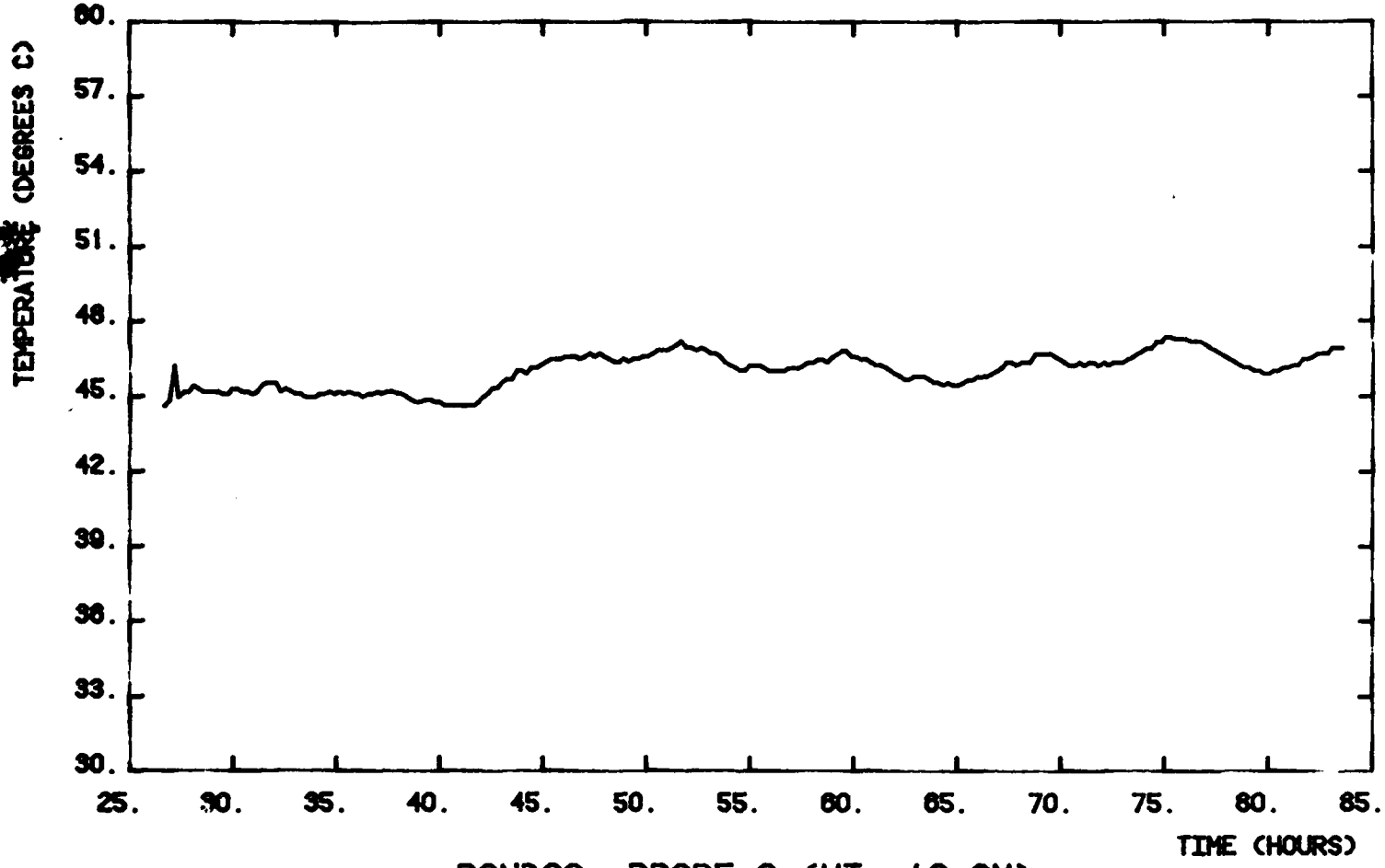

POND80, PROBE 8 (HT.=18.CM)

FIGURE 24e

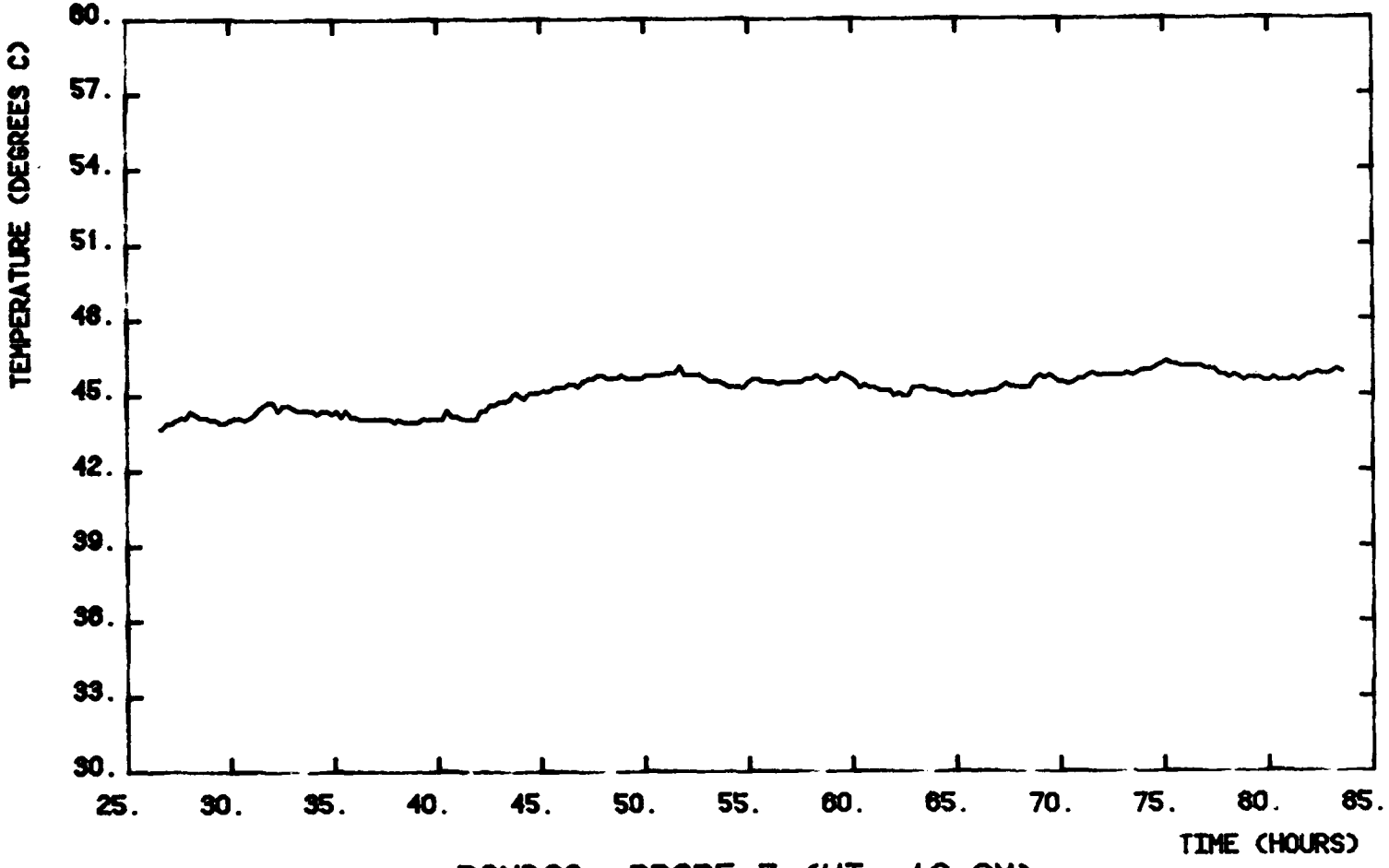

POND80, PROBE 7 (HT.=16.CM)

FIGURE 24f

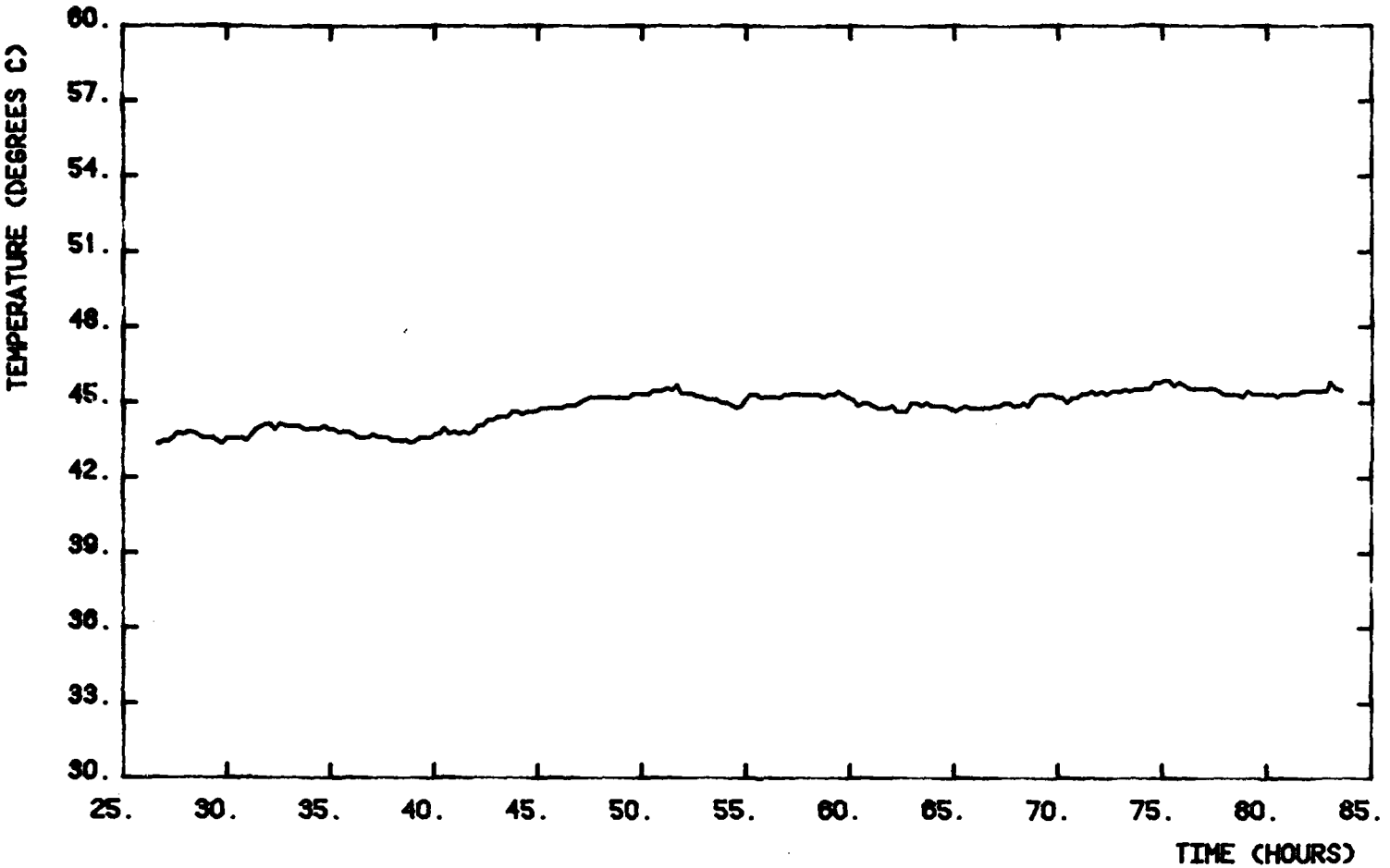

POND80, PROBE 6 (HT.=14.5CM)

FIGURE 24g

AD-A126 702 THE SALT-GRADIENT SOLAR POND(U) VON KARMAN INST FOR FLUID DYNAMICS RHODE-SAINT-GENESE (BELGIUM) S T BROWN FEB 83 EOARD-TR-83-4 AFOSR-82-0201

UNCLASSIFIED F/G 10/3 NL

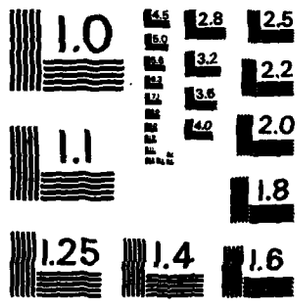

MICROCOPY RESOLUTION TEST CHART
NATIONAL BUREAU OF STANDARDS-1963-A

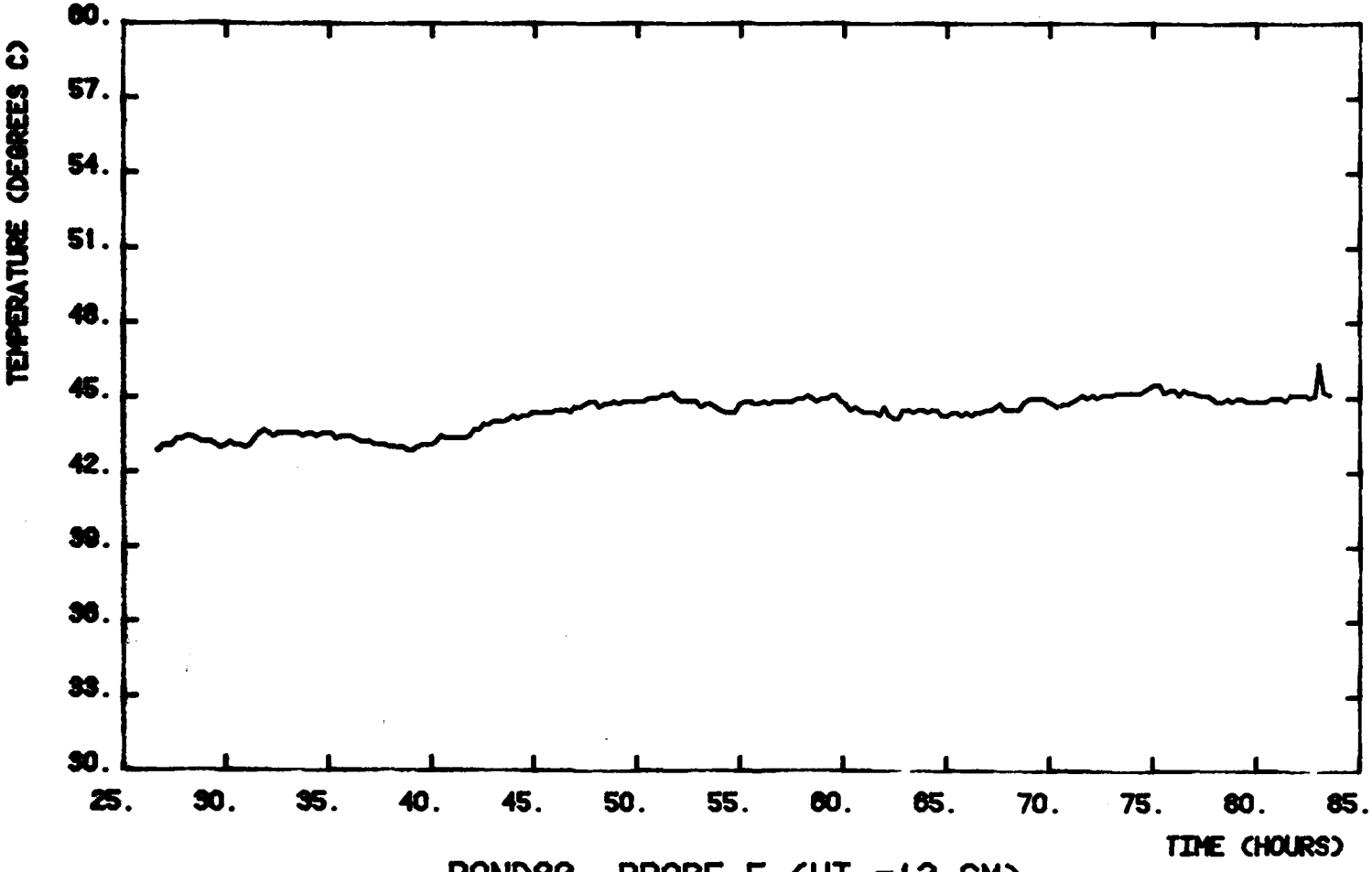

POND80, PROBE 5 (HT.=13.CM)

FIGURE 24h

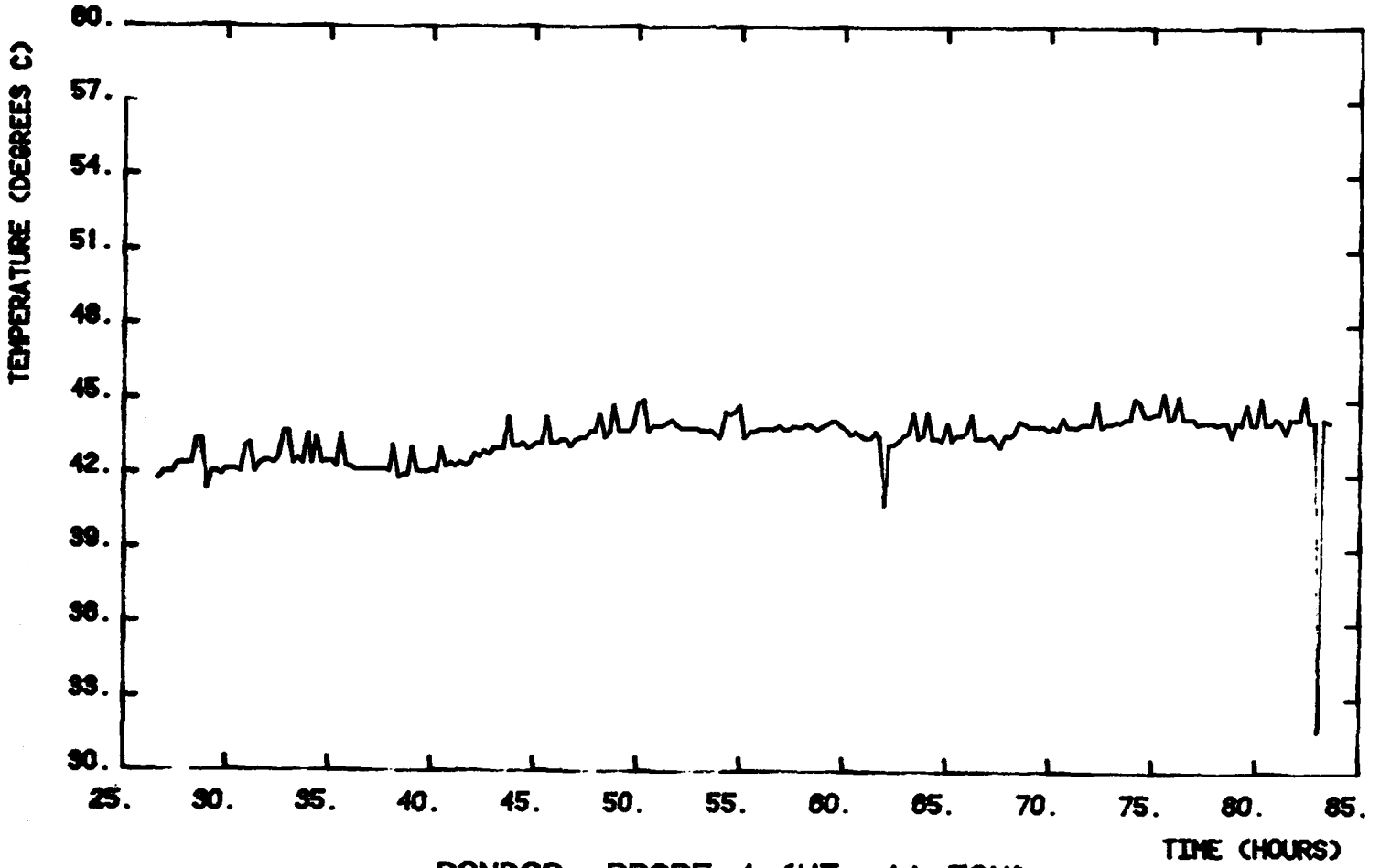

POND80, PROBE 4 (HT.=11.5CM)

FIGURE 24i

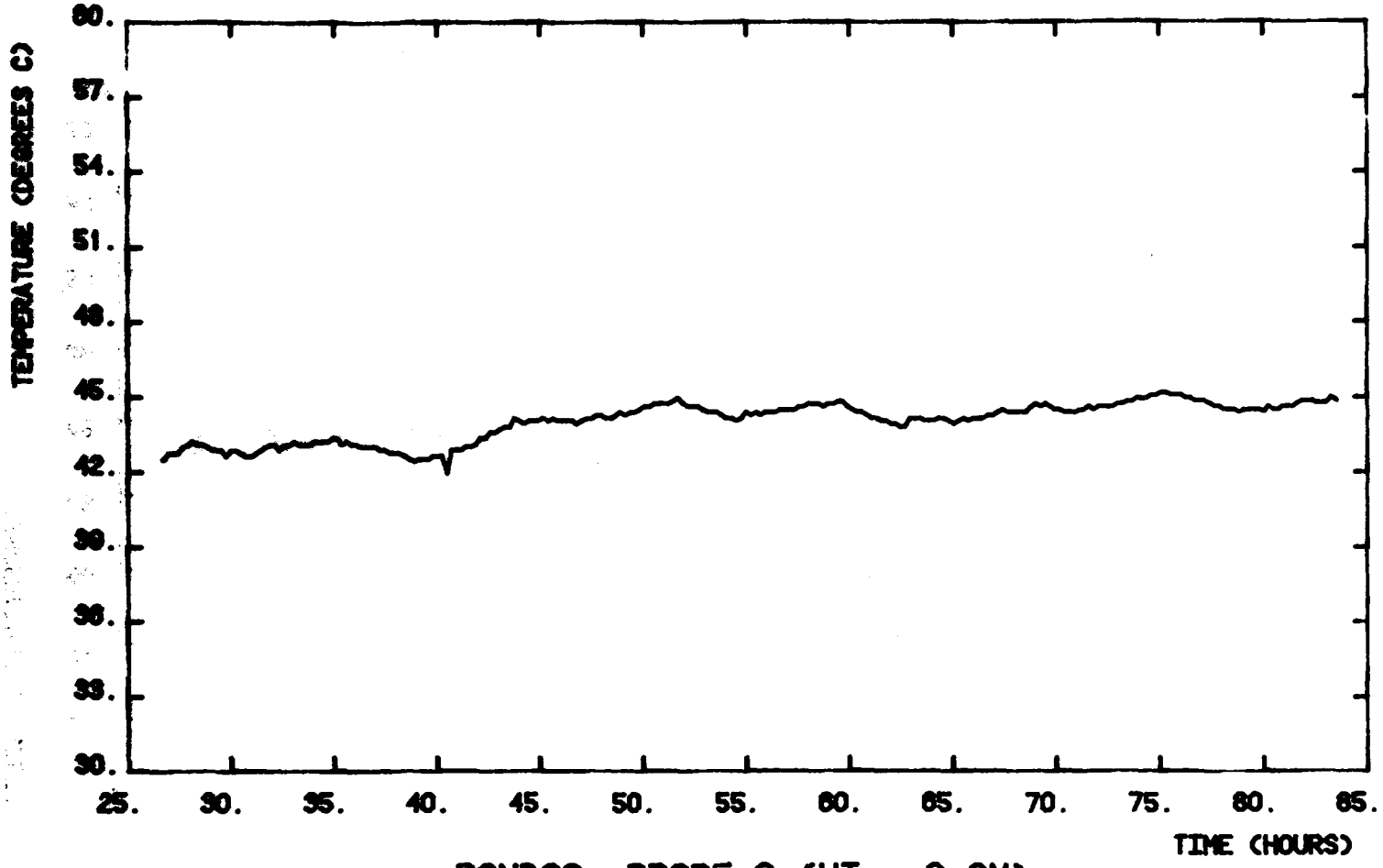

POND80, PROBE 3 (HT. =9.CM)

FIGURE 24j

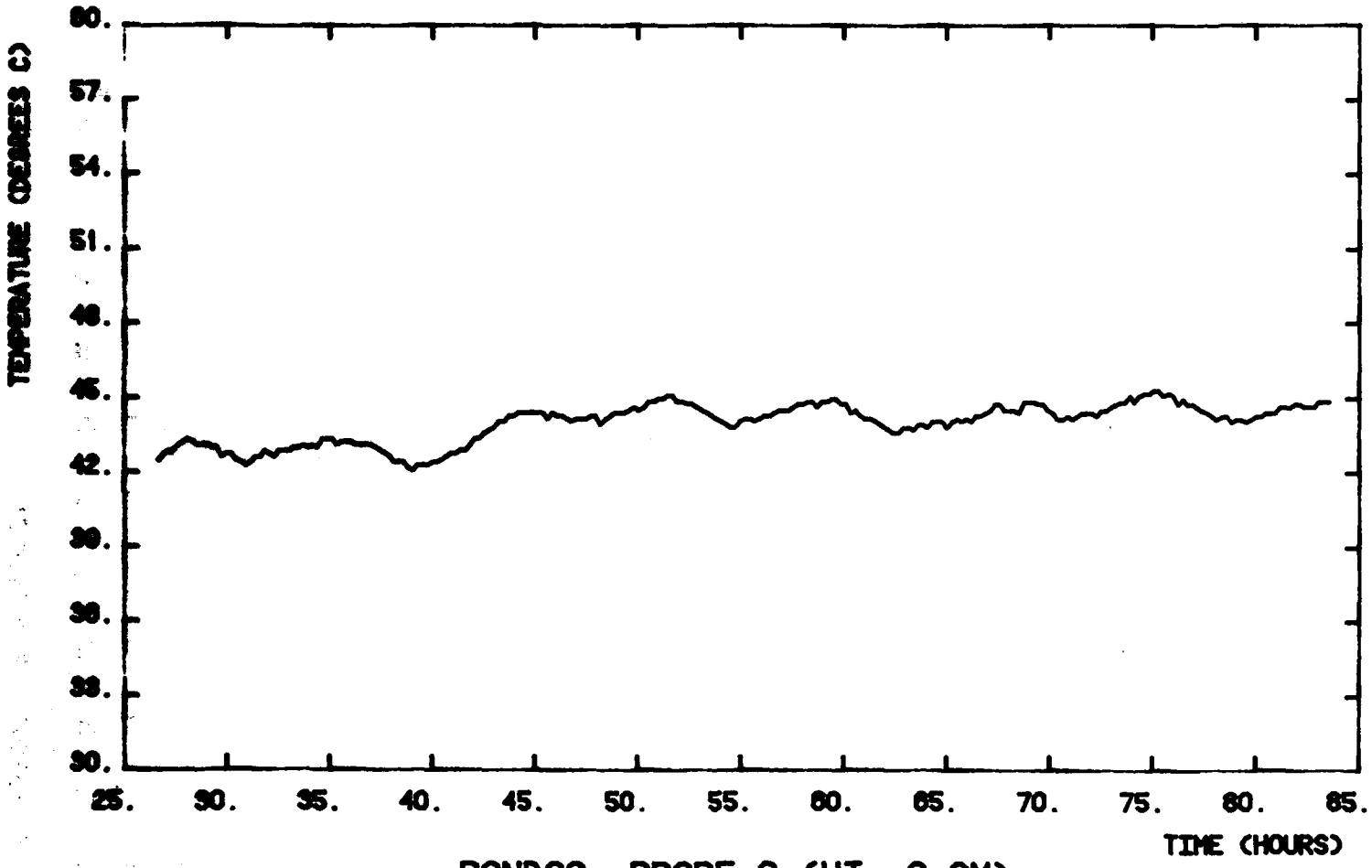

POND80, PROBE 2 (HT.=6.CM)

FIGURE 24k

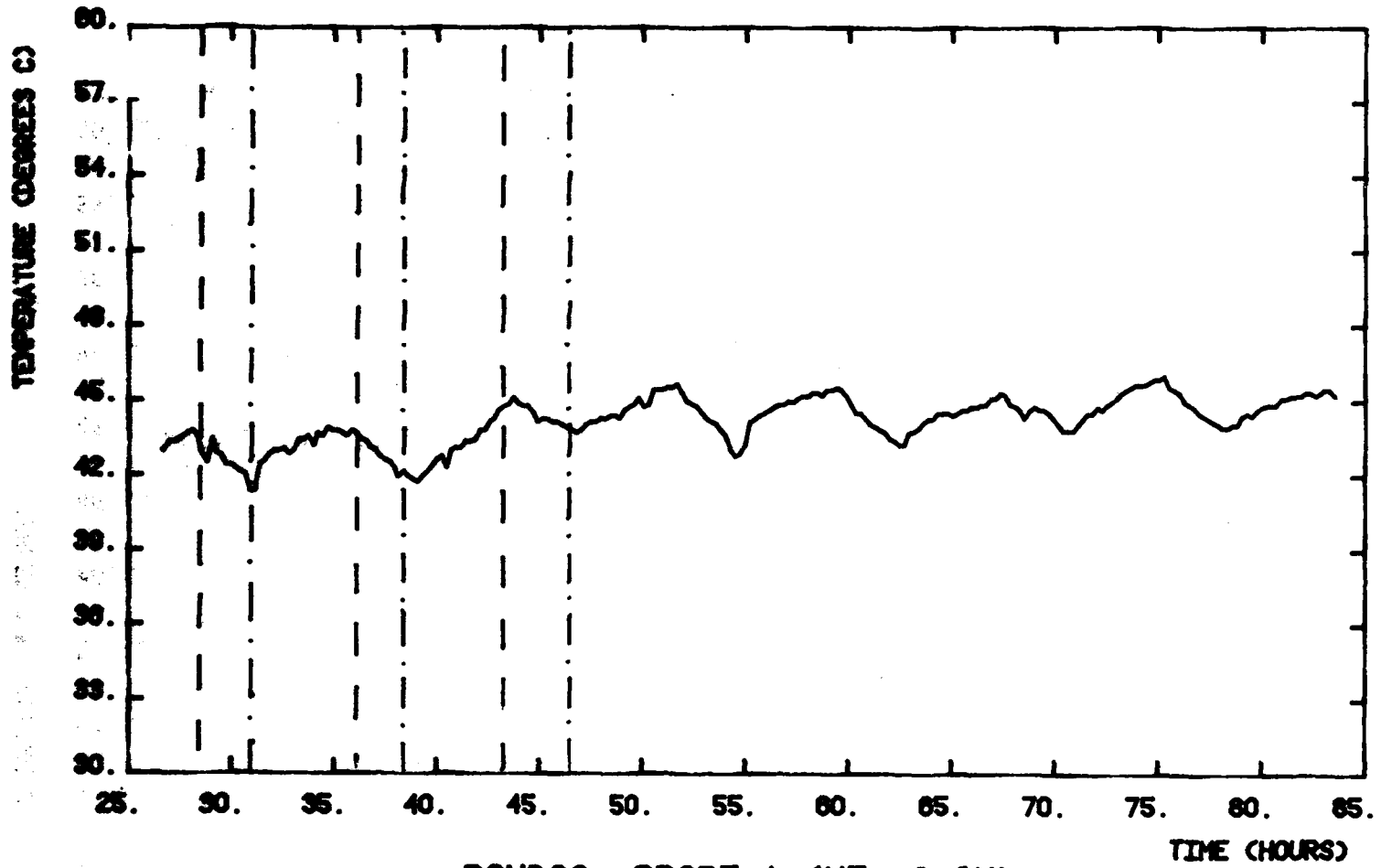

POND80, PROBE 1 (HT.=3.CM)

FIGURE 241

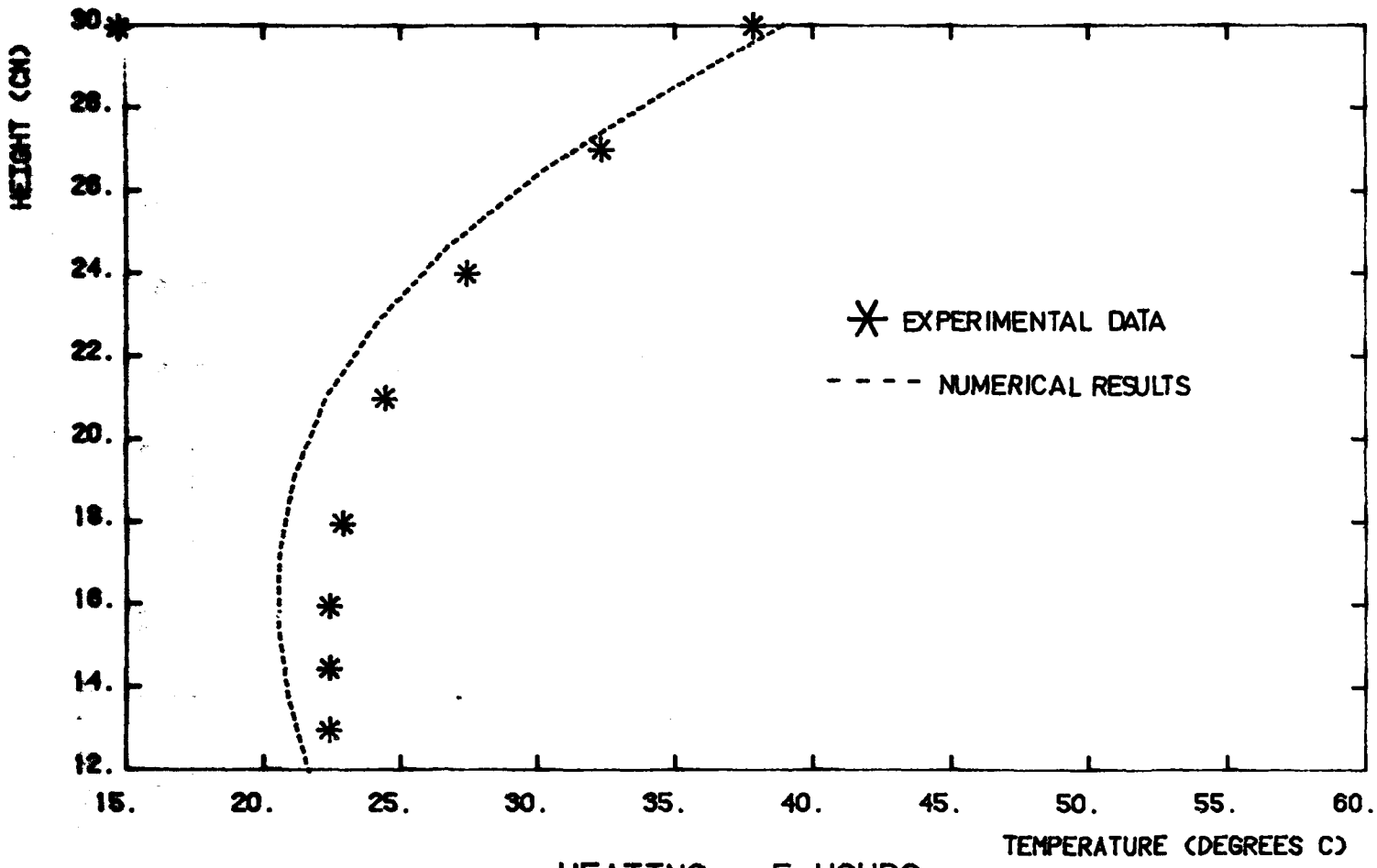

HEATING - 5 HOURS

FIGURE 25a

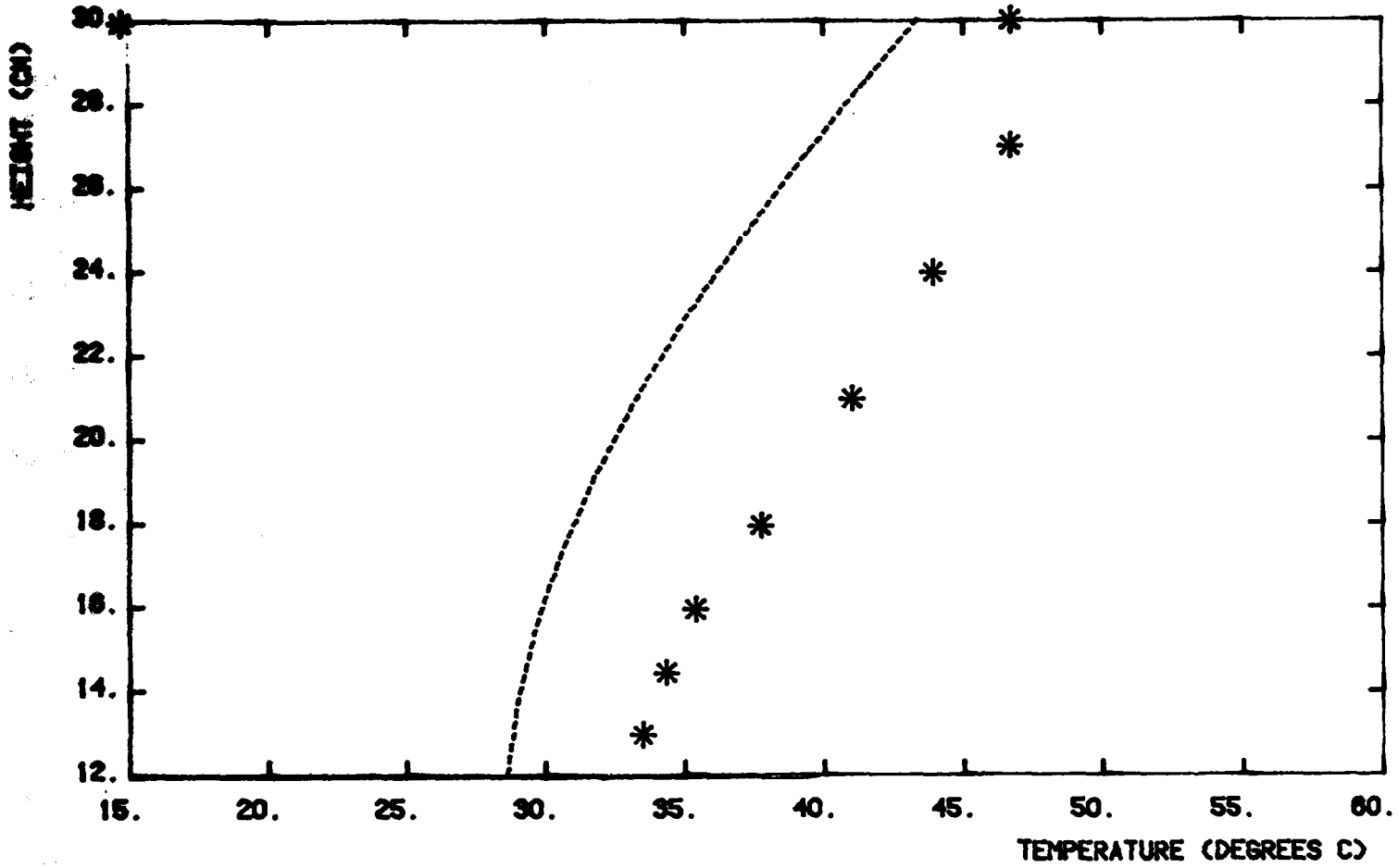

HEATING - 24 HOURS

FIGURE 25b

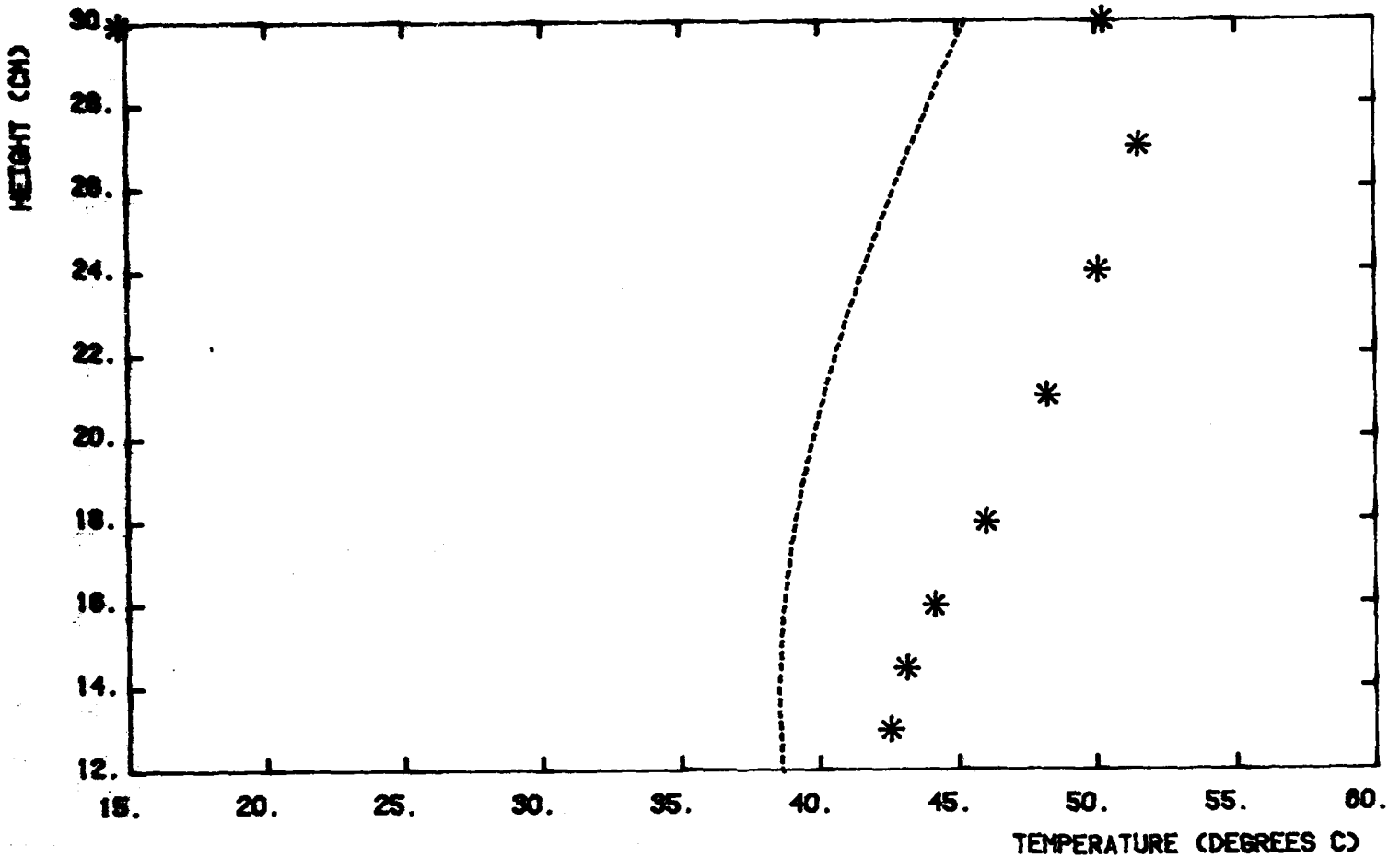

HEATING - 48 HOURS

FIGURE 25c

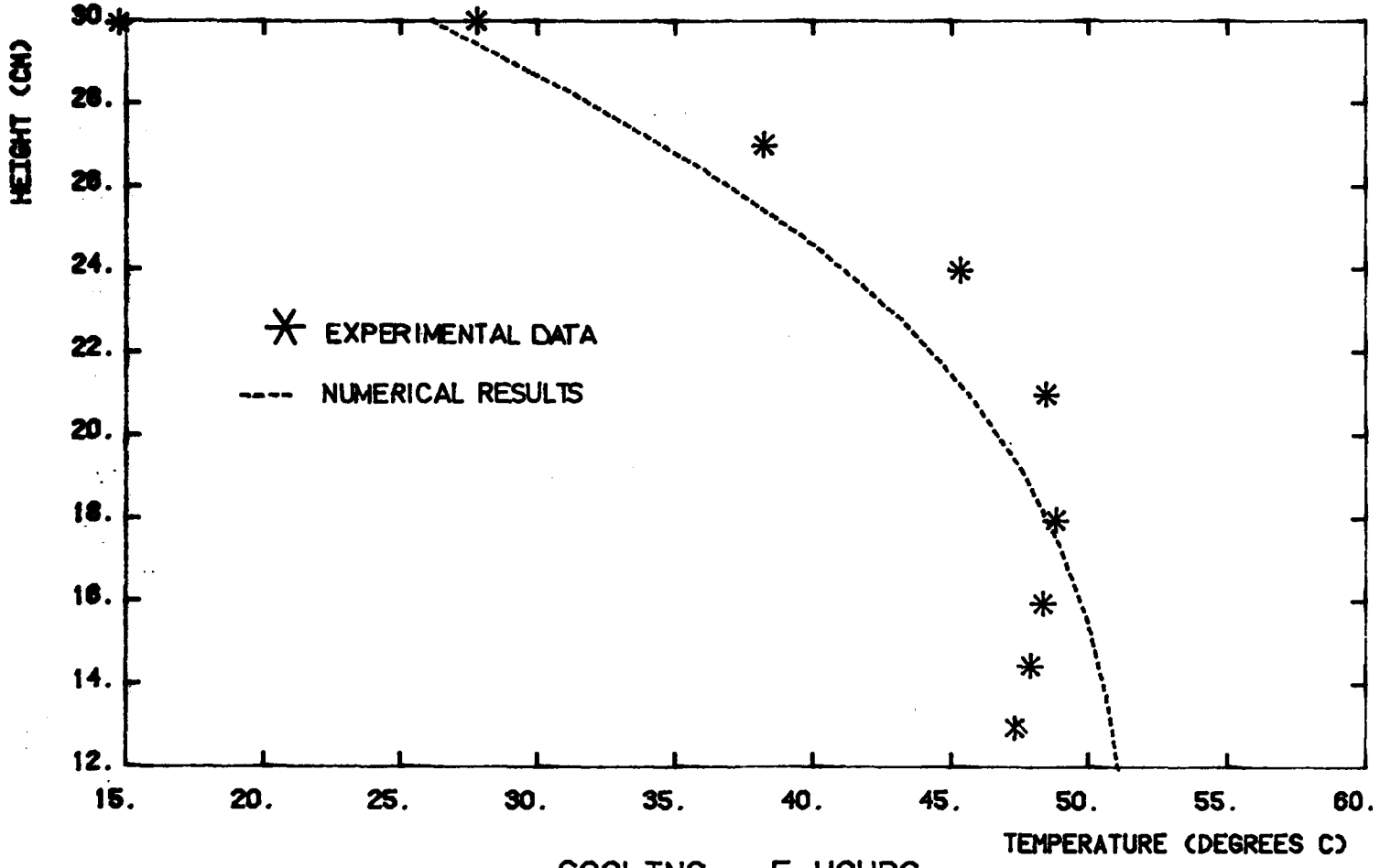

COOLING - 5 HOURS

FIGURE 26a

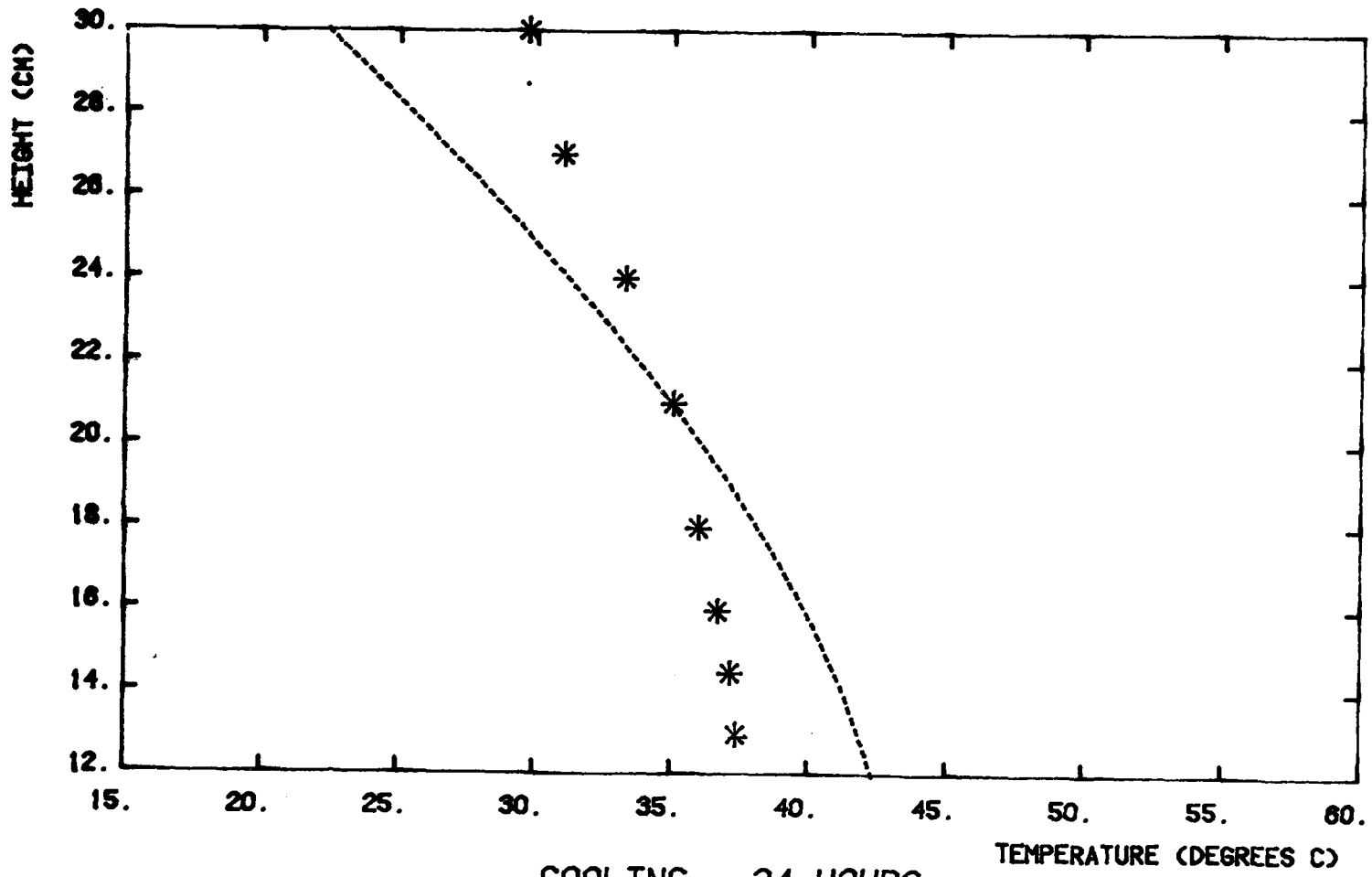

COOLING - 24 HOURS

FIGURE 26b

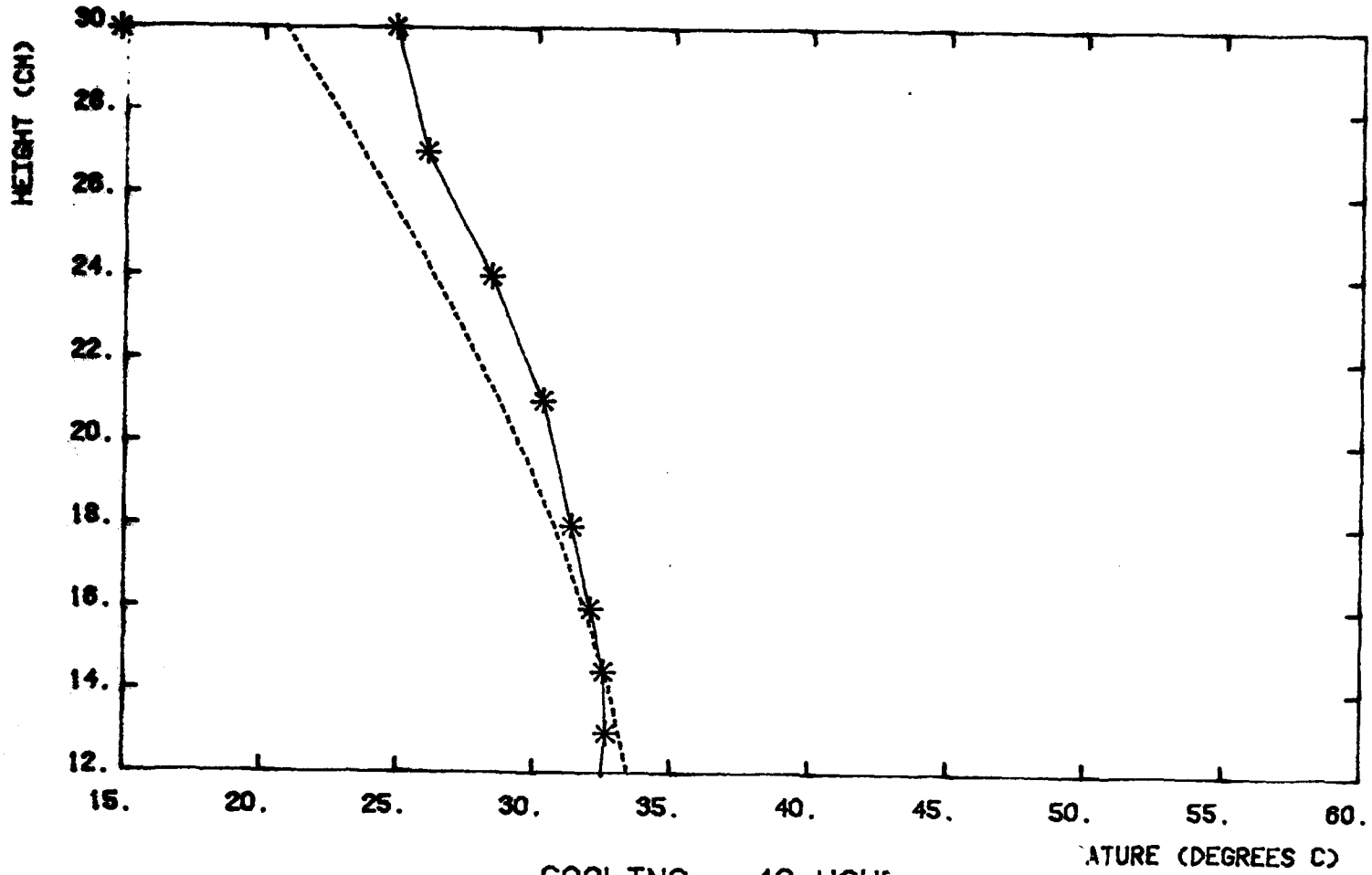

COOLING - 48 HOUR

FIGURE 26c

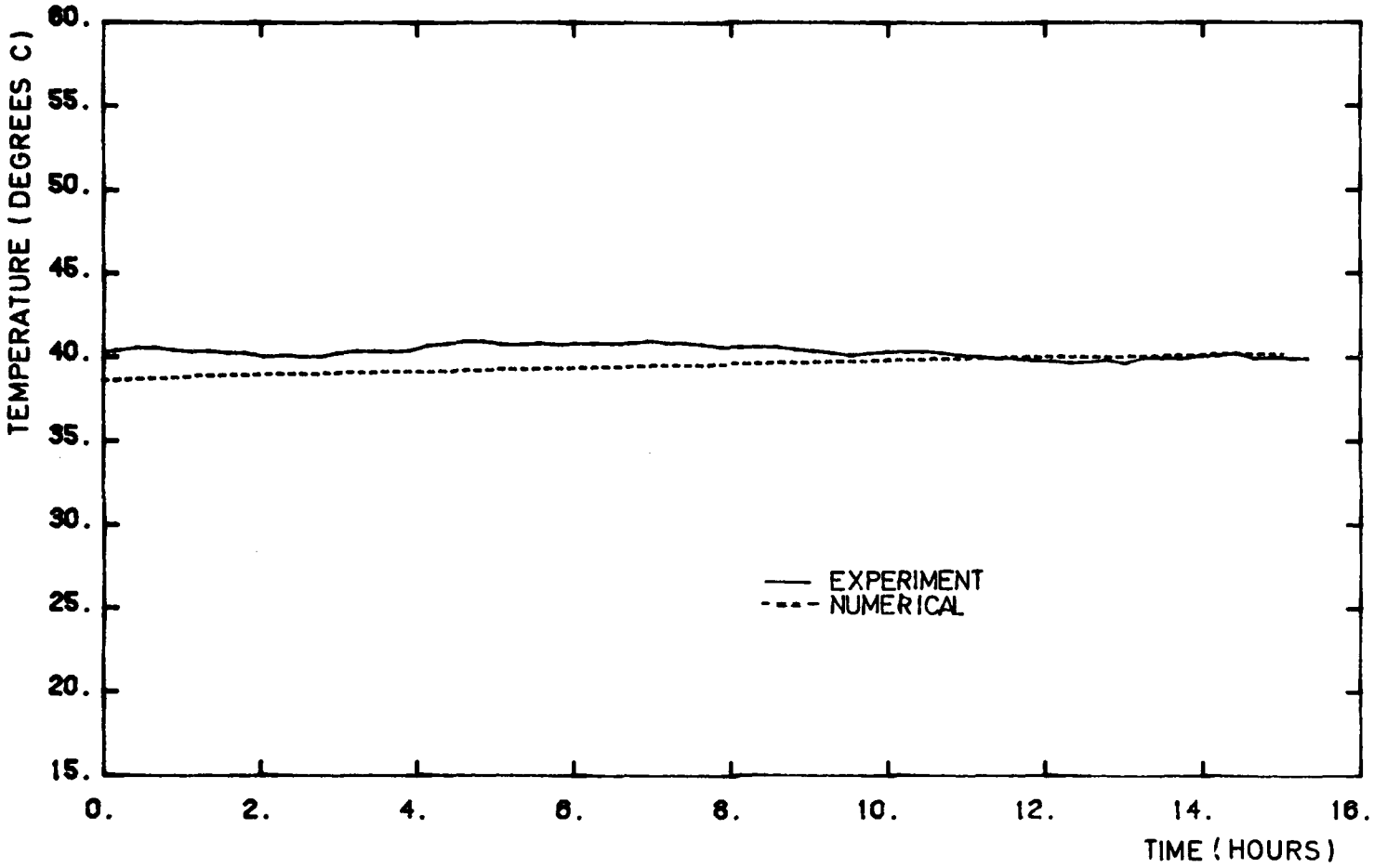

CYCLING - BOTTOM OF NCZ (HT.=12.CM)

FIGURE 27a

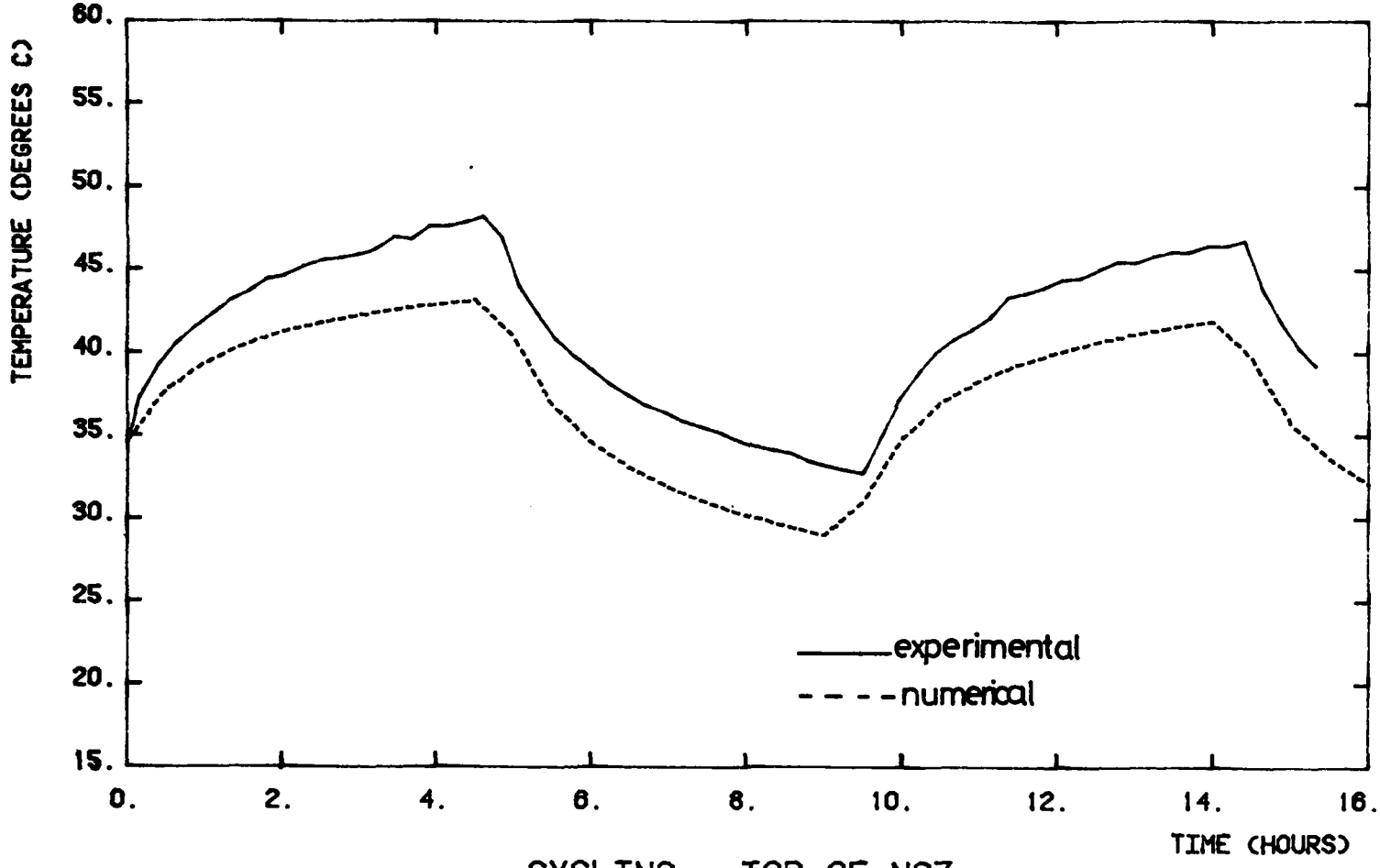

CYCLING - TOP OF NCZ

FIGURE 27b

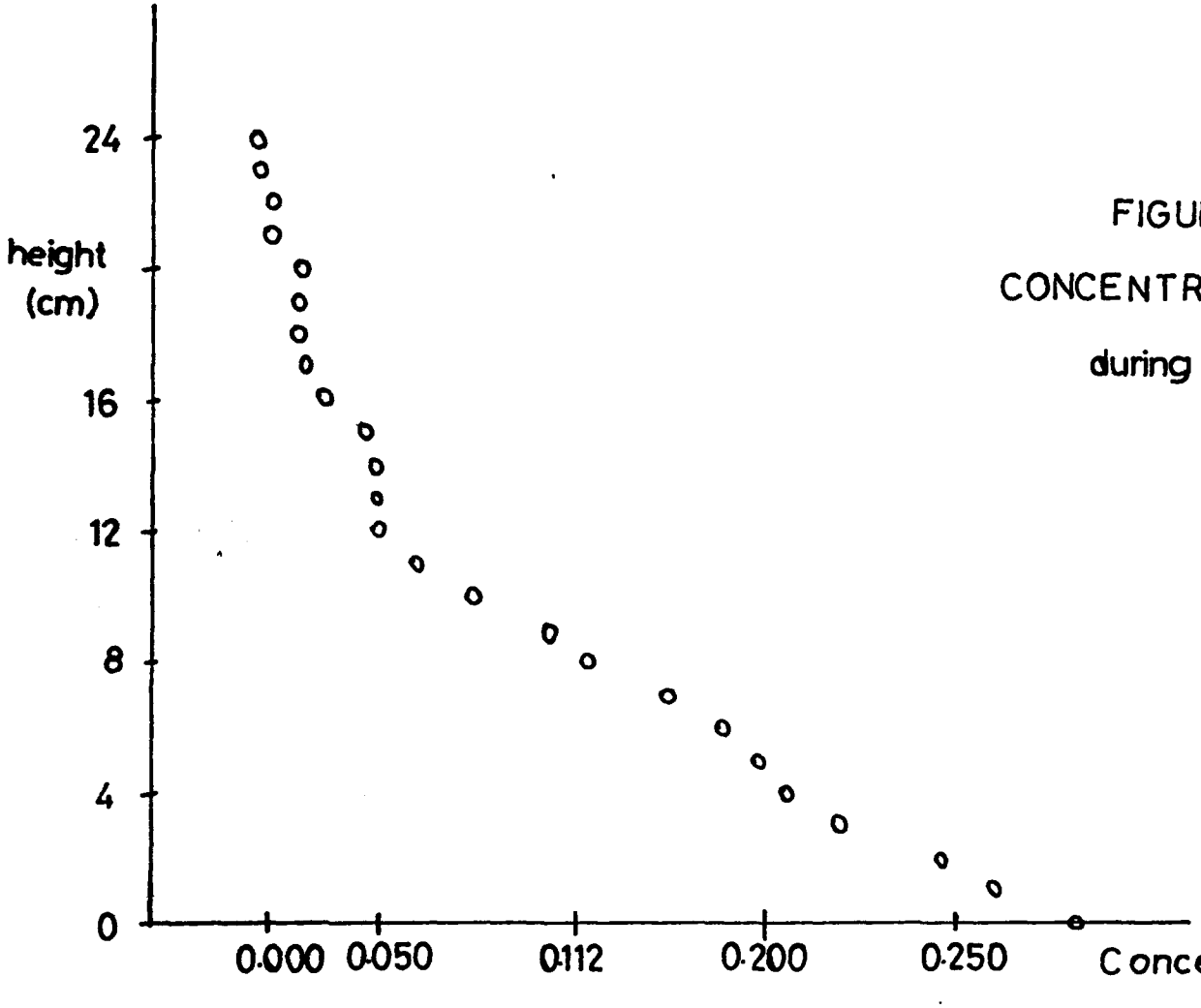

FIGURE 28a

CONCENTRATION PROFILE

during filling of last layer

FIGURE 28 b

CONCENTRATION PROFILE

3 days after filling

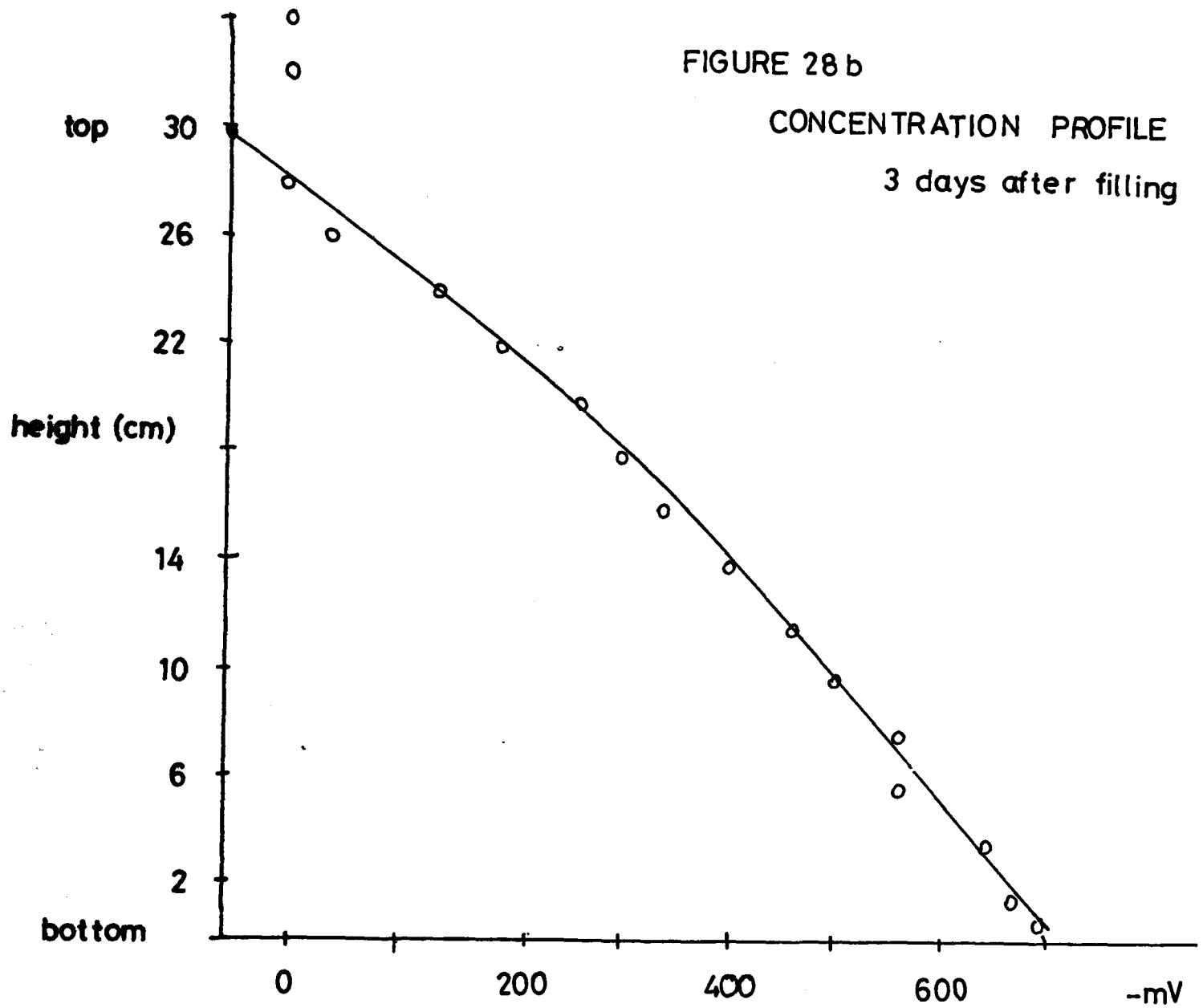

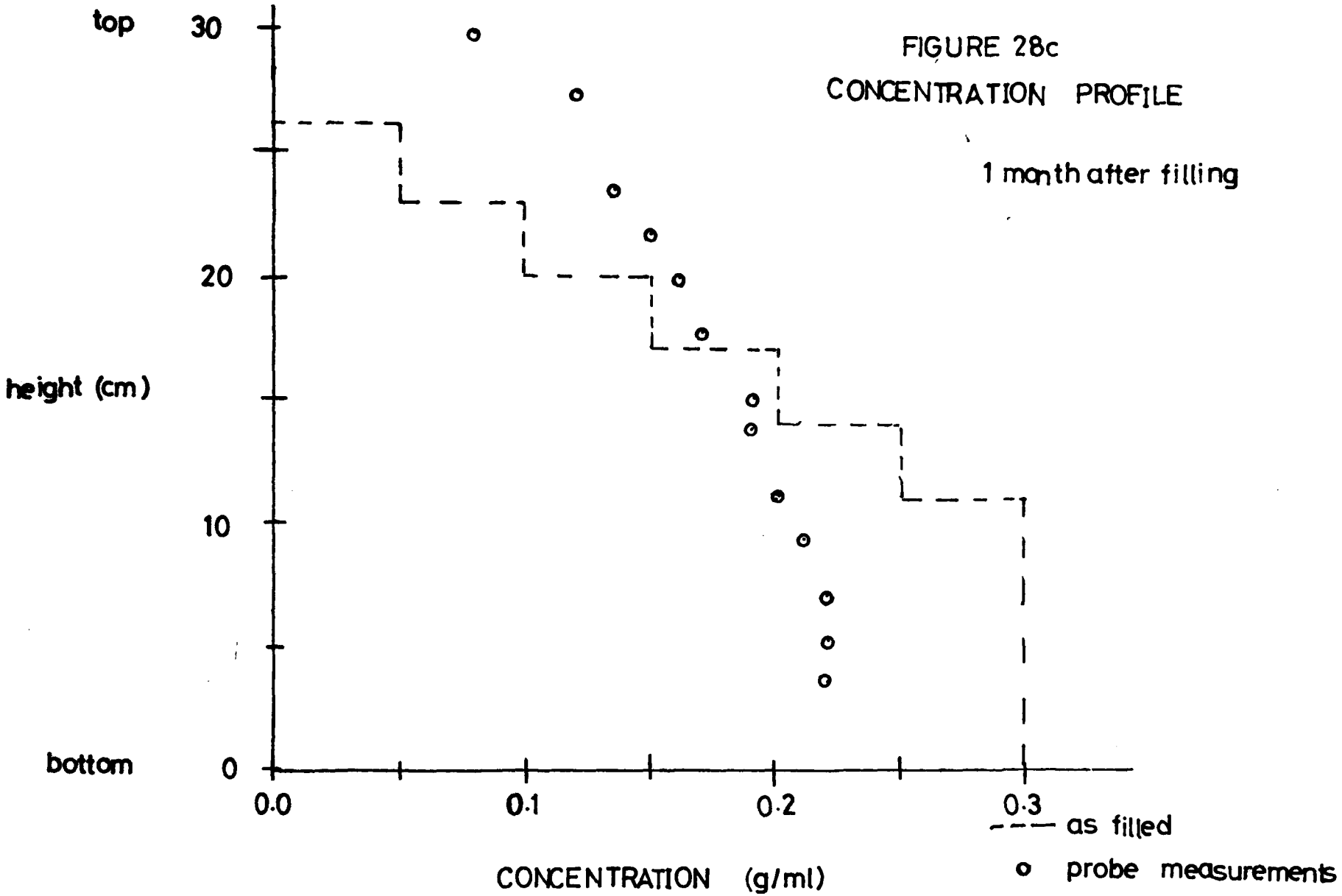

FIGURE 28c
CONCENTRATION PROFILE

1 month after filling

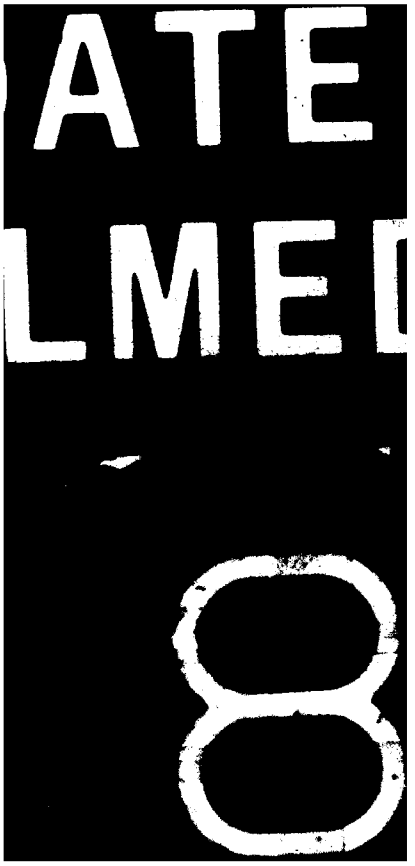
ATE
LMED
8